Sorting, missorting and spreading of Tau in neurons studied in microfluidic chambers

Dissertation

zur

Erlangung des Doktorgrades (Dr. rer. nat.)

der

Mathematisch-Naturwissenschaftlichen Fakultät

der

Rheinischen Friedrich-Wilhelms-Universität Bonn

vorgelegt von

Varun Venkatesh Balaji

Chennai, India

Bonn

2016

Angefertigt mit Genehmigung der Mathematisch-Naturwissenschaftlichen Fakultät der Rheinischen Friedrich-Wilhelms-Universität Bonn

1. Gutachter: Prof. Dr. Eckhard Mandelkow

2. Gutachter: Prof. Dr. Michael Hoch

Tag der Promotion: 13. Februar 2017

Erscheinungsjahr: 2017

Abbreviations ..... **iv**
Summary ..... **vi**
List of figures ..... **viii**
1 Introduction **1**
1.1 Alzheimer disease and other Tauopathies 1
1.2 Tau - a microtubule-associated protein 2
1.2.1 Isoforms of Tau 3
1.2.2 Tau domains and structure 3
1.2.3 Post-translational modifications (PTMs) of Tau 4
1.2.3.1 Phosphorylation of Tau 4
1.2.3.2 Other PTMs of Tau 6
1.2.4 Aggregation of Tau 6
1.3 The distribution and functions of Tau 6
1.3.1 Axonal localization of Tau protein and its functions 7
1.3.2 Somatodendritic localization of Tau protein & its potential toxic effects 7
1.3.3 Nuclear localization of Tau protein and its functions 8
1.4 Missorting of Tau into the somatodendritic compartment and its toxic effects 8
1.5 Proposed mechanisms underlying sorting and missorting of Tau 8
1.5.1 Preferential distribution and translation of Tau mRNA in axons 9
1.5.2 The retrograde diffusion barrier of Tau 9
1.5.3 Axonal transport of Tau 9
1.5.4 Higher affinity of Tau to microtubules in axons than in dendrites 10
1.5.5 Differential degradation of Tau protein in axonal and somatodendritic compartments 10
1.5.6 Mechanisms of Tau sorting 10
1.5.6.1 The ubiquitin-proteasome system (UPS) 10
1.5.6.2 Autophagy 12
1.5.6.3 The degradation of Tau by the proteasome and autophagy systems 14
1.5.6.4 Compromised autophagy and proteasome systems in AD 15
1.6 Microfluidic chambers (MFCs) – an ideal tool to enable local treatment and co-culture of neuronal populations 16
1.7 Spreading of Tau pathology in AD and other Tauopathies 18
1.7.1 Exosomes and spreading of Tau 19

1.8 Aims this study 21

2 Materials and Methods 22

2.1 Materials 22

2.1.1 Antibodies 22

2.1.2 Molecular weight markers 23

2.1.3 Kits 23

2.1.4 Cell culture media and reagents 23

2.1.5 Chemicals 24

2.1.6 Sofwares 24

2.1.7 List of equipments 24

2.1.8 Buffers 25

2.1.9 Microfluidic chambers 27

2.2 Methods 27

2.2.1 Preparation of primary neuronal cultures 27

2.2.2 Preparation & assembly of microfluidic chambers 29

2.2.3 Seeding of neurons in microfluidic chambers 29

2.2.4 Western blotting 30

2.2.5 LDH assay 33

2.2.6 Indirect immunofluorescence 34

2.2.7 Fluorescence insitu hybridization (FISH) 36

2.2.8 Methods used in studying transmission of Tau^{GFP} exosomes 38

2.2.9 Imaging techniques 39

3 Results 41

3.1 Localization of Tau in developing neurons 41

3.2 The role of protein degradation systems in the sorting of Tau 43

3.2.1 Investigation of the sorting mechanism of Tau in microfluidic chambers .43

3.2.2 Validation of the microfluidic chamber system for local treatment of compounds 44

3.2.3 The protein degradation inhibitors suppress protein degradation and are non-toxic to neurons cultured in microfluidic devices 46

3.2.4 Inhibition of the autophagy system in dendrites induces Tau missorting .49

3.2.5 Inhibition of the proteasome system in dendrites induces Tau missorting 51

3.2.6 Differential phosphorylation states of dendritic and axonal Tau 56

3.2.7 Isoforms of Tau degraded in dendrites by autophagy and the proteasome 60
3.2.8 Enhancement of the activity of autophagy or of the proteasome reduces Tau missorting 63
3.2.9 Accumulation of Tau protein in the dendrites via the inhibition of protein degradation systems results in loss of spines 66
3.2.10 Tau protein is locally synthesized in dendrites 68
3.2.11 Tau mRNA distributes to the dendrites, axons and cell bodies 73
3.3 Impact of experimental manipulations on the missorting of Tau protein. 75
3.4 Spreading of Tau protein via exosomes 80
3.4.1 Transmission of Tau^{GFP} exosomes can occur via axons 86
3.4.2 Synaptic contacts are required for the exosome-mediated transmission of Tau 87
3.4.3 Tau containing exosomes, independently of their origin, are transmitted across neuronal populations 94

4 Discussion 96
4.1 Sorting mechanisms of Tau protein 96
4.1.1 Developmental regulation of the distribution of Tau in neurons 96
4.1.2 Polarized distribution of Tau protein in neurons 96
4.1.3 The role of protein degradation systems in the axonal sorting of Tau protein 97
4.1.4 Protein degradation inhibition results in missorting of Tau with differential phosphorylation status and isoform distribution 99
4.1.5 Tau mRNA is present in the dendrites of neurons and is actively translated 100
4.1.6 Inhibition of protein degradation causes missorting of Tau into dendrites and spine loss 103
4.1.7 Chemical fixation can lead to artefacts of Tau mislocalization 103
4.2 Trans-synaptic transmission of Tau protein via exosomes 105

5 Bibliography 108

6 Appendix 120

7 Acknowledgement 123

Curriculum vitae 124

Abbreviations

AD – Alzheimer Disease

Aβ – Amyloid Beta

Ani – Anisomycin

Baf – Bafilomycin

BCA – Bicinchoninic acid

BSA – Bovine Serum Albumin

cAMP – cyclic Adenosine Mono Phosphate

CHX – Cycloheximide

CNS – Central Nervous System

DMSO – Dimethyl Sulfoxide

DIV – Days Invitro

Epo – Epoxomicin

E18 – Embryonic day 18

FA – Formaldehyde

FISH – Fluorescence Insitu Hybridization

Glu – Glutaraldehyde

GluR1 – Glutamate Receptor 1

IgG – Immunoglobulin

kDa – Kilo Dalton

Lac – Lactacystin

LDH – Lactate Dehydrogenase

MFC – Microfluidic Device

M – Molar

MAPs – Microtubule Associated Proteins

mg – milligram

mm – millimeter

mM – millimolar

mL – milliliter

MARK2 – Microtubule Affinity Regulating Kinase 2

NFTs – Neurofibrillary Tangles

OD – Optical Density

PTMs – Post Translational Modifications

PAGE – Poly Acrylamide Gel Electrophoresis

PVDF – Poly Vinylidene Difluoride

PBS – Phosphate Buffered Saline

PKA – Protein Kinase A

PP2A – Protein Phosphatase 2A

PP2B – Protein Phosphatase 2B

RD150 – Round Device 150

RT – Room Temperature

SDS – Sodium Dodecyl Sulfate

SEM – Standard Error of the Mean

SynPh - Synaptophysin

TCND1000 – Triple Chamber Neuron Device 1000

Tau^{GFP} – Human Tau tagged with Green Fluorescent Protein

Tau^{RFP} – Human Tau tagged with Red Fluorescent Protein

Tau^{CFP} – Human Tau tagged with Cyan Fluorescent Protein

UPS – Ubiqiuitin Proteasome System

UTR – Untranslated Region

Wor – Wortmannin

µg – Micro gram

µL – Micro liter

µm – Micro meter

µM – Micro molar

°C – degree Celsius

Summary

Tau is a microtubule associated protein which plays an important role in stabilizing microtubules (Mandelkow and Mandelkow, 2012). Tau is mainly an axonal protein but it is missorted into the somatodendritic compartment in Alzheimer disease (AD). This represents one of the earliest signs of neurodegeneration in AD (Braak et al., 1994). During early stages of development, Tau protein is ubiquitously expressed across all compartments of neurons whereas it becomes axonally sorted during differentiation and maturation (Zempel and Mandelkow, 2014). We investigated the sorting mechanisms of endogenous Tau in cultured primary neurons using microfluidic devices (MFCs) where cell compartments can be treated and observed separately. We found that blocking protein degradation pathways on the neuritic side of the microfluidic devices with the proteasomal or autophagy inhibitors (e.g. wortmannin, epoxomicin) increased the missorting of Tau into the dendrites on the neuritic side. This suggests that degradation of Tau in dendrites is a major determinant for the physiological axonal distribution of Tau. Notably, such missorted dendritic Tau showed a different phosphorylation pattern from axonal Tau, as it was phosphorylated mainly in the repeat domain (epitope of 12E8 antibody), but not in the proline-rich domains flanking the repeats (e.g. epitopes of PHF1 and AT8 antibodies). By contrast, the axonal Tau was phosphorylated at all three sites. The dendritically mislocalized Tau resulted in the loss of spines. Inhibition of local protein synthesis prevented the missorting of Tau induced by inhibition of protein degradation, indicating that the missorted dendritic Tau is locally synthesized. In support of this, Tau mRNA was detected not only in cell bodies and axons, but in dendrites as well. Taken together, the above results indicate that the protein degradation systems play an important role in the polarized distribution of Tau in neurons during differentiation.

Another hallmark of Tau-dependent pathology in Alzheimer disease is its spreading between anatomically connected neurons and brain regions in a stereotypic pattern (Braak stages). This implies a release of Tau into the extracellular space and re-uptake by other neurons (Wang and Mandelkow, 2016). The mechanism of Tau spreading is still a matter of debate. In the present study, we used microfluidic devices and showed that the trans-neuronal transfer of Tau protein can be achieved by exosomes (small membrane-bounded vesicles containing Tau) depending on synaptic connectivity. The spreading of GFP-Tau containing exosomes was

demonstrated directly by their uptake into neurons on the somal side, followed by transfer to second-order and third-order neurons in successive compartments of the MFCs. This implies the role of exosomes in the long distance spreading of Tau protein across different brain regions.

List of figures

Figure 1.1 Pathological hallmarks of Alzheimer disease 2

Figure 1.2 The six different isoforms of Tau protein 3

Figure 1.3 Phosphorylation sites of Tau protein and the epitopes of phosphorylation specific antibodies 5

Figure 1.4 The ubiquitin conjugation pathway 12

Figure 1.5 Cellular events of macroautophagy 14

Figure 1.6 Photographs and picture of microfluidic chambers 17

Figure 1.7 Mechanisms involved in the prion-like protein transmission in neurodegenerative diseases 20

Figure 2.1 Principle of LDH assay 34

Figure 2.2 Binding of the probe sets and the blocking probe (BL) to the target mRNA 36

Figure 2.3 Working schematic of the Quantigene ViewRNA ISH cell assay 37

Figure 3.1 Localization of Tau in developing neurons 42-43

Figure 3.2 Schematic representation of a microfluidic chamber showing separation of neurites from soma 44

Figure 3.3 Fluidic isolation in microfluidic chambers is intact even after 24hours.45-46

Figure 3.4 The protein degradation inhibitors used were active and non-toxic to neurons cultured in microfluidic chambers 48

Figure 3.5 The protein degradation inhibition by autophagy lead to Tau missorting 49-50

Figure 3.6 The protein degradation inhibition by the proteasome lead to Tau missorting 51-52

Figure 3.7 Quantification of dendrites with Tau missorting induced by protein degradation inhibitors 52

Figure 3.8 The protein degradation inhibition by autophagy is specific and lead to Tau missorting 53-54

Figure 3.9 The protein degradation inhibition by the proteasome is specific and lead to Tau missorting 55

Figure 3.10 Tau in dendrites is phosphorylated predominantly at the 12E8 site 57

Figure 3.11 Quantification of dendrites with missorted phosphorylated Tau induced by protein degradation inhibitors 60

Figure 3.12 1N isoform of Tau is degraded by autophagy and the proteasome in dendrites 62-63

Figure 3.13 Enhancement of the activity of autophagy by trehalose reduces Tau missorting into the dendrites.....65

Figure 3.14 Enhancement of the activity of the proteasome by rolipram reduces Tau missorting into the dendrites 66

Figure 3.15 Local treatment with protein degradation inhibitors suppresses protein degradation and lead to dendritic Tau mislocalization and spine loss 67-68

Figure 3.16 Protein translation inhibitors prevent Tau missorting 69-73

Figure 3.17 Fluorescence insitu hybridization reveals Tau mRNA across all compartments of the neuron 74-75

Figure 3.18 Tau redistributes into the somatodendritic compartment after experimental manipulations 77-79

Figure 3.19 Transmission of Tau^{GFP} exosomes from one neuronal population to the other in microfluidic chambers 82-85

Figure 3.20 Transmission of Tau^{GFP} exosomes from one neuronal population to the other can occur via axons 86

Figure 3.21 Synaptic contacts are required for exosome-mediated transmission of Tau^{GFP} 89-94

Figure 3.22 Tau containing exosomes are transmitted across neuronal populations independently of their origin.....95

Figure 4.1 & 4.3 Schematic representation of the different treatments and its consequences in neurons cultured in microfluidic chambers..... 98 &102

Figure 4.2 Schematic representation of the distribution of Tau mRNA in a neuron .101

Figure 4.4 Schematic representation of the spreading of exosomes containing Tau^{GFP} in neurons cultured in triple chamber microfluidic devices.....106

1 Introduction

1.1 Alzheimer disease and other Tauopathies

Alzheimer disease (AD) was first identified in 1907 by a German psychiatrist and pathologist, Dr. Alois Alzheimer in a post-mortem study on a 51-year old patient, Auguste D (Alzheimer, 1907). AD is the common form of dementia in developed nations and is one of the major health problems in aging populations. The dementia is characterized initially by synaptic loss (DeKosky and Scheff, 1990) followed by neuronal loss (Terry et al., 1981) and by progressive behavioral changes like loss of memory and other cognitive functions. It is estimated to cost the world 604 billion dollars/year and it is expected to triple by 2050 (Huang and Mucke, 2012).

AD, a progressive neurodegenerative disease is characterized by abnormal protein deposits of intracellular neurofibrillary tangles (NFTs) and extracellular senile plaques in the brain. While NFTs consists of the hyperphosphorylated microtubule binding protein - Tau (Mandelkow and Mandelkow, 1998), the senile plaques are composed of beta-amyloid protein (Aβ) generated from amyloid precursor protein (APP) through cleavage by β- secretase (β-site APP cleaving enzyme (BACE)) and γ-secretase - a multi-subunit complex composed of presenilin (PS), nicastrin, anterior pharynx-defective 1 (APH-1), and presenilin enhancer 2 (PEN-2) (Kovacs, 2009) **(Fig. 1.1).** Majority of AD cases (99%) are sporadic, which usually occur at a later stage around 65 years or older. Approximately 1% of AD is familial, which is caused by mutations of APP or presenilins and have an earlier onset of the disease around 50 years (Murrell et al., 1991). As familial APP or PS mutations promote the generation of Aβ, this has led to the proposal of the amyloid cascade hypothesis which posits that the deposition of Aβ is the primary event driving AD pathogenesis including tau pathology (Hardy and Allsop, 1991). However, accumulating evidence highlights the critical role of Tau pathology in AD. On one hand, Tau pathology appears to be necessary for Aβ-induced neurodegeneration as reducing Tau ameliorates Aβ-induced deficits invivo or in cultured cells (Roberson et al., 2007, Zempel and Mandelkow, 2014), on the other hand, Tau pathology does not necessarily occur downstream of Aβ deposits, as NFTs are also often detected in normal aged human brain in the absence of Aβ deposits, namely, primary age-related Tauopathy (PART)

(Braak and Del Tredici, 2014). Indeed, it is the NFTs not senile plaques that are correlated with the severity of dementia in AD (Arriagada et al., 1992).

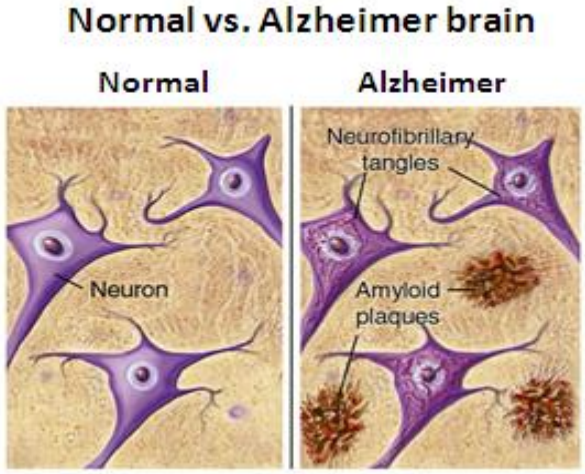

Figure 1.1: Pathological hallmarks of Alzheimer disease. The extracellular plaques consist of the Aß peptide, which accumulate between neurons. The twisted fibers found inside neurons are referred to as neurofibrillary tangles (NFTs) and consist primarily of the protein Tau which is involved in microtubule stabilization in healthy brains. In Alzheimer disease it dissociates from the microtubules thereby resulting in destabilization of microtubules and eventually in the formation of NFTs. The tangles get deposited in the regions of the brain involved in learning and memory and eventually can spread to other regions and are thought to lead to the degeneration of neurons (Figure adapted from http://www.brightfocus.org/alzheimers/infographic/amyloid-plaques-and-neurofibrillary-tangles).

Besides AD, Tau aggregation is also found in a wide range of neurodegenerative diseases termed Tauopathies, including progressive supranuclear palsy (PSP), corticobasal degeneration (CBD), argyrophilic grain disease (AGD), Pick disease (PiD), Huntington disease (HD), and frontotemporal dementia with parkinsonism-17 (*FTDP-17*) (Lee et al., 2001). The identification of Tau mutants of FTDP-17 in a group of familial tauopathies provided compelling evidence that Tau abnormalities alone are sufficient to cause Tauopathies (Lewis et al., 2000), thus establishing the key role of Tau in these neurodegenerative diseases.

1.2 Tau – a microtubule associated protein

Tau was discovered in 1975 in vitro, mainly as a factor involved in the assembly of tubulin subunits into the so called ‘36S’ rings and microtubules (Weingarten et al., 1975). Tau protein prepared from mammalian brain consists of a mixture of several related polypeptides of relative molecular weight ranging from 50 to 70kDa (Steiner et al., 1990). Tau belongs to a group of proteins termed microtubule associated proteins

(MAPs) which also includes MAP1A, MAP1B, MAP1C, MAP2 and MAP4 (Maccioni and Cambiazo, 1995). Distinct from other MAPs, Tau is a component of PHFs, and thus catches wide research interest.

1.2.1 Isoforms of Tau

Human Tau is encoded by a single gene comprising 16 exons on chromosome 17q21 (Neve et al., 1986). Exons 1, 4, 5, 7, 9, 11, 12 and 13 are constitutive while the others are subject to alternative splicing. Exons 0 and 1 contain the 5' untranslated sequences of *MAPT* mRNA, while Exon 14 is part of the 3' untranslated region of Tau mRNA. Exon 0 is part of the promoter, which is transcribed but not translated. The translation initiation codon ATG is in exon 1. Exons 4a, 6 and 8 are present only in mRNA of the peripheral tissue. The adult human brain contains six Tau isoforms which are generated via alternative splicing of exons E2, E3 and E10. These Tau isoforms differ by the presence of 0, 1 and 2 amino-terminal inserts (29 residues each, encoded by E2 and E3) (0N, 1N and 2N) in combination with the presence of 3 or 4 carboxy-terminal tandem repeat domains (3R or 4R, the 2nd repeat is encoded by E10) (Crowther et al., 1989, Andreadis et al., 1992) **(Fig. 1.2).**

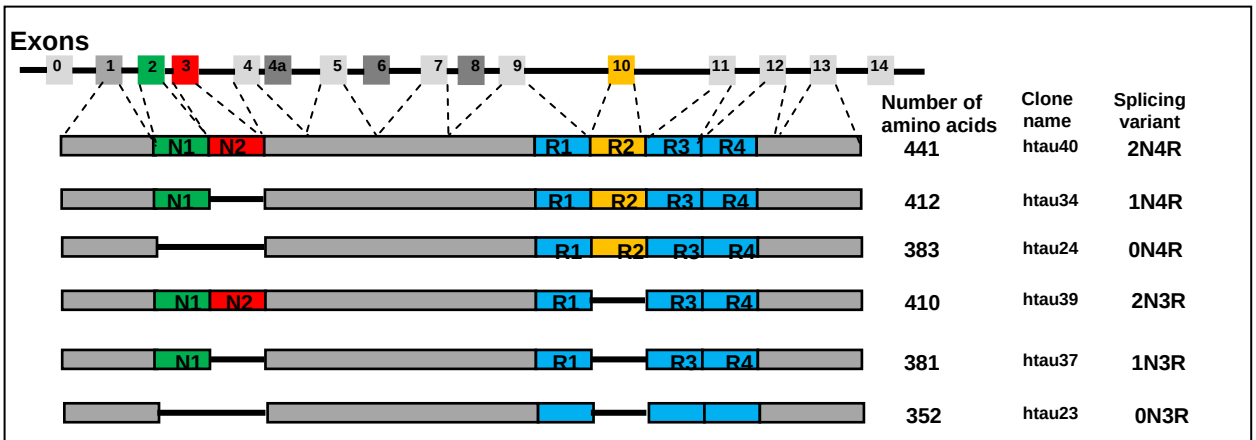

Fig. 1.2: The six different isoforms of Tau protein. Alternative splicing of exons 2, 3 and 10 results in six different Tau mRNAs translated into six different isoforms of Tau protein which differ by the presence of 0, 1 or 2 amino-terminal inserts (0N, 1N or 2N) and the presence or absence of repeat R2. This results in Tau isoforms of different number of aminoacids and molecular weight and are named as 3R or 4R species [Figure adapted from (Wang and Mandelkow, 2016)].

1.2.2 Tau domains and structure

Based on its microtubule interactions and amino acid character, Tau can be subdivided into two major domains: (1) the assembly domain in the C-terminal half

comprising the repeat domains plus flanking regions which binds to and stabilizes microtubules; (2) the projection domain in the N-terminal half, which does not bind to microtubules, but projects away from the microtubule surface. The middle region of Tau (aa 150-240) within the projection domain is a proline-rich domain. It contains: (1) seven PXXP motifs, which are binding sites for signalling proteins with SH3 domains, for instance, the tyrosine kinase fyn (Lee et al., 1998); (2) multiple threonine/proline (TP) or serine/proline (SP) motifs that are targets of proline-directed kinases which become hyperphosphorylated in AD and other Tauopathies.

1.2.3 Post-translational modifications (PTMs) of Tau

After synthesis, Tau is subjected to multiple post-translational modifications which appear to play critical roles in regulating Tau function, degradation and aggregation.

1.2.3.1 Phosphorylation of Tau

Tau is normally a phosphoprotein. Its phosphorylation is developmentally regulated so that fetal Tau (~7 phosphates per molecule) is more highly phosphorylated than adult Tau (~2 phosphates) (Kenessey and Yen, 1993). However, in AD, the phosphorylation of Tau is increased to ~8 phosphates per molecule, about 3-4 times more than controls (Kopke et al., 1993). There are up to 85 potential phosphorylation sites (80 Ser/Thr, 5 Tyr) in the longest isoform of Tau (2N4R). Owing to the unfolded structure of Tau, most of these sites are accessible, with ~45 of them observed experimentally (Hanger et al., 2009).

The kinases which phosphorylate Tau can be divided into three categories: (i) Proline directed serine/threonine kinases (PDPKs) such as glycogen synthase kinase 3β (GSK-3β), cyclin-dependent kinases (cdk5/cdc2), mitogen-activated protein kinase (MAPK), stress-activated kinases (e.g. JNK and p38), etc that phosphorylate Tau at SP/TP motifs clustering in the flanking regions of Tau. In AD and other Tauopathies, these SP/TP motifs are abnormally phosphorylated, generating epitopes for diagnostic antibodies AT8 (S202/T205), AT180 (T231/S235), PHF1 (S396/S404) etc that are widely used for labeling pathological Tau **(Fig. 1.3)** (ii) Non-proline directed serine/threonine kinases such as Microtubule-Affinity Regulating Kinase (MARK), Ca^{2+}/Calmodulin-dependent protein kinase II (CaMPK II), cyclic AMP dependent kinase (PKA) and Casein Kinase II, which phosphorylate Tau at the KXGS motifs in

the repeat domain (Schneider and Mandelkow, 2008). (iii) tyrosine Kinases including the Src family kinases - Fyn kinase, Lck, Src, Syk, c-Abl phosphorylate the five tyrosine residues in all isoforms of Tau (Lebouvier et al., 2009).

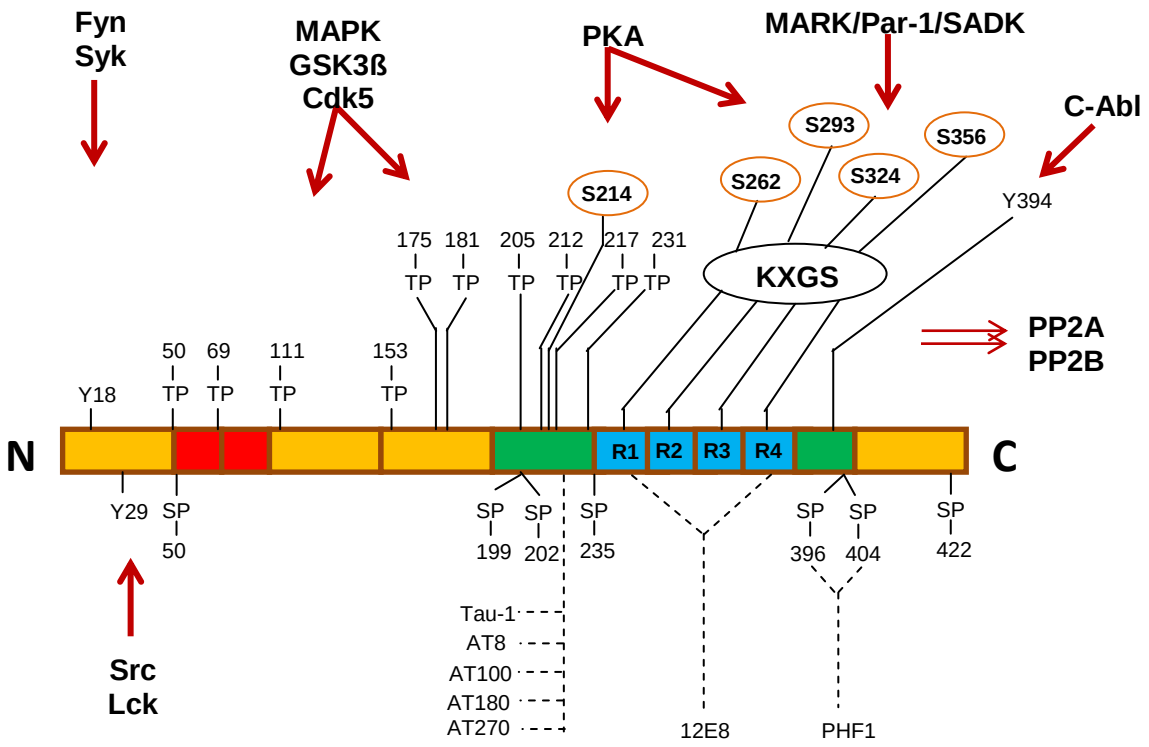

Fig. 1.3: Phosphorylation sites of Tau protein and the epitopes of phosphorylation specific antibodies. Various kinases and phosphatases target different phosphorylation sites of Tau protein. Phosphorylation of the SP/TP motifs by MAPK, GSK3ß and Cdk5 has a slight modulating effect on the microtubule binding of Tau, but phosphorylation at the KXGS motifs and at S214 by MARK, PKA or SADK can reduce its affinity to microtubules. The Src family kinases phosphorylate the tyrosine residues of Tau. The phosphatases, PP2A and PP2B dephosphorylate Tau. The epitopes of the different phospho-Tau specific antibodies have been indicated [Figure adapted from (Schneider and Mandelkow, 2008)].

Phosphorylation plays a critical role in regulating both physiological and pathological functions of Tau. Phosphorylation may fine-tune the binding of Tau to microtubules and therefore regulates the stabilization and assembly of microtubules. The hyperphosphorylation of Tau is observed in NFTs from all Tauopathies, and thereby has been implicated to play a role in driving Tau aggregation. However, this issue remains a matter of debate (see below). In addition, abnormal phosphorylation of Tau may retard its degradation and thus contributes to its accumulation and aggregation.

1.2.3.2 Other PTMs of Tau

Tau is also subjected to other post-translational modifications. The abnormally phosphorylated Tau in AD brain was also glycosylated (Wang et al., 1996). Additionally, the KXGS motifs are hypoacetylated and hyperphosphorylated in AD patients and in a mouse model of Tauopathy (Cook et al., 2014).

1.2.4 Aggregation of Tau

The aggregation of Tau depends on two short hexapeptide motifs at the beginning of R2 and R3 (VQIINK and VQIVYK) of Tau that show propensity for β-structure (von Bergen et al., 2000). Disruption of these motifs by introducing proline mutations - β-structure breaker abrogate the tendency of Tau for aggregation; on the contrary, strengthening the β-structure by mutations (e.g. ΔK280 or P301L) accelerates Tau aggregation (Khlistunova et al., 2007, Mocanu et al., 2008).

Notably, phosphorylation at sites S262/S356 in the repeat region and S214 detaches Tau from microtubules and can infact protect Tau against aggregation (Schneider et al., 1999). Finally, Tau aggregation can be induced efficiently by polyanionic cofactors, regardless of phosphorylation, suggesting that phosphorylation is not necessary for Tau aggregation. Thus, it is possible that unknown cofactors trigger Tau aggregation in the Alzheimer brain, while phosphorylation may accelerate aggregation indirectly, for example by detaching Tau from microtubules (Wang and Mandelkow, 2012). Additionally, in a cell model of Tauopathy, stepwise proteolysis of Tau harboring the ΔK280 mutation resulted in the aggregation of Tau (Wang et al., 2009, Wang et al., 2007), highlighting the critical role of truncation of Tau in aggregation.

1.3 The distribution and functions of Tau

Tau protein is mainly found in neurons, but debatably also in many non-neuronal cells (Migheli et al., 1988). In neurons, the subcellular distribution of Tau is developmentally regulated. Before developmental differentiation, Tau distributes evenly in the cell body and neurites. Later, when axons emerge and neurons are polarized, Tau becomes enriched in axons (Mandell and Banker, 1995), with minor amounts in dendrites and nuclei.

1.3.1 Axonal localization of Tau protein and its functions

In neurons, Tau mainly distributes into the axons where it interacts with microtubules through the repeat domain and flanking regions and thereby stabilizes microtubules and promotes microtubule assembly (Mandelkow and Mandelkow, 2012). In addition, Tau seems to be essential for axonal elongation and maturation, as knockdown of Tau in cultured neurons inhibits neurite formation (Caceres and Kosik, 1990), whereas overexpression of Tau promotes neurite formation (Knops et al., 1991, Biernat and Mandelkow, 1999). Besides Tau's role in regulating microtubule dynamics and neuronal polarization, it may also regulate axonal transport via different mechanisms in terms of influencing the function of motor proteins - dynein and kinesin which transport cargos toward the minus-end (toward the cell body) and plus- end of microtubules (toward the axonal terminus), respectively (Stamer et al., 2002).

1.3.2 Somatodendritic localization of Tau protein and its potential toxic effects

There is only a small amount of Tau found in dendrites but a recent study showed that the dendritic Tau may be involved in the regulation of synaptic plasticity, since pharmacological synaptic activation induces translocation of endogenous Tau from the dendritic shaft to the excitatory synapses in cultured neurons or acute hippocampal slices (Frandemiche et al., 2014). In addition, the postsynaptic Tau has been proposed to be essential for long term depression (LTD), which becomes defective in Tau knockout mice (Kimura et al., 2014, Regan et al., 2016). Finally, the dendritic Tau appears to be essential for Aβ-induced neurotoxicity (Zempel et al., 2013). The dendritic Tau could serve as a protein scaffold to deliver the kinase FYN to postsynaptic sites, where it phosphorylates the subunit 2 of the NMDA receptor (NR2B), resulting in the stabilization of the interaction of this receptor with the postsynaptic density protein 95 (PSD95), powering up glutamatergic signalling and thereby enhancing Aβ toxicity (Ittner et al., 2010). Additionally, in cell culture studies, NMDA receptor activation was shown to phosphorylate Tau in dendrites thereby regulating its interaction with the PSD95-Fyn-NMDA receptor complex with potential implications in AD (Mondragon-Rodriguez et al., 2012). These findings highlight the toxic role of Tau in the somatodendritic compartment.

1.3.3 Nuclear localization of Tau protein and its functions

In addition to its localization in the axons and somatodendritic compartment, Tau protein can also localize to the nucleus and could interact with the DNA and protect it as a response to stress (Sultan et al., 2011).

1.4 Missorting of Tau into the somatodendritic compartment and its toxic effects

Given the different subcellular functions of Tau, the impairment of the polarized distribution of Tau may thereby lead to neuronal dysfunction. In AD, the missorting of Tau into the somatodendritic compartment represented one of the earliest signs of neurodegeneration. The missorting of Tau starts as a granular staining of the soma, which precedes the formation of NFTs and the loss of synapses (Braak et al., 1994). The mis-located dendritic Tau may cause neurotoxicity due to its toxic gain-of-function. For example, in cultured primary neurons, overexpression of Tau causes the missorting of Tau into the dendrites, where it binds to microtubules, leading to inhibition of vesicle and mitochondrial transport, loss of ATP and eventually loss of spines. These defects can be rescued by expressing the kinase MARK2 which detaches Tau from microtubules via its phosphorylation (Thies and Mandelkow, 2007). In addition, Aβ or other stressors may induce missorting of Tau in cultured neurons. In these cases, the missorted dendritic Tau may mediate toxicity by promoting the translocation of tubulin tyrosine ligase-like enzyme 6 (TTLL6) into dendrites, followed by polyglutamylation of microtubules, recruitment of spastin to microtubules and severing of microtubules by spastin (Zempel et al., 2013). Notably, the missorting of hyperphosphorylated Tau into the dendrites and spines may induce cognitive deficits even in the absence of signs of neurodegeneration. This may be because hyperphosphorylated Tau enters spines possibly through an actin-based process, resulting in synaptic dysfunction by preventing the synaptic recruitment of AMPA and NMDA receptors (Hoover et al., 2010).

1.5 Proposed mechanisms underlying sorting and missorting of Tau

Given the impact of the distribution of Tau on its physiological and pathological functions, it is of interest to study the mechanisms underlying sorting and missorting

of Tau. Some hypotheses to explain the polarized distribution of Tau are in the following chapter –

1.5.1 Preferential distribution and translation of Tau mRNA in axons

The localization of Tau mRNA to the cell body and the proximal region of axons (Litman et al., 1993) might play a role in the axonal localization of Tau protein although this is a matter of debate. Indeed, the cis-acting sequences at the 3' UTR of Tau mRNA act as a zip code in its targeting to the axons (Aronov et al., 2001) and also play an essential role in its stabilization. In addition to the 3' UTR, the 5' UTR of Tau mRNA is also involved in the regulation of its translation in axons (Morita and Sobue, 2009). Aside from its localization in axons, Tau mRNA has also been identified in the proximal region of dendrites (Kosik et al., 1989), although no clear evidence exists. Therefore, the localization and translation of Tau mRNA in dendrites remains to be elucidated in detail.

1.5.2 The retrograde diffusion barrier of Tau

Recently, the polarized distribution of Tau has been attributed to the existence of a novel retrograde diffusion barrier at the axon initial segment. This barrier allows the anterograde flow of Tau into the axons, while preventing the retrograde flow back of the axonal Tau into the somatodendritic compartment, leading to the axonal retention of Tau (Li et al., 2011).

1.5.3 Axonal transport of Tau

The fast transport of Tau protein into the axons after its synthesis in the somatodendritic compartment has been proposed to explain the varying pattern of the localization of Tau protein in axons and its mRNA in the soma (Kosik et al., 1989). However, the evidence that Tau undergoes fast axonal transport is still missing. Instead, the slow axonal co-transport of Tau with tubulin into the axon (Tytell et al., 1984) and/or the piggy backing of Tau on tubulin fragments (Konzack et al., 2007) may contribute to the axonal localization of Tau. Indeed, active transport could contribute to the distribution of Tau over longer distances.

1.5.4 Higher affinity of Tau to microtubules in axons than in dendrites

Another factor which might contribute to the polarized distribution of Tau is the differential affinity of Tau to microtubules in axons versus dendrites. The process of extraction of soluble proteins before fixing them revealed a tighter binding of Tau to the microtubules in axons than in dendrites (Kanai and Hirokawa, 1995).

1.5.5 Differential degradation of Tau protein in axonal and somatodendritic compartments

Finally, it has been speculated that the clearance of Tau is different in the somatodendritic compartment compared to the axons and thus may lead to the polarized distribution of Tau in neurons. This hypothesis is based on a single observation: when biotinylated Tau is injected into cultured neurons, it distributes across all compartments of the neuron for 24hrs. Afterwards the amount of Tau in the somatodendritic compartment (but not in axons) is gradually reduced and finally disappeared completely while Tau in the axons stays (Hirokawa et al., 1996). It has never been tested whether the disappearance of Tau in the somatodendritic compartment is indeed due to the clearance of Tau by the protein degradation systems.

1.5.6 Mechanisms of Tau sorting

As described above, the polarized distribution of Tau in neurons has been proposed to be regulated at both the mRNA and protein level via several mechanisms, however, the involvement of each mechanism in the sorting of Tau remains unclear. Since we and other groups recently showed that the protein degradation systems – autophagy and proteasome play an important role in preventing Tau aggregation and neurodegeneration (Wang et al., 2009, Kruger et al., 2012, Han et al., 2014), we wanted to understand whether the protein degradation systems indeed are involved in the sorting of Tau.

1.5.6.1 The ubiquitin-proteasome system (UPS)

The UPS plays an important role in the extra-lysosomal degradation of proteins in the cytosol, nucleus, endoplasmic reticulum and the cytoskeleton (Coux et al., 1996).

The UPS degrades target proteins earmarked with another small protein, ubiquitin, which is then directed towards the 26S proteasome for degradation.

The 26S proteasome complex

The 26S proteasome is an ATP-dependent protease complex of over 2.5 megadaltons composed of three major subunits – a 20S catalytic core, which has the proteolytic activities and two 19S regulatory subunits on either end of the 20S catalytic core. The two ATPase containing 19S regulatory subunits unfold the substrate and translocate it to the 20S subunit (Wong and Cuervo, 2010) where it is then degraded.

The ubiquitin conjugation pathway

Ubiquitin is an 8.5kDa protein composed of 76 residues with seven lysine residues. Ubiquitin and ubiquitin-like proteins (Ubls) are produced as inactive precursor moieties which are processed by the deubiquitinating enzymes (DUBs) or the ULPs (Ubl specific proteases) to expose their glycine carboxylate residue. The processed ubiquitin is then activated by the ubiquitin-activating enzyme, E1, transferred to the ubiquitin-conjugating enzyme, E2 and finally conjugated to the lysine of the substrate with the help of the ubiquitin ligase, E3 (Kerscher et al., 2006) **(Fig. 1.4).**

Small molecules that can suppress the activity of the proteasome system include epoxomicin, lactacystin, MG132, etc. Due to the non-specific effects of MG132 (Braun et al., 2005), epoxomicin and lactacystin have been used in our study. On the other hand, well known activators of the proteasome include RNA aptamers (single stranded nucleic acids capable of repressing the enzymatic activity of proteins they bind to) (Lee et al., 2015) and a pharmacological stimulator, rolipram (Myeku et al., 2016) which is one of the best chemical activators of the proteasome.

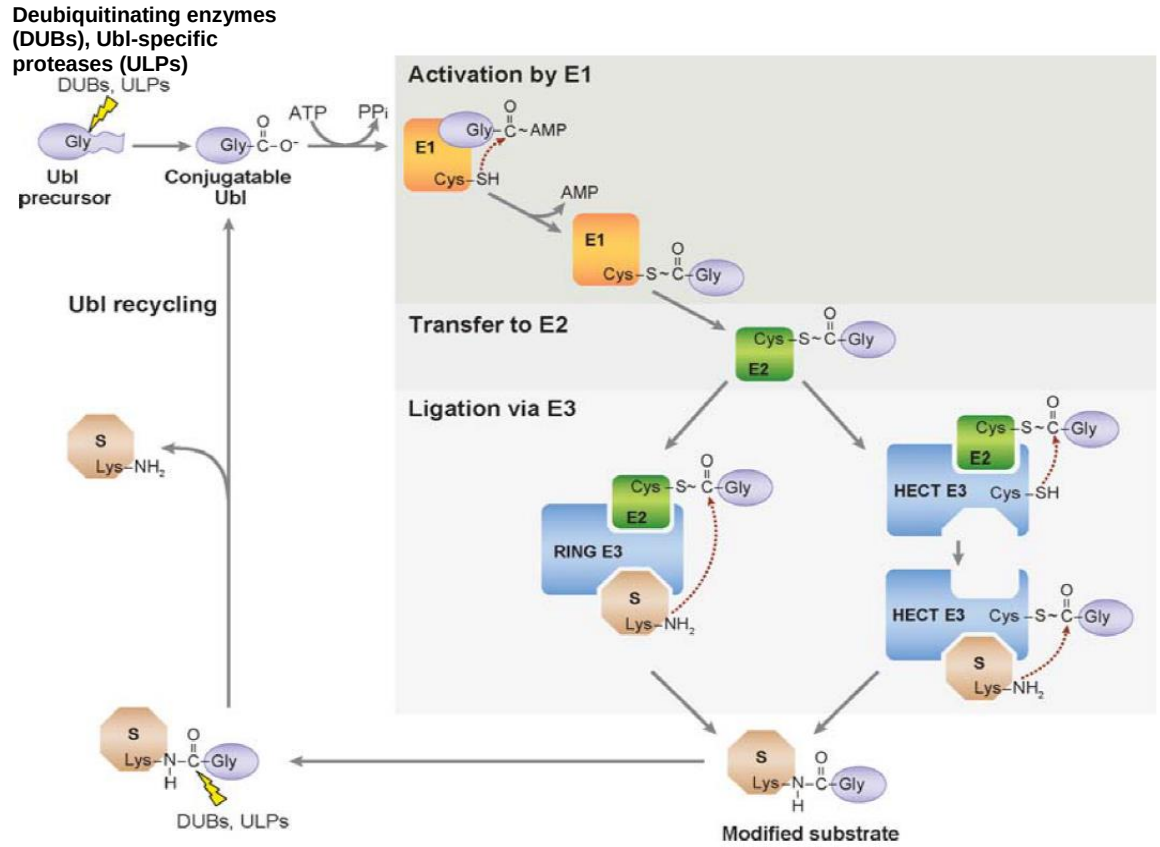

Fig. 1.4: The ubiquitin conjugation pathway. The processed Ubl is activated by E1 (Orange box) transferred to E2 (green box) and ligated to substrate via E3 (Blue boxes) enzymes. After the ligation step, the DUBs and ULPs act to remove the ubiquitin from the substrates for Ubl recycling [Figure reproduced from (Kerscher et al., 2006)].

1.5.6.2 Autophagy

Another important protein degradation pathway, autophagy, is involved in the removal of damaged organelles, protein aggregates, etc using lysosomes as a powerful tool. Autophagy can be classified into three main types based on the site of cargo sequestration such as microautophagy, macroautophagy and chaperone-mediated autophagy (Klionsky, 2013).

In microautophagy, the lysosomal membrane invaginates engulfing the cytoplasmic contents (Marzella et al., 1981) whereas in chaperone-mediated autophagy (CMA), the proteins are targeted to the lysosomes for degradation (Cuervo and Wong, 2014). Although the involvement of microautophagy in Tau degradation has not been reported the role of CMA in Tau degradation has been widely studied (Wang et al., 2009).

Macroautophagy

Macroautophagy (hereafter referred to as 'autophagy') involves the engulfment of the contents of the cytoplasm into double or multi-membraned vesicles which are targeted to the lysosomes for degradation. Hence macroautophagy is considered to be a 'non-selective' form of autophagy (Yang and Klionsky, 2010) involving autophagosome formation through four main steps – vesicle nucleation or phagophore formation, vesicle elongation, docking and fusion, breakdown and degradation **(Fig 1.5).**

In mammals, autophagy is stimulated by the deprivation of insulin or nutrients which inhibit the mammalian target of rapamycin (mTOR) which in turn inhibits UNC51-like kinase - ULK1 thereby activating the class III PI3Kinase, which encompasses the vacuolar protein sorting protein (Vps34). The Vps34 phosphorylates phosphatidylinositol to phosphatidylinositol 3-phosphate (PI3P) which is involved in membrane trafficking. The PI3P generated by the Vps34 activity interacts with the PI3P effectors – WIPI1 and WIPI2 (Nixon, 2013) followed by the elongation of the isolation membrane by the two conjugation systems - autophagy related protein 12 (Atg12) and autophagy related protein 8 (Atg8) conjugation systems. Although not well characterized, autophagolysosomal fusion in mammals involves the lysosomal membrane binding protein LAMP2 and GTP binding protein Rab7. Finally, the cathepsins B,D and L are involved in the degradation of the autophagosomal content (Levine and Kroemer, 2008).

Under physiological conditions, autophagy is induced by amino acid deprivation. Other important activators of autophagy include rapamycin, a lipophilic antibiotic and trehalose, a disaccharide (Rubinsztein et al., 2007, Sarkar et al., 2007).

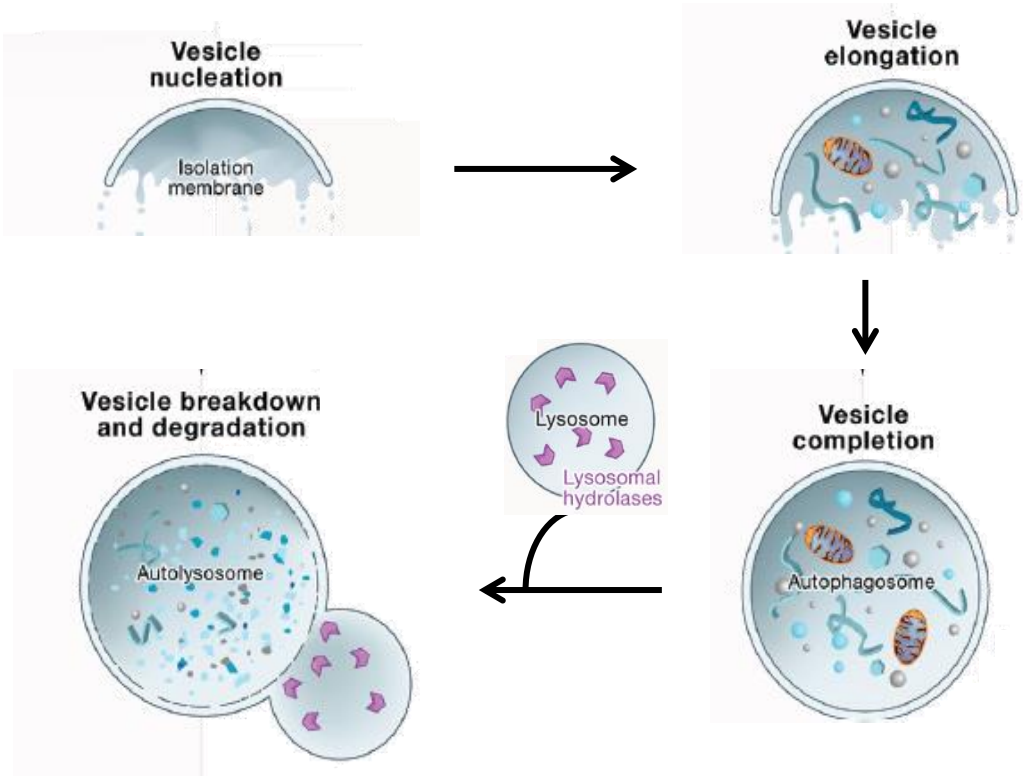

Fig. 1.5: Cellular events of macroautophagy. The formation of autophagosomes in macroautophagy involves four main steps – vesicle nucleation, elongation, completion, breakdown and degradation. The fusion of lysosomes with autophagosomes results in the formation of autolysosomes where the engulfed material is degraded. While the PI3kinases are involved in the initial steps of macroautophagy, the Atg proteins are mainly involved in the vesicle elongation. The LAMP, Rab and the SNARE proteins are involved in the docking and fusion steps [Figure adapted from (Levine and Kroemer, 2008)].

The class I PI3kinases inhibit autophagy whereas the class III PI3kinases activate autophagy by promoting the formation of autophagosomes. The early stage inhibitors of autophagy such as 3-methyladenine (3MA), wortmannin and LY294002 inhibit both the class I and class III PI3 kinases (Rubinsztein et al., 2007). Unexpectedly, 3MA blocks class I PI3kinase persistently whereas it transiently blocks class III PI3kinase (Wu et al., 2010). Contrary to the effect of 3MA, wortmannin blocks class III PI3kinases persistently whereas its effect on class I PI3kinases is transient which makes it a more suitable inhibitor of autophagy among the others (Yang et al., 2013). Another potent inhibitor of autophagy, Bafilomycin A1, prevents the maturation of autophagosomes by preventing the fusion of autophagosomes with lysosomes (Yamamoto et al., 1998).

1.5.6.3 The degradation of Tau by the proteasome and autophagy systems

Both cell culture and in vitro studies support the proteasomal degradation of Tau. Tau protein ubiquitinated via the lysine 63 polyubiquitin chain could be directed to the 26S

proteasome and subsequently deubiquitinated and degraded (Babu et al., 2005). Moreover, the accumulation of Tau has been confirmed using proteasomal inhibitors (Hamano et al., 2009) whereas proteasomal enhancers led to Tau clearance and improved cognition (Myeku et al., 2016). In addition to the proteasomal degradation of Tau, several studies indicate the role of autophagy in degrading Tau. In a cell model of Tau aggregation, stimulating autophagy can reduce Tau aggregation; whereas, inhibiting autophagy can promote Tau aggregation (Wang et al., 2009). Stimulating autophagy also reduces the Tau level in cultured primary neurons, regardless of the phosphorylation state of Tau (Kruger et al., 2012). This indicates that stimulation of autophagy could be a potential therapeutic approach for Tauopathies.

1.5.6.4 Compromised autophagy and proteasome systems in AD

In AD, both proteasome and autophagy become compromised, which may contribute to Tau missorting and Tau aggregation. Proteasome inhibition has been well known to be involved in the pathogenesis in AD. The oligomers and aggregates of Tau (Ren et al., 2007) and the oligomers of Aß could bind to the 20S proteasome and inhibit its peptidase activity (Keck et al., 2003, Tseng et al., 2008) resulting in the accumulation of the ubiquitin conjugates of Tau and Aß. The decrease in the proteasomal activity in AD could be attributed to the increased accumulation of Tau aggregates and/or oligomers which can in turn block the entry pore of the proteasome. In addition to the impairment of the proteasome, autophagy impairment is also well known to be involved in the pathogenesis in AD. Although the induction of macroautophagy and the accumulation of immature forms of autophagic vacuoles were identified in dystrophic neurites in the neocortex of AD brain samples (Nixon et al., 2005), these findings are caused by the impairment of the late steps of autophagy, i.e. the impaired clearance of autophagosomes rather than the initial steps (Boland et al., 2008). Drugs like methylene blue are currently being tested in our lab which activate autophagy (Congdon et al., 2012) and have shown to reduce the level of pathological Tau species with improved learning and memory in a transgenic mouse model of tauopathy (Hochgrafe et al., 2015). Methylene Blue is thought to inhibit Tau aggregation and propagation in AD besides activating autophagy. So Methylene Blue can serve as a novel therapeutic strategy.

Although autophagy and proteasome could degrade Tau efficiently, potential problems exist in inhibiting the pathways in neuronal cultures to test their role in Tau sorting. For example, our previous study showed that inhibition of the proteasome or the autophagy system in primary neurons induced pronounced neurotoxicity (Kruger et al., 2012). Besides this, the inhibition of the proteasomal pathway activates autophagy (Ding et al., 2007) whereas inhibition of autophagy compromises the proteasomal system (Korolchuk et al., 2009) thereby increasing the level of proteasomal substrates. In order to avoid compensation by the two protein degradation pathways and to avoid the potential toxic effects of the compounds used, we sought to carry out our studies in neurons cultured in compartmentalized devices such as the microfluidic chambers which enable local treatments of neurons for long periods of time.

1.6 Microfluidic chambers (MFCs) - an ideal tool to enable local treatment and co-culture of neuronal populations

Microfluidic chambers allow to control, monitor and manipulate cellular microenvironments. The device is fabricated in polydimethylsiloxane (PDMS), an optically transparent material, making it suitable for sophisticated microscopic techniques. The device contains two mirror image compartments. There are four reservoirs or wells serving as loading inlets and the two wells on each side are connected by channels **(Fig. 1.6a).** The cells, when added to a well, are drawn into the connecting channels by capillary action. The two connecting channels on each side are in turn connected by 100-120 microgrooves with varying lengths. The size of the grooves is small enough to prevent the cell bodies of the neurons to pass to the other side. So the microgrooves act as ‘filters’ allowing the passage of neurites only to the other side (Taylor et al., 2005). Microfluidic chambers allow fluidic isolation of microenvironments on the somal or neuritic side by establishing a volume difference between the two compartments, with lesser volume on the side of treatment **(Fig. 1.6b)**. The hydrostatic pressure difference resulting from the fluidic isolation facilitates slow but continuous flow across microgrooves which counteracts diffusion of small molecules from the added side (e.g. neuritic side) to the other side (e.g. somal side) (Taylor et al., 2003), enabling the restriction of local treatments for more than 20 hours.

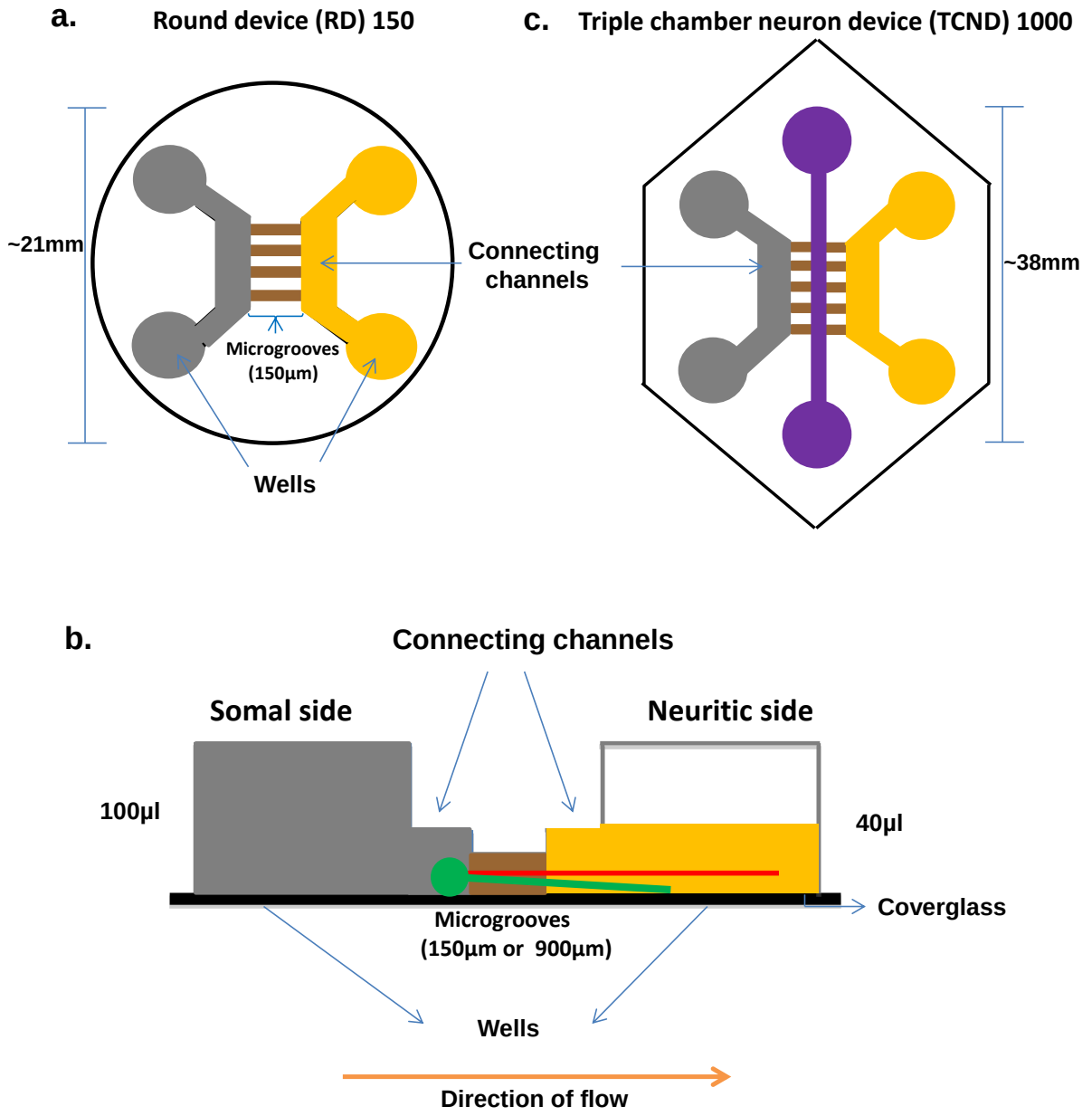

Fig. 1.6: Photographs and picture of microfluidic chambers. (a) Photograph of a microfluidic chamber (RD-Round device 150, top view) showing all the four wells with a diameter of ~6mm and a height of 4mm. The two wells on each side are connected by a channel which is 2mm wide, 7mm long and 100µm tall. The connecting channels are inturn connected by microgrooves (brown) which are 150µm long with a height of ~3µm and a width of 10µm. The representation shows the two wells on each side and their connecting channels in grey and yellow. (b) Schematic diagram of the side view of a microfluidic chamber indicating fluidic isolation. The somal side is shaded in grey and the neuritic side in yellow. Fluidic isolation is acheived by removing a small volume of medium (60 µl) from the neuritic side which can be detected by a lower liquid level on the neuritic side. Therefore the flow of liquid occurs from the somal to the neuritic side (orange arrow) (c) Photograph of a microfluidic device (TCND-triple chamber neuron device 1000, top view) showing all the six wells and their connecting channels. The wells have a diameter of ~8mm and a height of 4mm. The first (grey) and the third (yellow) connecting channels have a length of 7mm, a width of 1.5mm and a height of 0.1mm, whereas the central chamber (purple) has a width of 1mm, length of 15mm and a height of 0.1mm.. It contains two 500µm microgroove barriers (brown) which are 10µm wide with a height of 3µm [Figure adapted from http://xonamicrofluidics.com/ and from (Taylor et al., 2005)].

1.7 Spreading of Tau pathology in AD and other Tauopathies

In AD, Tau aggregates appear in a hierarchical pattern, first in the entorhinal cortex, then in the hippocampus and later to the surrounding areas. Based on this sequential appearance, AD can be classified into 6 stages - Tau pathology initiates at the entorhinal cortex (Braak stages I and II), then spreads subsequently to the hippocampus (Braak stages III and IV) and finally to the broader regions of the neocortex and hippocampus (Braak stages V and VI) (Braak and Braak, 1991). Up to date, the mechanism underlying the progression of Tau pathology remains elusive.

One hypothesis assumes that the hierarchical propagation of Tau pathology is due to the differential vulnerability of brain regions. In line with this view, in AD, the neurons prone to developing NFTs are projection neurons with long axons that are only poorly myelinated (Braak and Braak, 1996). They are intrinsically vulnerable, because (1) they have high energy requirements that may subject them to chronic oxidative stress (Yan et al., 2013); (2) their poor myelination increases their exposure to toxic environmental conditions, as myelin sheaths provide a mechanical barrier against pathogens and provide trophic support and protection against oxidative stress (Nave and Werner, 2014, Fruhbeis et al., 2013). A second hypothesis is based on the observation that neurons affected by Tau pathology are often anatomically connected (Hyman et al., 1984). Thus, Tau pathology may be due to the neuronal connectivity. The agent causing the spread of pathology e.g., stress granules, cytokines, trophic factors, etc, has also been a matter of debate. One current hypothesis holds that Tau itself spreads from cell to cell. These Tau species could act as seeds to induce the aggregation of Tau in the recipient neurons. Since this spreading pattern is similar to the propagation of prion pathology, Tau can thus be regarded as a prion-like protein **(Fig. 1.7)**. Consistent with this hypothesis, internalization of extracellular Tau aggregates induces a misfolded state of intracellular Tau (Frost et al., 2009). Additionally, formation of Tau aggregates was identified in mice injected with brain extracts from P301S mice (Clavaguera et al., 2009) or with extracts from humans who died from various Tauopathies (Clavaguera et al., 2013). The spreading of Tau followed a cell type specific pattern in AD and CBD (Boluda et al., 2015).

The advancement of NFTs from the entorhinal cortex to neurons of the trans-synaptic circuit (de Calignon et al., 2012) and the trans-synaptic spreading of Tau pathology

along anatomically connected brain regions (Liu et al., 2012) highlights the role of synapses in the spreading of Tau pathology. Preformed Tau aggregates could also spread independently of synaptic connections indicating the existence of non-synaptic mechanisms for Tau pathology spreading (Peeraer et al., 2015). Currently, there is a debate on what Tau species are transmitted between neurons. Proposed candidates are Tau oligomers or short fibrils (Guerrero-Munoz et al., 2015), although any of the Tau species might be transmitted in association with extracellular vesicles, particularly exosomes.

1.7.1 Exosomes and spreading of Tau

Exosomes are small membranous vesicles (50-150nm) (Lynch et al., 2009) formed by the endocytosis of molecules. The endosomes are either recycled to the plasma membrane or fuse with multivesicular bodies (MVBs). The subsequent fusion of the MVBs with the plasma membrane releases exosomes (Dujardin et al., 2014a). Exosomes are secreted by a wide variety of cell types including neurons (Faure et al., 2006). It has been reported that α-synuclein, prion protein and β-amyloid are present in exosomes (Fevrier et al., 2004, Kunadt et al., 2015, Rajendran et al., 2006). Exosomes isolated from the conditioned medium of cultured cell lines over-expressing Tau or CSF from AD patients may contain Tau (Saman et al., 2012, Simon et al., 2012), although this is a matter of debate. Interestingly, exosomes can be released at neuronal presynaptic terminals and taken up by postsynapses at *Drosophila* neuromuscular junctions (NMJ) (Korkut et al., 2013), and therefore qualify as carriers for trans-synaptic transmission of proteins. Thus, it would be of interest to investigate whether exosomes are involved in the trans-synaptic spreading of Tau pathology.

Microfluidic chambers have been used to study the spreading of different forms of Tau. Using neurons cultured in microfluidic devices, only low molecular weight aggregates and short fibrils of Tau were taken up and trafficked anterogradely or retrogradely (Wu et al., 2013). Another study reported the uptake and trafficking of Tau monomers and oligomers towards the axon terminals (Usenovic et al., 2015). Using three chambered microfluidic devices, the importance of synapses in the transmission of Tau aggregates (Calafate et al., 2015) as well as transsynaptic transmission of phosphorylated high molecular weight Tau species (Takeda et al., 2015) was demonstrated.

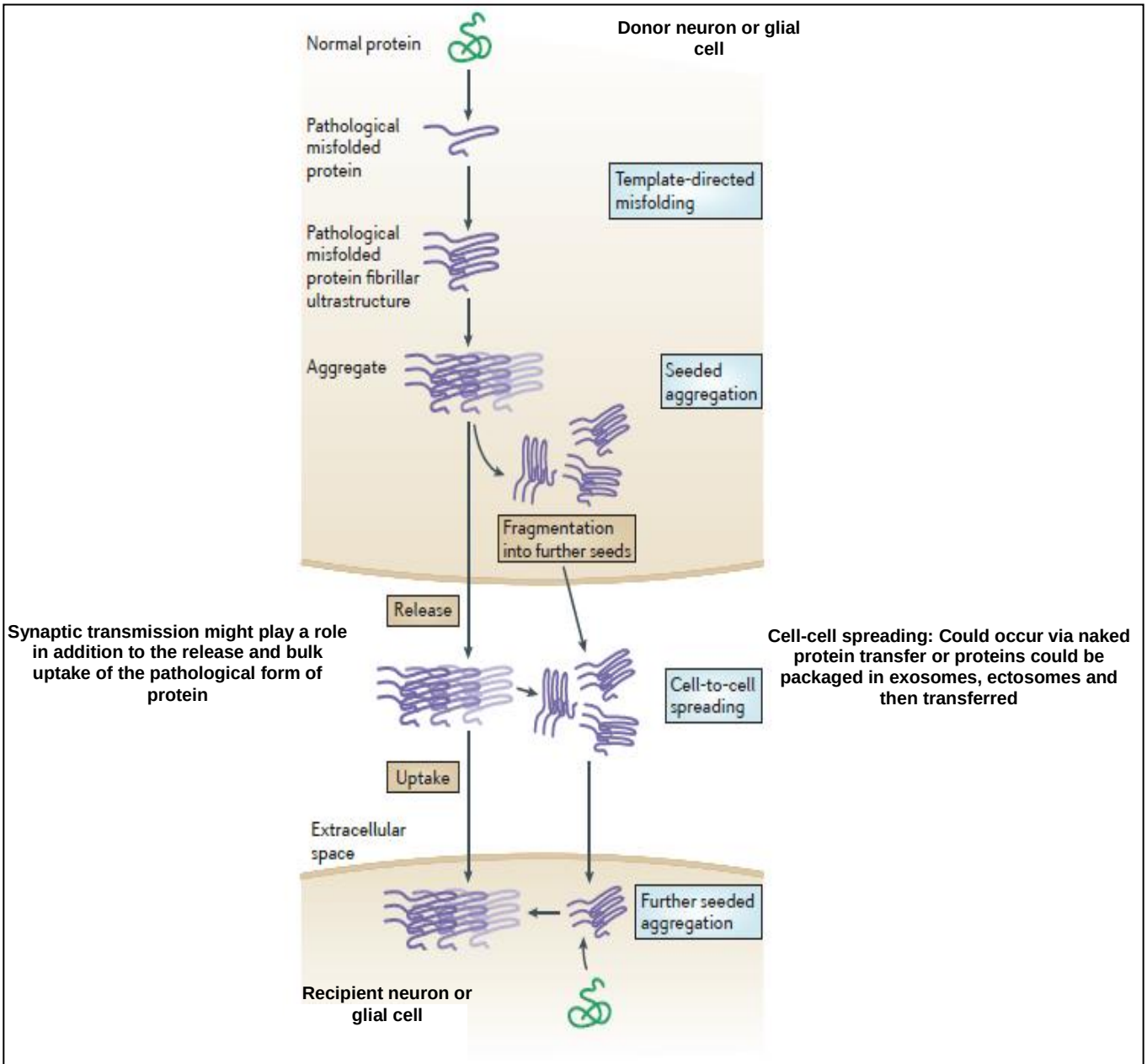

Fig. 1.7: Mechanisms involved in the prion-like protein transmission in neurodegenerative diseases. The pathological misfolded protein aggregates in the donor cell is released either in its aggregated form or fragmented into seeds which are then released. The released protein is then taken up by the recipient cell by bulk endocytosis either in its naked form or packaged in extracellular vesicles like exosomes, ectosomes, etc. The other possible mechanism of pathological protein spreading from one cell to the other is via direct synaptic transfer. The daughter seeds entering the neighboring cells might get missorted and could initiate further aggregation and spreading [Figure adapted from (Brettschneider et al., 2015)].

1.8 Aims of this study

The aims of this study were to use Microfluidic chambers (MFCs) to investigate the mechanism of Tau sorting and Tau spreading. MFCs allow one to treat neurons locally at the distal part of the dendrites or axons (Taylor et al., 2005) for prolonged periods of time. This allows one to address specific questions regarding the intracellular generation, distribution, and transcellular migration of Tau.

The following questions were investigated using MFCs:

1. The role of the protein degradation systems (proteasome, autophagy) for the clearance and missorting of Tau

2. The toxic effect of Tau accumulation in dendrites

3. The localization and translation of Tau mRNA in dendrites

4. The trans-synaptic spreading of Tau via exosomes

2 Materials and Methods

2.1 Materials

All chemicals were purchased from Calbiochem, Sigma, Affymetrix or Enzo.

2.1.1 Antibodies:

Primary antibodies:

Antibody	Company
K9JA	Dako
PHF1	Peter Davies
AT8	Pierce
12E8	Elan pharmaceuticals
ß actin	Sigma
p62 (SQSTM1)	Abnova
DA9	Peter Davies
Ubiquitin	Dako
MAP2 (Mouse)	Sigma
MAP2 (Chicken)	Millipore
SA4473	Eurogentec
YL1/2	Serotec
Flotillin	BD trans
GluR1	Chemicon
Synaptophysin	Sigma

Secondary antibodies:

All secondary antibodies – Amca, Cy2, CF488, A488, Cy3, Tritc, Cy5, CF647 and A647 were purchased from dianova.

Dyes for cell culture:

DiI	Cytoskeleton
Rhodamine Phalloidin	Molecular Probes

2.1.2 Molecular weight markers:

Protein magic marker	Fermentas
Page ruler prestained protein ladder	Fermentas

2.1.3 Kits

ECL western blotting detection kit	Amersham
ViewRNA™ ISH Cell Assay for Fluorescence RNA *In Situ* Hybridization (RNA FISH) kit	Affymetrix
BCA kit (Bicinchoninic acid kit)	Sigma
Cytotoxicity detection kit	Roche Applied Science

2.1.4 Cell culture media and reagents:

Neurobasal medium	Gibco (Life technologies)
Dulbecco's PBS	Sigma
Donor Horse serum	Sigma
NS-21	PAN-biotech
Penicillin/ Streptomycin	PAN-biotech
Pyruvate	Sigma
L-Glutamine	PAA
Trypsin-EDTA	Sigma
Hank's BSS	Sigma

Ham's F12	PAA
Fetal Bovine Serum	Millipore

2.1.5 Chemicals

The protein degradation inhibitors - Wortmannin, Bafilomycin, Epoxomicin and Lactacystin were purchased from Calbiochem. The protein synthesis inhibitors - cycloheximide and anisomycin were purchased from Sigma, Munich, Germany. Trehalose was purchased from Sigma and Rolipram was purchased from Enzo. Unless stated otherwise all the above chemicals (except trehalose) were prepared in DMSO.

2.1.6 Softwares

AIDA	Fuji
LSM700 Image processing software, ZEN	Zeiss
EndNote X7	Thomson Reuters, UK
Image J 1.49o	NIH, USA
XFluor4	Tecan

2.1.7 List of equipments:

Centrifuges & Vortex

Centrifuge 5804	Eppendorf
Mini spin – Table top centrifuge	Eppendorf
Vortex - Genie 2	Scientific industries,INC

Cell culture hood & incubators

Cell culture hood	Scanlaf
37 °C CO2 incubator	Thermo Scientific
37°C waterbath	Memmert GmbH

Microscope

LSM 700	Zeiss
Episcope/Apotome	Zeiss
Fluoview 1000	Olympus

Other equipments

37°C incubator/shaker	Biozym
Fujifilm LAS4000 camera	Fuji
TECAN plate reader	Safire

2.1.8 Buffers

10X Blotting Buffer	480mM Tris-HCl, 390mM Glycine, 50% Methanol, 1% SDS
1X SDS Running Buffer	0.025M Tris-HCl, 0.192M Glycine, 0.1% SDS
10X TBST	100mM Tris-HCl pH 7.5, 1.5M NaCl, 5%

	Tween 20
5X SDS Sample Buffer	1.25M Tris-HCl pH 6.8, Glycerol, 50% SDS, 0.25% Bromophenol Blue
2X SDS Sample Buffer	0.5M Tris-HCl pH 6.8, Glycerol, 10% SDS, 0.1% Bromophenol Blue
Lysis Buffer	50mM Tris HCl, pH 7.4, 150mM NaCl, 1mM EDTA,1mM EGTA, 1% Triton X-100

Lysis Buffer:

Tris HCl pH 7.4	50mM
Sodium chloride	150mM
EDTA	1mM
EGTA	1mM
Triton X-100	1%

For western blot sample preparation:

Stock protease solution

One tablet from Complete mini protease inhibitor cocktail (Roche diagnostics, USA) is dissolved in 2mL distilled water to prepare a 25X stock protease solution.

Working protease solution:

Reagent	Volume added
Sodium orthovanadate (2mM)	4µL

Stock protease	160µL
Okadaic acid	1µL
Glycerol – 3- phosphate (60mM)	40µL

The above mixture is diluted in 795µL lysis buffer to prepare 1000µL working solution.

2.1.9 Microfluidic chambers

Round device with 150µm microgroove barrier (RD150)	Xona microfluidics
Round device with 900µm microgroove barrier (RD900)	Xona microfluidics
Triple chamber neuron device with 1000µm microgroove barrier (TCND1000)	Xona microfluidics

2.2 Methods:

2.2.1 Preparation of primary neuronal cultures

Rat dissection and primary neuron preparation:

Cortical or hippocampal neurons were prepared from embryonic day 18 (E18) rat embryos and cultured according to Banker's protocol. The instruments for dissection were sterilized with ethanol and placed inside the laminar flow hood. Before anaesthetizing the rats, few dishes were filled with Hank's BSS (HBSS) and pre-cooled on ice. Using 2 to 3mL isofluorane (Sigma-Aldrich), the rat was anaesthesized followed by the rinsing of its abdomen with 70% ethanol, incision and removal of its uterus. The fetuses were then removed from the uterus and their heads were sectioned immediately and placed in one of the dishes with cold Hank's BSS. Under

a dissection microscope the brains were dissected out and submerged inside the HBSS in the dishes on ice. After removing the cerebral hemispheres, the cortex was cut in half and thalamus was removed completely. The tissues were then turned and the meninges were peeled off. The tissues containing both the cortex and hippocampus were then transferred into a new petridish with HBSS. Under a dissection microscope, the hippocampus from each tissue was cut gently using a small scissor. The same procedure was repeated for all of the cerebral hemispheres from all embryos.

Finally, the separated hippocampus and cortical tissues were transferred to 15 ml and 50 ml falcon tubes respectively. The HBSS is then removed and to the cortical and the hippocampal tissues were added ~5mL and ~2mL trypsin respectively and placed in 37°C water bath for 8 minutes. The trypsination reaction was stopped by adding plating medium (Neurobasal medium with supplements) or HBSS with Horse serum to each tube. When the tissue gets settled down in the tubes, the supernatant containing both trypsin and medium is removed. Subsequently, around 1mL HBSS pre-warmed at 37°C was added to each tube and the tissues were gently dissociated by pipetting them up and down. The dissociated cells were then filled with pre-warmed HBSS and ~10µL of this suspension was mixed with 10µL of trypan blue for 5 mins at room temperature to identify the number of dead cells. Next, 10µL of the trypan blue-treated cell suspension was added in a Neubauer chamber for cell counting under a bright field microscope. The number of trypan blue staining negative cells in the four grids was counted and the cell density was calculated according the formula: cell density (no./ml)= cell number/4 X 10^4 X dilution factor.

Prior to plating of neurons in 24-well or the 6-well plates, the autoclaved coverglasses were coated with poly-D-lysine dissolved in Dulbecco's PBS for 2 days in 37°C incubator. On the day of seeding of neurons, the plates were washed thrice with prewarmed Dulbecco's PBS. Once the primary neuronal cultures were prepared, the cells were seeded in the 6-well and 24-well plates with neurobasal medium (supplemented with penicillin/streptomycin, L-Glutamine, Horse serum, pyruvate and NS-21) pre-warmed in the 37°C incubator. For hippocampal neurons, 0.6 × 10^5 cells and 3 ×10^5 cells were plated in each well in 24-well plates and in 6-well plates respectively. After 4 days, the cultures were treated with 5µg/mL cytosine arabinoside (Sigma, Munich, Germany) to suppress glial growth.

2.2.2 Preparation & assembly of microfluidic chambers:

Preparation of microfluidic chambers and coverglasses

For culturing of neurons in microfluidic chambers, the coverglasses (Deckgläser round coverglasses, 25mm or Deckgläser microscopic coverglasses, 24 X 50mm) used to assemble the microfluidic chambers with, were autoclaved, and then coated with 1mg/mL poly-D-lysine dissolved in autoclaved water for 2 days in 37°C incubator. On the day of primary neuron preparation, the coverglasses were washed three times with autoclaved water to remove unbound poly-D-lysine. The coverglasses were subsequently dried inside the cell culture hood for 2 to 3hrs with the coated side facing upwards. The microfluidic chambers were sequentially washed once with 70% ethanol and once with autoclaved water and dried for 2 to 3hrs.

Just before the seeding of neurons, the dried microfluidic chambers were taken with a sterile forceps and placed gently on the coated coverglass with the feature side (side of the chamber containing the entry ports to the connecting channels and microgrooves) facing downwards. Next, the chamber is gently pressed against the coverglass with the forceps on all its regions and the assembly of the chamber with coverglass is carefully lifted up by holding the coverglass. The setup is then flipped to check if the bonding is formed without air bubbles. If the presence of any gaps is visible then the chamber is carefully removed from the coverglass and once more placed and gently pressed against the coverglass. Once the assembly is done, the setup is placed inside a 6-well plate or a dish. The same procedure is repeated for all the chambers. One of the wells of the 6-well plates is left empty but later filled with water to avoid evaporation of medium from the chambers in the other wells.

2.2.3 Seeding of neurons in microfluidic chambers:

Around 1mL of the dissociated neurons was precipitated by centrifugation at 300Xg for 5 mins. The supernatant was then removed carefully without disturbing the cell pellet, and the cell pellets were resuspended in ~ 200 – 500µL of neurobasal medium The cell density was measured again and adjusted to ~6 × 10^6 cells/ml with neurobasal medium. Then 5µL of the cell suspension was taken in a 10µL pipette and dispensed carefully with the pipette tip placed at the junction of one well and its connecting channel. The cell suspension is drawn quickly by capillary action across the connecting channel. The chamber was then incubated inside the 37°C incubator

for 5 mins for the cells to attach to the coverglass. Afterwards, cells were seeded in another well on the same side following the same procedure. After another 5mins of incubation, neurobasal medium is added to all the wells of each chamber with more medium added on the cell-seeded side so that the hydrostatic pressure difference could drive more cells into the connection channel and attach near the microgrooves. This would enable more neurons to project dendrites through the microgrooves to the neuritic side. After 4 days, the chambers were treated with 5µg/mL cytosine arabinoside (Sigma, Munich, Germany) to suppress glial growth.

In cases of neuronal co-culture, once the first order neurons cultured on one side of the microfluidic chambers have reached 14 Days in vitro (DIV), another population of neurons were seeded on the other side (called as the 'neuritic side'). The neurons were left to grow for additional 10 to 11 days.

For local treatment of neurons grown in microfluidic devices, around 60 µl of medium was removed from the side to be treated to achieve fluidic isolation (see **Fig 1.6b** in Introduction).

2.2.4 Western Blotting

Sample preparation for western blot

The neurons in 6-well plates were briefly washed with cold 1x PBS and 100µL of the lysis buffer containing protease and phosphatase inhibitors were added to each well. Subsequently, the cells were then scrapped off the wells using a cell scrapper (24x24cm, blade width 13mm) and collected in 1.5mL eppendorf tubes and kept in ice for 20 minutes to completely disassemble microtubules. If required, the tubes are centrifuged at 14,000 rpm for 20mins at 4°C. To 40µL of the supernatant, 5x sample buffer was added and heated at 95°C for 5mins. The remaining of the supernatant was used for protein estimation to ensure equal loading. The samples were then stored at -20°C refrigerator until used.

Protein estimation by bicinchoninic acid (BCA) assay

The formation of the purple-coloured product in the BCA assay involves the macromolecular structure of protein, peptide bonds and the presence of four amino acids (Cysteine, Cystine, Tryptophan, Tyrosine). The protein concentrations are determined with reference to a standard protein such as bovine serum albumin

(BSA). A set of dilutions of the standard BSA of known concentrations were prepared and measured together with the protein sample of unknown concentration in a 24-well plate.

Standard (Volume in µL)

H_2O	25	20	15	10	0
BSA (1µg/µL)	0	5	10	15	25

The BCA solution was prepared by mixing one part of copper sulfate (Sigma-Aldrich) with 50 parts of BCA (Sigma). Each well of the 24-well plate with or without protein was made upto 25µL with water and to that 200 µl of BCA reagent was added. The 24-well plate was then incubated at 37°C in dark for 30 minutes. The absorbance was then measured at 562nm using TECAN infinite M200 plate reader.

Sodium dodecyl sulfate polyacrylamide gel electrophoresis (SDS-PAGE)

SDS-PAGE (sodium dodecyl sulfate polyacrylamide gel electrophoresis) was performed to electrophoretically separate the proteins based on their molecular weight according to a modified protocol (Matsudaira and Burgess, 1978). Using SDS, the protein is first denatured and as a result of the protein's binding with SDS, it obtains a negative charge. Followed by the addition of SDS, the proteins are heated to 95°C together with DTT to enhance denaturation.

The denatured proteins are then applied to the wells of the polyacrylamide gel submerged in running buffer and an electric current is applied across the gel which results in the negatively-charged proteins to migrate depending on their size. The protein separation is performed using a discontinuous buffer system in SDS-PAGE. Early on, the proteins focus into a single sharp band in the stacking gel. A change of pH and the elimination of the ion gradient in the resolving gel enable the proteins to separate by the molecular size sieving.

A setup with glass plates oriented vertically containing 1 mm spacers in between was used for casting gels. Separating gel and stacking gel were prepared as first

described by Ornstein, 1964. The casting of the SDS-PAGE gels were done as following: First the separating gel (composition described in the table below) was poured between the assembled glass plates followed by covering with a layer of isopropanol. Once the separating gel has polymerized, the layer of isopropanol was removed and washed with water. The stacking gel (composition described in the table below) was poured over the polymerized separating gel. Immediately following this, the comb was placed in between all the gel plates.

Components	**Separating gel 10%**	**Separating gel 17%**	**Stacking gel 4%**
	mL	**mL**	**mL**
40% Acrylamide/Bis acrylamide (37.5:1)	15	25.6	5.4
1M Tris HCl, pH 8.8	22	22	-
0.25M Tris HCl, pH 6.8	-	-	27
10% SDS	0.6	0.6	0.54
TEMED	0.12	0.12	0.108
10% APS	0.065	0.065	0.15
H_2O	22	11.5	-
H_2O + Bromophenol Blue	-	-	20.9

When the stacking gel solution is polymerized, the entire gel setup was placed in the electrophoresis chamber filled with the 1x SDS running buffer. The comb was then removed and the protein sample was mixed with 5x SDS sample buffer and heated to 95°C for 5 minutes. The denatured protein samples were then loaded in the wells of

the stacking gel. The molecular weight marker and page ruler were also loaded in the other wells and electrophoresis was performed at 170 volts for 1hour.

Blotting

After electrophoresis, SDS gels were equilibrated in western blotting buffer (1x). The proteins in the gel were then transferred on to a methanol activated PVDF membrane by using electric current of 100mA for 60 minutes. Following electroblotting, the membrane was blocked in 4% milk dissolved in TBST (1x) overnight. Subsequently, the membrane was incubated with specific primary antibody (diluted in TBST) at 37°C for 1 hour or overnight at 4°C. Following incubation with the primary antibody, the membrane was washed three times with 1X TBST and incubated with a peroxidase conjugated secondary antibody (diluted in TBST) at 37°C for 1 hour. The membrane was again washed three times with 1X TBST. The ECL based detection system was used to detect the luminescent product of the secondary antibody.

Detection by Enhanced Chemiluminescence method

A mixture of solutions A and B from the ECL kit (GE-Healthcare) is prepared in a 1:1 ratio and added to the membrane and incubated in dark for 5mins. Air bubbles were removed and the membrane is developed inside the ImageQuant LAS4000 western blot developer machine (GE-Healthcare).

2.2.5 LDH assay:

The LDH measurement is a colorimetric assay for the quantification of cell death and cell lysis. This method is based on measuring the activity of Lactate dehydrogenase (LDH), a soluble cytosolic enzyme which is released as a result of the loss of membrane integrity. So the amount of released enzyme correlate with the amount lysed/dead cells and can be used as an indicator of membrane integrity. For the measurement of cytotoxicity, the Detection Kit from Roche Applied Science was used according to manufacturer's instructions.

LDH kit (Roche Applied Science, Indianapolis, IN, USA) measures the release and activity of LDH present in the culture medium in a two-step reaction. In the first step, oxidation of lactate to pyruvate results in the reduction of NAD+ to NADH and H+ catalyzed by LDH. In the second step, diaphorase acts as a catalyst to transfer the H/H+ from NADH and H+ to the tetrazolium salt INT (2-[4-iodophenyl]-3-[4-

nitrophenyl]-5-phenyltetrazolium chloride) which is reduced to formazan, a red coloured product which absorbs strongly at 490nm **(Fig 2.1)**.

Primary neurons were seeded at a density of 3×10^6 cells in microfluidic chambers. After 3 weeks the neurons were treated with the different protein degradation inhibitors on the neuritic side for 24 hours. After treatment of neurons in microfluidic chambers with the different protein degradation inhibitors, the medium from the somal and the neuritic sides were collected in eppendorf tubes separately.

The dye (composed of INT and sodium lactate) and the catalyst (Diaphorase/NAD+ mixture) from the cytotoxicity detection kit were mixed in a ratio of 45:1. Then 50µL of medium from the somal and neuritic sides of each chamber from each condition were mixed with 50µL of the above mixture in a 96 well plate and incubated at room temperature in dark for 30minutes. Then the reaction was stopped by the addition of 10µL of 1N HCl and incubated again for 1hour at 4°C. After incubation, the absorbance was measured at 490nm.

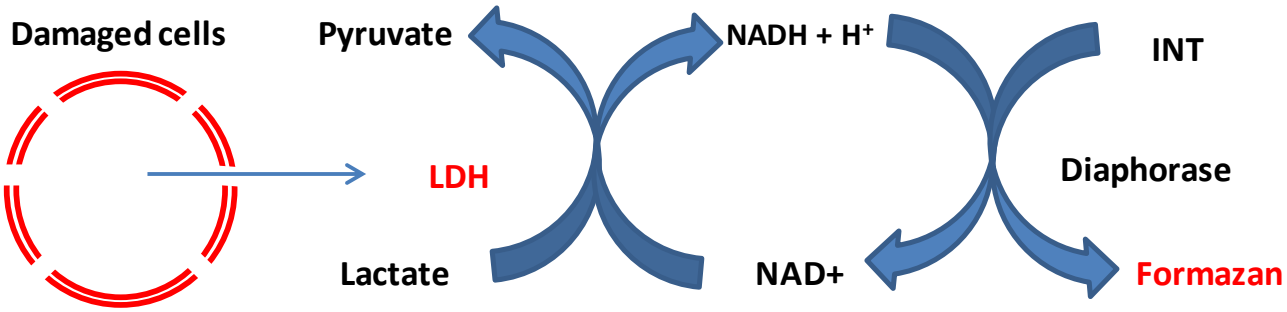

Fig. 2.1: Principle of LDH assay. The enzyme, lactate dehydrogenase (LDH) released into the medium from damaged cells catalyzes the oxidation of lactate to pyruvate and reduces NAD^+ to NADH and H^+. The enzyme diaphorase transfers the H^+ from NADH and H^+ to the tetrazolium salt (INT) which is then converted to red-coloured formazan which absorbs at 490nm (Figure adapted from www.thermofisher.com).

2.2.6 Indirect Immunofluorescence:

Indirect immunofluorescence is a two-step procedure where the cells are first labeled with target-specific, unlabeled primary antibodies which are then recognized by the addition of secondary antibodies that are conjugated with fluorophores. Since multiple secondary antibody molecules can bind to each primary antibody, this method provides signal amplification by increasing the number of fluorophore

molecules per antigen, which cannot be achieved with a direct immunofluorescence assay.

After treatment of the primary neurons in microfluidic chambers, the chambers were slowly and carefully removed from the coverglass to make sure that no damage occurs to the neurons. Once the chamber was removed, the coverglass was immediately placed in a fixing solution containing 3.7% Formaldehyde (Sigma)/4% Sucrose in PBS (pH 7.4) for 30 minutes at 37°C (Deshpande et al., 2008). The cells were then washed three times with 1XPBS, permeabilized with 0.1% triton X-100 for 10 minutes at room temperature and afterwards blocked in 5% BSA for 1hr at room temperature followed by incubation with the primary antibodies for 1hr at 37°C or overnight at 4°C. Subsequently, the cells were washed with 1X PBS for three times each for 10 minutes to remove unbound primary antibodies. After washing, the cells were incubated with secondary antibodies for 1hr at 37°C. This is followed by washing with 1X PBS for three times each for 5mins. Finally the cells were washed with distilled water once and mounted on microscopic slides using Fluoromount G mounting medium (Beckman Coulter, USA).

Primary antibody	**Dilution**
K9JA	1:1000
MAP2 (Sigma)	1:200
MAP2 (Abcam)	1:100
p62	1:500
12E8	1:1000
PHF1	1:1000
AT8	1:1500
Ubiquitin	1:50

SA4473	1:50
YL 1/2	1:1000
Flotillin	1:500
GluR1	1:100
Synaptophysin	1:500

The following secondary antibodies were used: Amca, Cy2, A488, CF488, Cy3, Tritc, Cy5 and A647. All of these fluorescently labeled secondary antibodies were used at a dilution of 1:200.

2.2.7 Fluorescence in situ hybridization

The fluorescence in situ hybridization was done using a 'ViewRNA™ ISH Cell Assay for Fluorescence RNA *In Situ*Hybridization (RNA FISH)' kit from Panomics, according to the manufacturer's protocol.

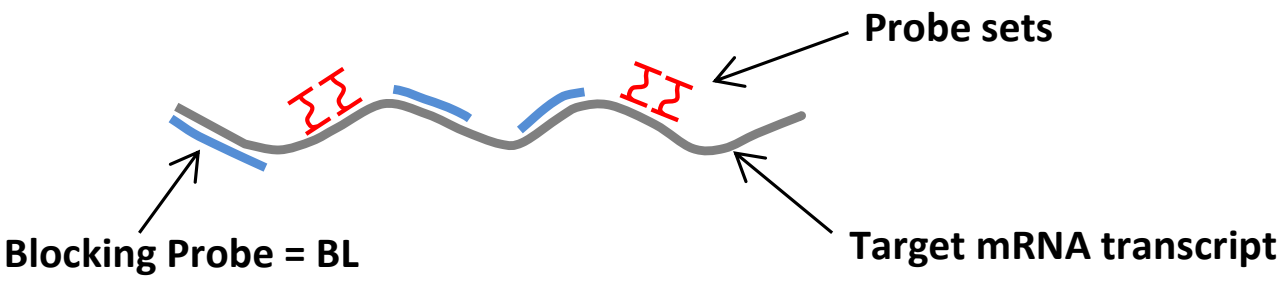

Fig. 2.2: Binding of the probe sets and the blocking probe (BL) to the target mRNA. Following fixation of neurons they are permeabilized and incubated with the probe set mix which contains the probe sets (red) and the blocking probe (BL, blue). 20 pairs of the target specific probe sets bind to the target RNA transcript building the landing platform for the branched DNA which is formed in the next steps. The naked RNA sequence inbetween the probe sets are covered by the addition of target specific blocking probes to build a chimeric DNA/RNA double strand (Figure provided by Affymetrix).

The target – rat Tau mRNA is 5159 bases long. The coding region of rat Tau mRNA is 145-1269. The probe set covers region 123-1158 of the rat Tau sense mRNA **(Fig 2.2)**. Once the probe set binds to the target mRNA, the preamplifier molecules hybridize to their respective pair of probe set oligonucleotides followed by the binding of multiple Amplifier molecules to their respective preamplifiers. Next, several label

probe oligonucleotides with the fluorescent dye hybridize to the corresponding amplifiers. Since the probe sets, pre amplifiers, amplifiers and label probe mixes are DNA oligos, the amplification of signal follow a so called 'branched DNA' pattern **(Fig 2.3)**. By this technology, an 8,000 fold amplification of signal occurs for one mRNA transcript.

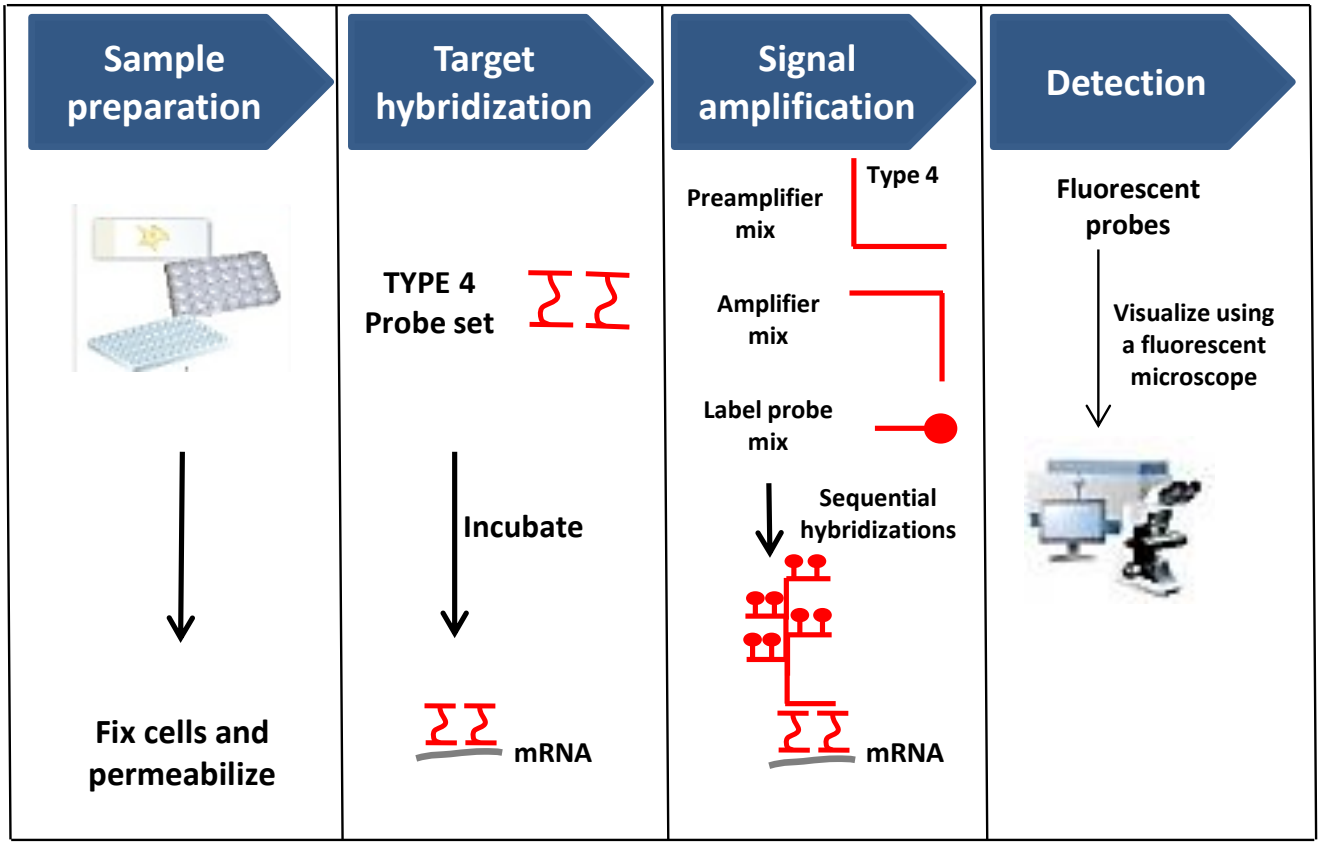

Fig. 2.3: Working schematic of the Quantigene ViewRNA ISH cell assay. The cells were first fixed and permeabilized followed by digestion with the protease to allow accessibility. Target specific probe set is then added which binds to the target RNA as described above. Signal amplification then occurs by the branched DNA technology via a sequential hybridization of the preamplifier, amplifier and the label probe mixes. A fully assembled signal "amplification" tree with all the probe sets bound to the target mRNA transcript produces a 8000 fold amplification for that transcript. Finally, the target mRNAs can be visualized with a fluorescence microscope (Figure adapted from Affymetrix 'QuantiGene ViewRNA ISH Cell Assay User Manual').

In brief, neurons were fixed with 3.7% Formaldehyde (sigma) / 4% sucrose for 30 minutes at 37 °C, then permeabilized with the detergent solution (Panomics) for 5 minutes and washed twice with PBS. Afterwards, the neurons were digested with the protease (1:10000, panomics) for 10 minutes at room temperature and washed thrice

with 1X PBS. The cells were incubated with the probe set for rat Tau mRNA diluted in pre-warmed diluent (1:100, panomics) at 40°C for 3 hours. After washing with the 'washing buffer' (panomics) thrice each for 2 minutes, neurons were incubated with pre-amplifier, Amplifier and Label probe mix in respective pre-warmed diluents (1:25, panomics) each for 30 minutes at 40°C, with washes in between for 2 minutes with washing buffer (panomics). Finally the neurons were washed in washing buffer thrice and blocked in 5% BSA for 1 hour at room temperature, followed by incubation with primary antibodies - K9JA (1:1000, DAKO) and MAP2 (1:200, Sigma) for 1 hour at 37°C. After washing with PBS thrice, the neurons were incubated for 1 hour with Cy3 labelled (1:200) and A647 labeled secondary antibodies (1:200, Dianova, USA). After secondary incubation the cells were washed thrice with PBS and the coverslips were mounted using prolong gold anti-fade reagent.

2.2.8 Methods used in studying transmission of Tau^{GFP} exosomes

Tranfections in cell culture

Transfections of N2a cells with Tau construct (human Tau tagged with GFP at the N terminus (longest isoform in CNS, 2N4R or hTau40, for short Tau^{GFP})) were performed with lipofectamine 2000 (Invitrogen) according to manufacturer´s manual. Twenty-four hours after transfection, the conditioned medium was removed followed by washing of the cells with warm PBS and split into new flasks. Cortical neurons were infected with adeno-virus expressing the same Tau construct tagged with CFP at the N-terminus (Tau^{CFP}).

Exosome purification

Exosomes were purified from conditioned medium of N2a cells or cultured cortical neurons (DIV14-21) as described previously (Thery et al., 2006). Briefly, conditioned medium was collected and centrifuged at 300 × g for 10 minutes to remove cells. The supernatant was then sequentially centrifuged at 2000 × g for 10 minutes to remove dead cells and at 10,000 × g for 30 minutes to remove cell debris. Afterwards, the supernatant was then isolated and centrifuged at 100,000 × g for 70 minutes. The pellet (exosomes + contaminating proteins) was washed with PBS to eliminate contaminated proteins and centrifuged at 100,000 × g for 70 minutes to collect

purified exosomes. The exosomes were then used for treatment of cultured primary neurons.

Treatment of exosomes in microfluidic chambers

Primary rat hippocampal neurons were co-cultured in both the connecting channels of microfluidic chambers (Xona microfluidics, USA) with 150µm and 900µm long microgrooves. When the 1st order neurons are aged DIV14, 2nd order neurons were seeded on the other connecting channel and allowed to grow until it reaches DIV4 or DIV10/11. At the time of treatment with exosomes, the 1st order neurons were at DIV18 or DIV25 and the second order neurons were at DIV4 or DIV10/11. The treatment of exosomes was done in the 1st order neurons by adding 10µL of the exosomal preparation to 40µL of medium in each well for 24hrs. For control experiments to test the possibility of exosomal release, microfluidic chambers with 150µm microgrooves with only the 1st order neurons were treated with exosomes (10µL in each well containing 40µL medium) for 24hrs. After 24hrs, the chambers were removed and cells fixed for immunofluorescence as described above.

2.2.9 Imaging techniques

Confocal imaging

The stained cells were observed with a 40x and a 63x objective on a LSM700 microscope (Zeiss, Oberkochen, Germany) using lasers, beam splitters and filters according to the fluorophores. The smart-setup of the ZEN software was used to select the different lasers for imaging different fluorescent dyes. The laser power was used at 1.0% to avoid saturation of the dyes. A Z-stack of the images was taken, which was merged using the 'maximum intensity projection' option in the ZEN software.

Time lapse imaging

Imaging in episcope was done with a 40x objective and 1x optical zoom with a AxioCam MR R3 camera and a 1X camera adapter. All imaging in episcope (Zeiss, Oberkochen, Germany) were done using a HXP lamp with appropriate filter sets and an apotome image was created using the 'apotome' option in the ZEN software and the Z stacks merged using 'orthogonal projection' of the apotome image. For time lapse imaging in microfluidic chambers, a Z stack with a thickness of around 40µM

was imaged for every 5mins for up to 20hours. The microfluidic chamber was imaged by closing it with a lid supplied with considerable amount of humidity to avoid evaporation of small amounts of the medium during imaging up to 20hours (when diffusion of the A488 dye in microfluidic chambers was tested to validate fluidic isolation). For live imaging of DiI added to neurons in microfluidic chambers, a Fluoview1000 confocal microscope (Olympus, Hamburg, Germany) with a 60X objective live-cell imaging chamber and ZDC system for Z-drift compensation was used for image acquisition. During imaging, the microfluidic chambers were kept inside the imaging chamber (37°C, 65% humidity, supplied with 5% CO_2). Live imaging was done for every half an hour for up to 3hrs.

3 Results

3.1 Localization of Tau in developing neurons

Tau is mainly an axonal protein in mature neurons, but during different stages of neuronal polarization, Tau displays a distinct distribution pattern. Although Tau is mainly sorted into the axons after seven to ten days in culture (Mandell and Banker, 1995), it is not clear when this exactly happened.

In order to confirm the localization of endogenous Tau in cultured neurons and to find the exact time point of the axonal localization of Tau, we fixed the neurons at different stages of development. In very young neurons starting from DIV1 until DIV9 **(Fig. 3.1a, i-v)**, Tau protein is ubiquitously expressed in all cellular compartments. Starting from DIV7, the staining of Tau becomes progressively weaker in the somatodendritic compartment. Axonal localization is clearly seen at DIV10, when Tau staining diminishes in the somatodendritic compartment, resulting in a striking difference of Tau staining between DIV9 and DIV10 **(Fig. 3.1a, compare v & vi and quantification in Fig. 3.1b)**. At more mature ages (DIV14 - DIV21), Tau localization is mainly found in the axons with only basal levels in the somatodendritic compartment **(Fig. 3.1a, vii, viii and quantification in Fig. 3.1b)**. This is consistent with early findings (Mandell and Banker, 1995).

Fig. 3.1. a. Localization of Tau in developing neurons

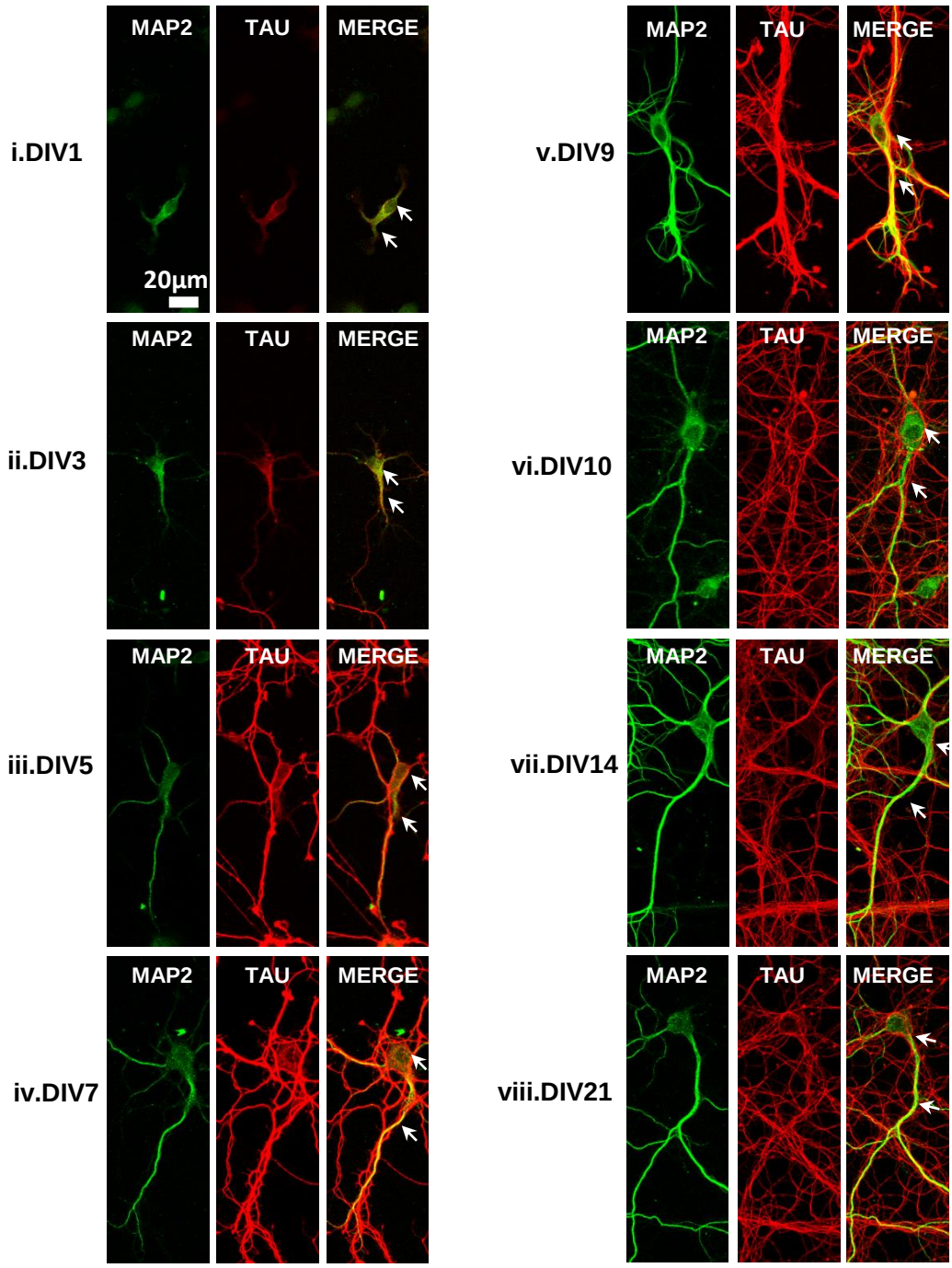

(a, i-viii) Rat hippocampal neurons (DIV 1-21) cultured in 24-well coverglasses were fixed and stained at different ages. Each panel represents a double immunostaining for MAP2 (green) and Tau (red). (i-v) Tau is distributed abundantly in soma and the processes of all neurons from DIV1-DIV9 as indicated by arrows in the merged panels. MAP2 in contrast is absent from axons as early as DIV3 (ii). (vi-viii) At DIV10, Tau immunoreactivity disappears from the somatodendritic compartment and Tau is sorted mainly to the axons. At DIV14 and DIV21, a more stringent axonal localization is observed (indicated by arrows). Scale bar = 20µm.

Fig 3.1. b. Quantification of neurons at different ages with Tau missorting

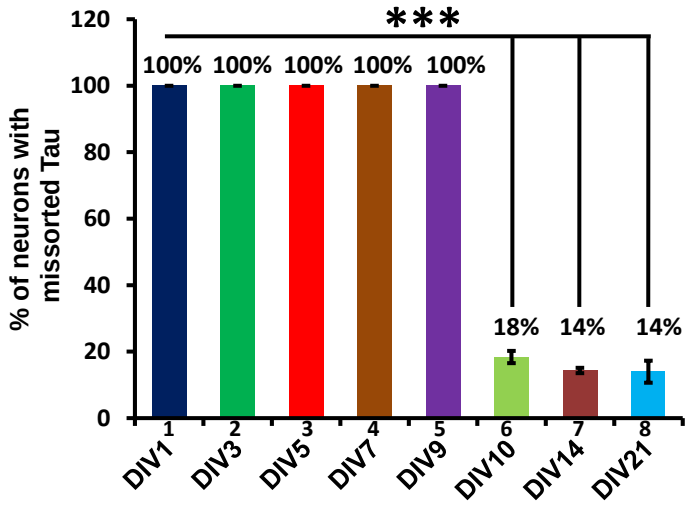

(b) Quantification of neurons at different ages with Tau missorting reveals 100% of neurons from DIV1-DIV9 (bars 1-5) showing Tau localization across all compartments. Whereas from DIV10 onwards, an axonal sorting of Tau is observed (bars 6-8). Error bars, SEM from *n* = 65-130 neurons from 3 independent cultures in each stage. ***$p < 0.005$ using Student's *t* test.

3.2 The role of protein degradation systems in the sorting of Tau

How the ubiquitous distribution of Tau in young neurons is shifted to the mainly axonal distribution in mature neurons is not clear. As Tau is a substrate of both the proteasome and autophagy, we tested whether one or both of them is indeed involved in the sorting of Tau.

3.2.1 Investigation of the sorting mechanism of Tau in microfluidic chambers

To investigate the role of the degradation systems in the sorting of Tau, we examined whether suppression of the activity of the proteasome or autophagy by inhibitors would increase the dendritic Tau level leading to the missorting of Tau. Our previous study had shown that inhibition of either the proteasome or autophagy in primary neurons for a time longer than 6hrs induced pronounced neurotoxicity, while a shorter time less than 6hrs did not affect Tau level at all (probably due to the long half-life of Tau) or even reduced the level of Tau due to the compensatory activation of the proteasome (Kruger et al., 2012). Thus, in order to test the role of the protein degradation systems in the sorting of Tau, we wanted to treat primary neurons for a long time without inducing pronounced neurotoxicity and compensation. We took advantage of microfluidic devices, which allow neuronal cell bodies to grow on one side (somal side) while neurites grow through the microgrooves to the other side

(neuritic side) **(Fig. 3.2)**. We chose to use microfluidic devices with short microgrooves (150µm), which allow some dendrites to grow to the neuritic side. We focused on dendrites growing to the neuritic side which were treated with the proteasome or autophagy inhibitors.

Fig. 3.2: Schematic representation of a microfluidic chamber showing separation of neurites from soma

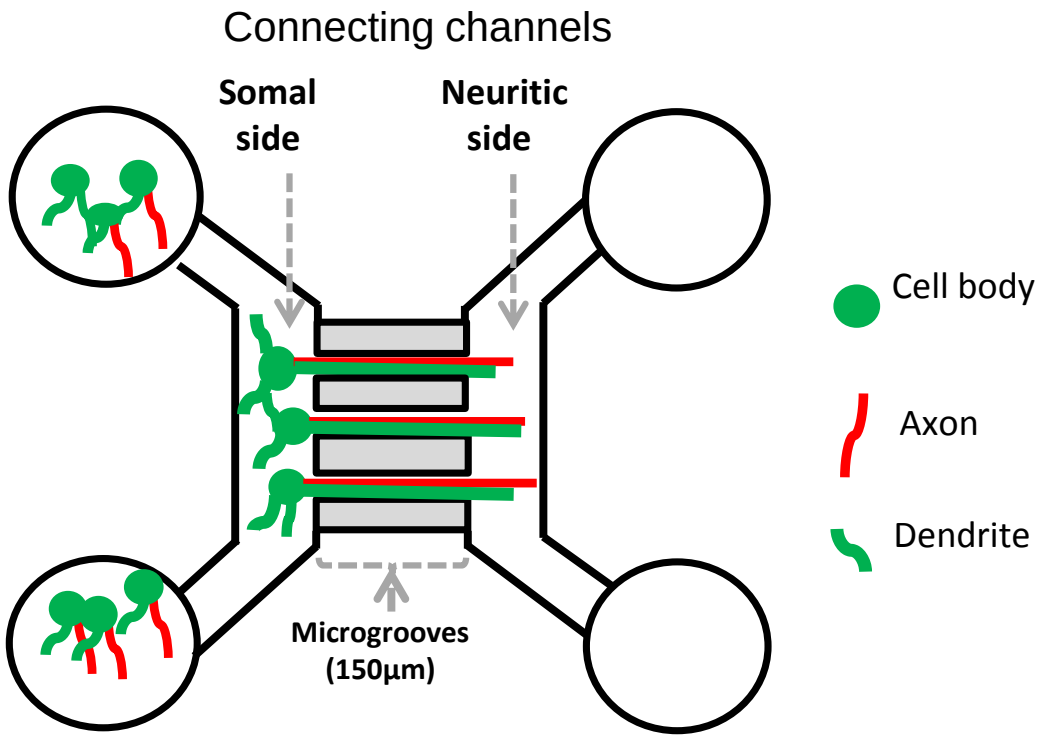

Microfluidic chamber showing the somal and neuritic sides (connecting channels) connected by microgrooves which have a length of 150µm and a width of 10 µm. The somal side contains cell bodies, dendrites (green) and axons (red). The neuritic side contains only axons and dendrites. The microgrooves do not allow the entry of the cell bodies so that only the neurites can pass through from the somal to the neuritic side.

3.2.2 Validation of the microfluidic chamber system for local treatment of compounds

Although some recent studies showed that the application of fluidic isolation in microfluidic chambers can sustain the local treatments for over 20 hours (Taylor et al., 2005), we tested the fluidic integrity of the microfluidic chamber system by applying Alexa 488 IgG (Wu et al., 2013) on either the neuritic or the somal side for 24 hours. While strong fluorescence signals were detected on the somal side (Upper panel) or on the neuritic side (Lower panel), no trace of Alexa 488 IgG was found on

the opposite side which was not treated **(Fig. 3.3a)**. This result demonstrated that fluidic isolation was intact for over 24 hours in our culture system.

We further validated the fluidic integrity using A488 fluorescent dye (0.1mM, 0.7kDa) to ensure that our inhibitors that were small in size (<1kDa) would not diffuse to the opposite side. After applying fluidic isolation in a microfluidic chamber (with 150µm long microgroove) without cells, the A488 dye was added to the side of lesser volume and imaged live for over 20hrs. Representative images at different time points starting from less than 5min up to 20hrs are shown **(Fig. 3.3b)**. There was no leakage of the dye either in the microgrooves or to the other side of the chamber even after 20hrs. This proved that fluidic isolation was intact for long time periods, which enabled us to carry out experiments.

Fig. 3.3. a. Fluidic isolation in microfluidic chambers is intact even after 24 hours

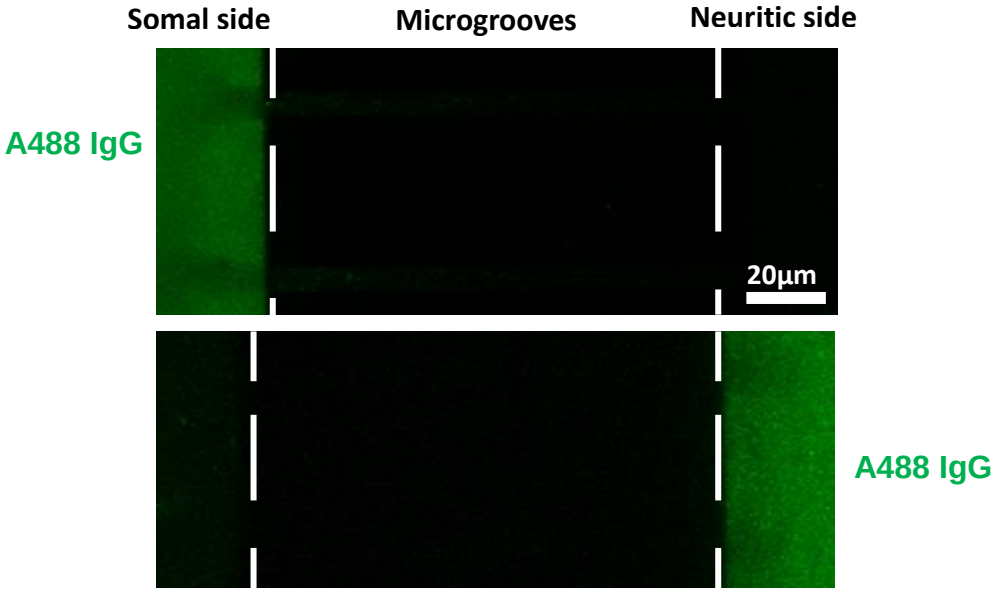

(a) After achieving fluidic isolation, Alexa-488 labelled IgG (green) was added either to the somal side (upper panel) or to the neuritic side (lower panel) for 24 hours. In this case fluidic isolation was achieved by maintaining a volume difference of around 60 µL between the somal and neuritic sides. Note that strong fluorescent signals were detected on the antibody-treated side, while no fluorescence is visible on the opposite side even after 24hrs. Scale bar = 20µm.

Fig. 3.3. b. Fluidic isolation in microfluidic chambers is intact even after 20 hours

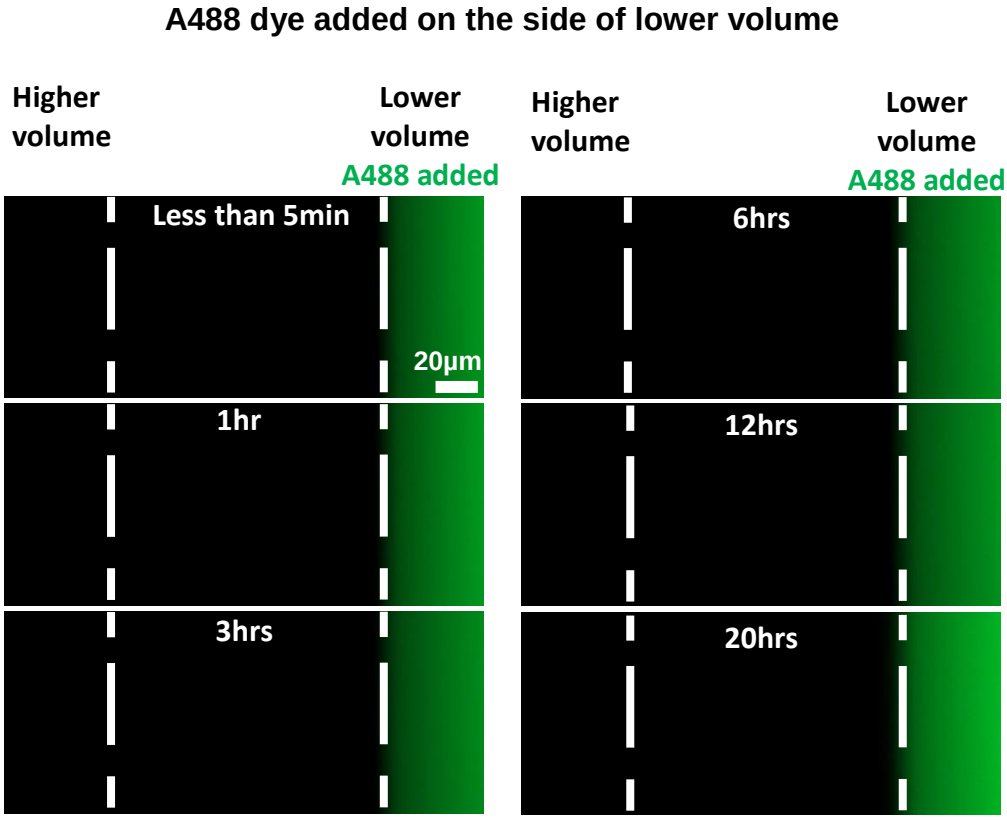

(b) Time lapse imaging of a microfluidic chamber (without cells) where the dye A488dye (0.1mM) was added on the side of lower volume as indicated. Images represent different time points starting from less than 5 min up to 20hrs. Note that there is no fluorescence of the A488 dye in the microgrooves and on the opposite side, indicating that there is no diffusion of the A488 dye to the opposite side. This validates the integrity of fluidic isolation in microfluidic chambers. Scale bar = 20µm.

3.2.3 The degradation inhibitors suppress protein degradation and are non-toxic to neurons cultured in microfluidic devices

We first tested the efficacy of the protein degradation inhibitors to be used in our experiments. Wortmannin (Harold et al., 2007) and bafilomycin (Rubinsztein et al., 2009) have been used classically for the inhibition of autophagy. Likewise epoxomicin and lactacystin (Yew et al., 2005) have been used for the inhibition of the proteasome. We measured the efficacy of these inhibitors by monitoring the amount of the autophagy substrate - p62 (Itakura and Mizushima, 2011) or the proteasomal substrates - ubiquitinated proteins (Myeku et al., 2016) via western blotting. An increase in the level of p62 was found in neuronal cultures treated with the autophagy inhibitors (bafilomycin or wortmannin) **(Fig. 3.4a).** A similar increase of

ubiquitinated proteins was found after treatment with the proteasome inhibitors (lactacystin or epoxomicin) **(Fig. 3.4b)**. This result shows that the protein degradation inhibitors used were active.

Next, we wanted to measure the toxicity of the different protein degradation inhibitors used in our study. In order to suppress the protein degradation systems, we treated neurons on the neuritic side of the microfluidic devices with either the autophagy inhibitors - wortmannin or bafilomycin or with the proteasomal inhibitors - epoxomicin or lactacystin for 24 hours. We then assessed the potential neurotoxicity induced by these treatments using the LDH release assay. As expected, the local application of these inhibitors on the neuritic side did not cause cytotoxicity on the somal or on the neuritic side**,** as the control and the treated neurons showed similar level of LDH release at both the somal and neuritic sides respectively **(Fig. 3.4c)**. This is in contrast to the dramatic cell death induced by overall treatment of primary neurons with degradation inhibitors as has been previously reported by us (Kruger et al., 2012). Notably, much higher LDH release was detected in the somal side than the neuritic side. This might be because the somal side contains cell bodies and also much more dendrites and axons than the neuritic side. This result shows that the protein degradation inhibitors used were non-toxic when applied locally.

Fig. 3.4: The protein degradation inhibitors used were active

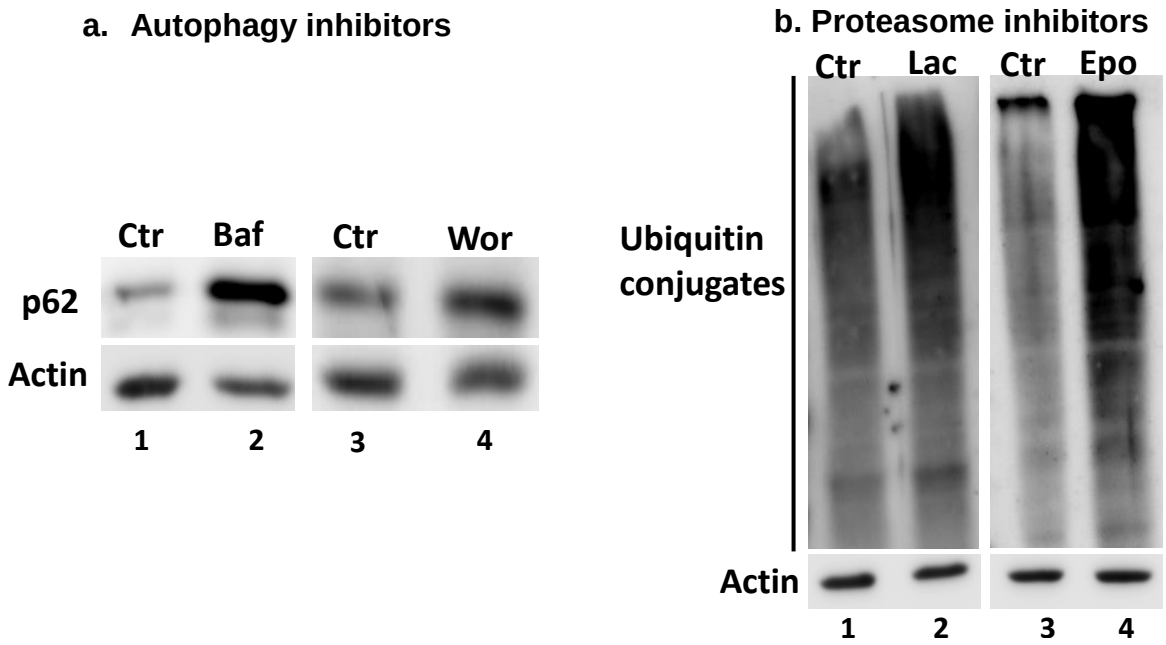

Rat hippocampal neurons (DIV 21 – 25) were treated with the different autophagy or proteasomal inhibitors - Wortmannin (inhibits autophagy, 1 µM, 24hrs), Bafilomycin (inhibits autophagy, 0.2µM, 24hrs), Epoxomicin (inhibits the proteasome, 0.2 µM, 24hrs), Lactacystin (inhibits the proteasome, 0.5 µM 24hrs). The samples were collected and western blots were carried out using the antibodies for the autophagy and proteasome substrates – p62 and ubiquitinated substrates respectively.
(a) Treatment with the autophagy inhibitors - bafilomycin (compare lanes 1 and 2) or wortmannin (compare lanes 3 and 4) lead to an increase in the autophagy substrate - p62.
(b) Treatment with the proteasomal inhibitors - lactacystin (compare lanes 1 and 2) or epoxomicin (compare lanes 3 and 4) lead to an increased level of ubiquitin conjugates.

Fig 3.4. c. Local treatment with the protein degradation inhibitors does not induce toxicity

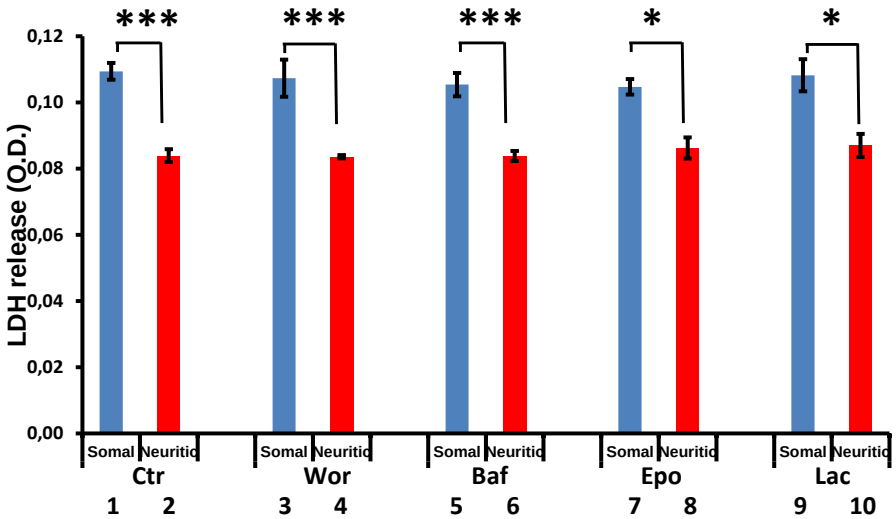

Neurons were treated with the autophagy (bars 3 – 6) or proteasomal (bars 7 – 10) inhibitors on the neuritic side for 24h. The medium from the somal and neuritic sides were collected for LDH release assay.
(c) Cytotoxicity measured with LDH release assay. Protein degradation inhibitors applied only on the neuritic side did not result in a significant increase in LDH release either on the neuritic side [compare red bars of DMSO (Ctr, bar 2) vs inhibitor treated cultures (bars 4, 6, 8 & 10)] or on the somal side [compare blue bars of DMSO (Ctr, bar 1) vs inhibitor treated cultures (bars 3, 5, 7 & 9)]. Error bars, SEM from n = 4-8 chambers in each condition. *$p < 0.05$, ***$p < 0.005$ using Student's t test.

3.2.4 Inhibition of the autophagy system in dendrites induces Tau missorting

In order to test the role of the protein degradation system - autophagy on the missorting of Tau, we treated neurons on the neuritic side of the microfluidic devices with the autophagy inhibitors – wortmannin or bafilomycin for 24 hours and then checked the Tau distribution. Axons and dendrites were monitored with Tau antibody - K9JA and with an antibody against the dendritic marker - MAP2 respectively. Compared to the control neurons treated with vehicle (DMSO) **(Fig. 3.5a)** which showed ~16% (16.7±3.11%) Tau missorting, wortmannin **(Fig. 3.5b,** 75.6±6.72%**)** and bafilomycin **(Fig. 3.5c,** 56.1±5.28%**)** treated cultures showed a significantly higher percentage (~50-80%) of dendrites with Tau accumulation on the neuritic side **(quantification in Fig. 3.7a).** This result indicates that the disappearance of Tau from dendrites during differentiation is caused by autophagic degradation.

Fig 3.5: The protein degradation inhibition by autophagy lead to Tau missorting

a. Vehicle ctr (DMSO, <0.1%)

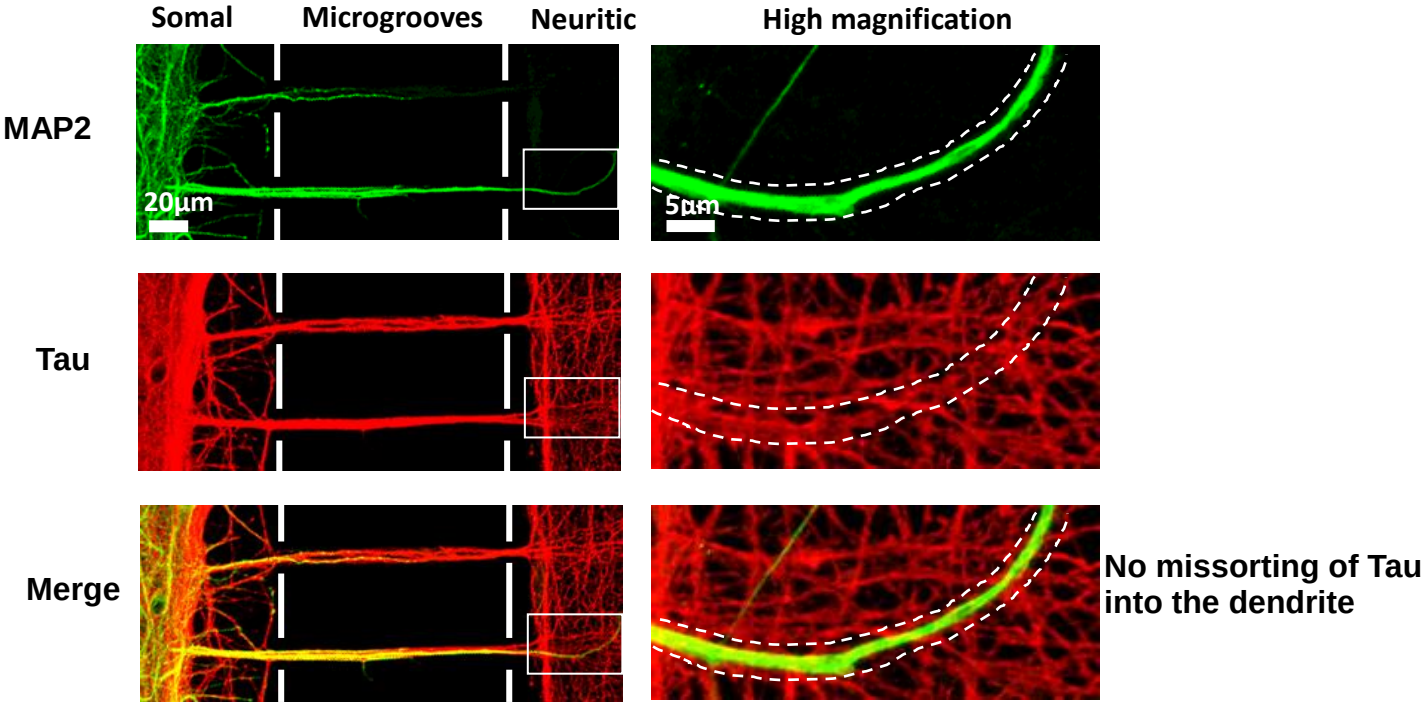

Rat hippocampal neurons (DIV 21-25) cultured in microfluidic devices were treated on the neuritic side for 24h with DMSO (control, a). The dendrites were stained with MAP2 antibody (green) and total Tau with K9JA antibody (red). Magnified images of the insets are shown on the right with a pair of eye-guiding dotted lines to highlight a dendrite with or without Tau.
(a) In the vehicle-treated control (DMSO, <0.1%), Tau is predominantly localized to the axons [see merged images at the bottom in (a)]. Only a small fraction of dendrites colocalizes with Tau. Scale bars in the main images = 20µm, in insets = 5µm.

Fig 3.5: The protein degradation inhibition by autophagy lead to Tau missorting

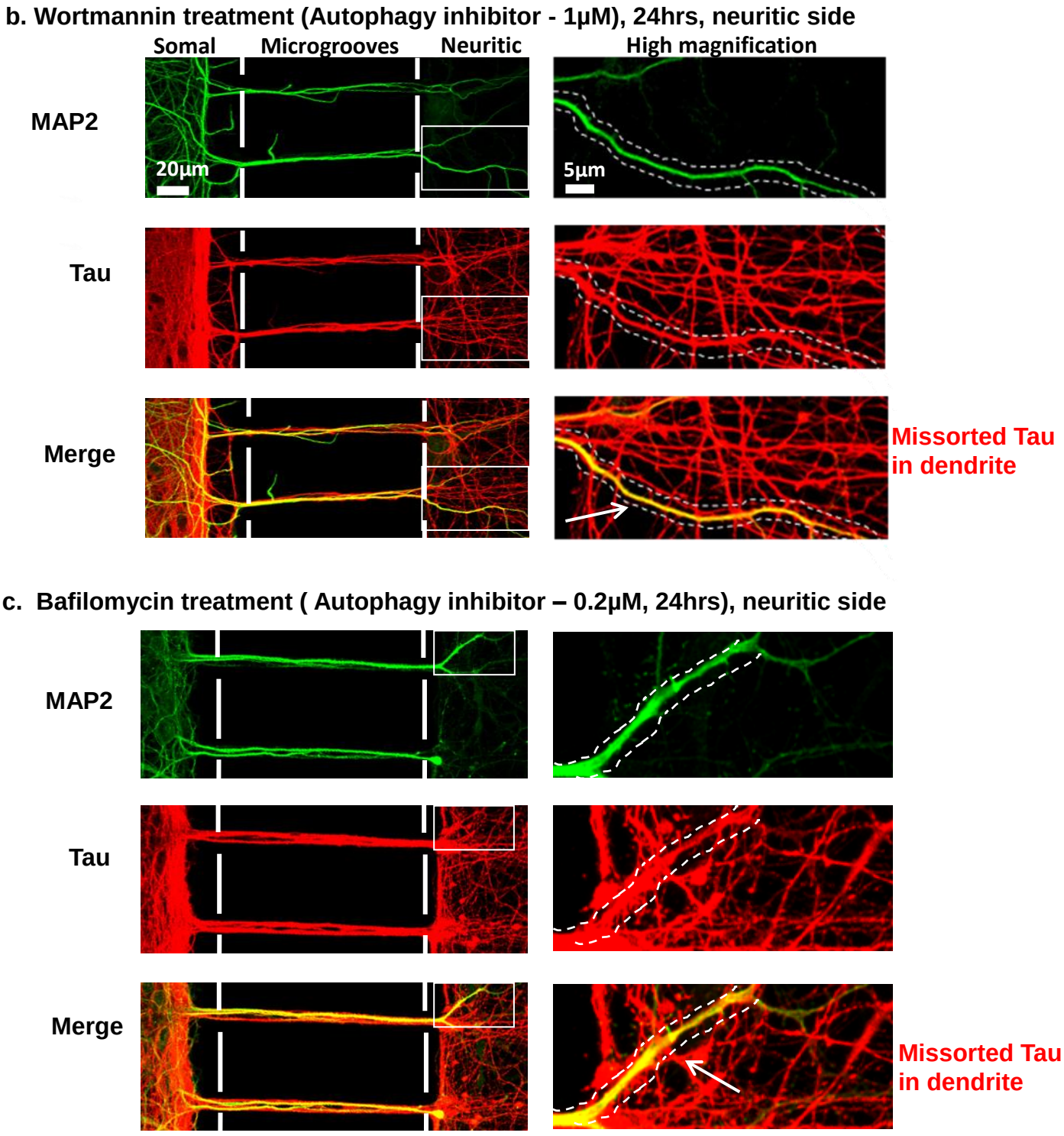

Treatment on the neuritic side for 24h with the autophagy inhibitors - wortmannin (b) or bafilomycin (c) **(b & c)** In cultures treated with wortmannin (b, 1µM, 24hrs) or with bafilomycin (c, 0.2µM, 24hrs), the fraction of dendrites with Tau increases strongly (see quantification in 3.7a) where a clear colocalization of Tau with MAP2 (merged images at the bottom in b & c, indicated by arrows) could be seen. Scale bars in the main images = 20µm, in insets = 5µm.

3.2.5 Inhibition of the proteasome system in dendrites induces Tau missorting

In order to test the influence of the other protein degradation system – the proteasome on the missorting of Tau, we treated neurons on the neuritic side with the proteasome inhibitors – epoxomicin or lactacystin for 24 hours and then checked the Tau distribution. Axons and dendrites were monitored with Tau antibody - K9JA and with antibody against - MAP2, a dendritic marker. Compared to the control neurons treated with vehicle (DMSO) **(Fig. 3.5a)** which showed ~16% (16.7±3.11%) Tau missorting, epoxomicin showed ~76% (75.9±3%) Tau missorting **(Fig. 3.6a)** and lactacystin showed ~69% (68.9±3.73%) Tau missorting **(Fig. 3.6b).** This result demonstrates that the disappearance of dendritic Tau during differentiation can be achieved either by autophagic or proteasomal degradation.

Fig 3.6: The protein degradation inhibition by the proteasome lead to Tau missorting

a. Epoxomicin treatment (Proteasome inhibitor – 0.2µM), 24hrs, neuritic side

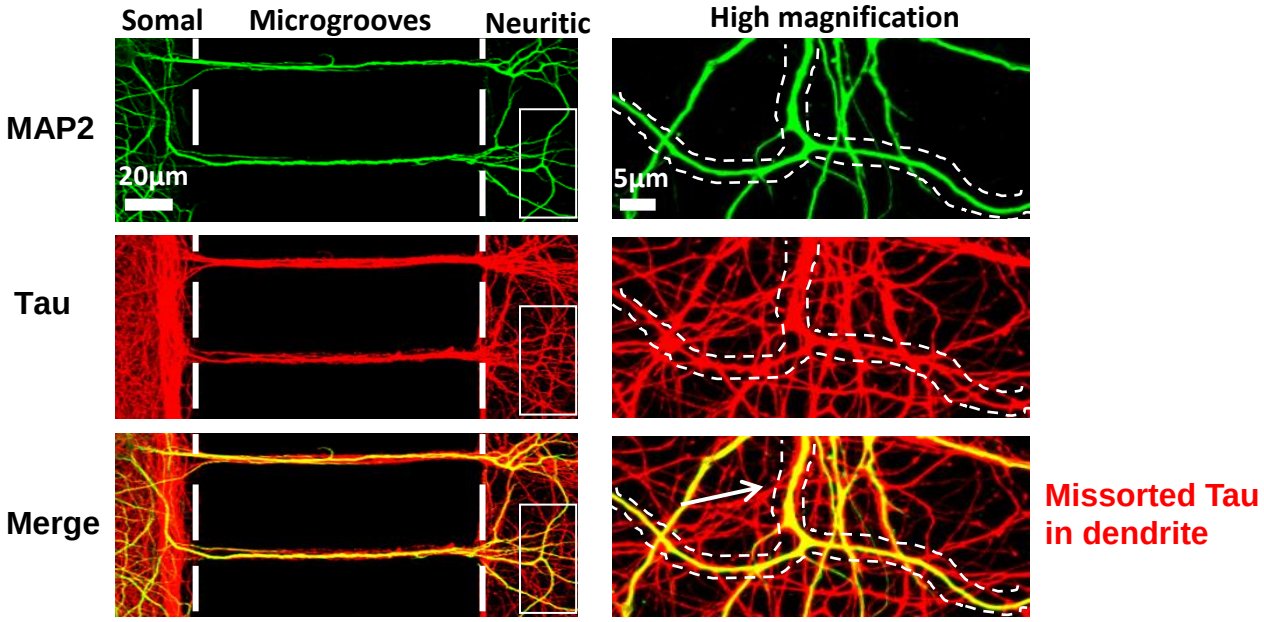

Rat hippocampal neurons (DIV 21-25) cultured in microfluidic devices were treated on the neuritic side for 24 h with the proteasome inhibitor - epoxomicin (a). The dendrites were stained with MAP2 antibody (green) and total Tau with K9JA antibody (red). Magnified images of the insets are shown on the right with a pair of eye-guiding dotted lines to highlight a dendrite with or without Tau.
(a) In cultures treated with epoxomicin (a, 0.2µM, 24hrs), the fraction of dendrites with Tau increases strongly (see quantification in 3.7a) where a clear colocalization of Tau with MAP2 (merged images at the bottom in a, indicated by arrow) could be seen. Scale bars in the main images = 20µm, in insets = 5µm.

Fig 3.6: The protein degradation inhibition by the proteasome lead to Tau missorting

b. Lactacystin treatment (Proteasome inhibitor – 0.5µM, 24hrs), neuritic side

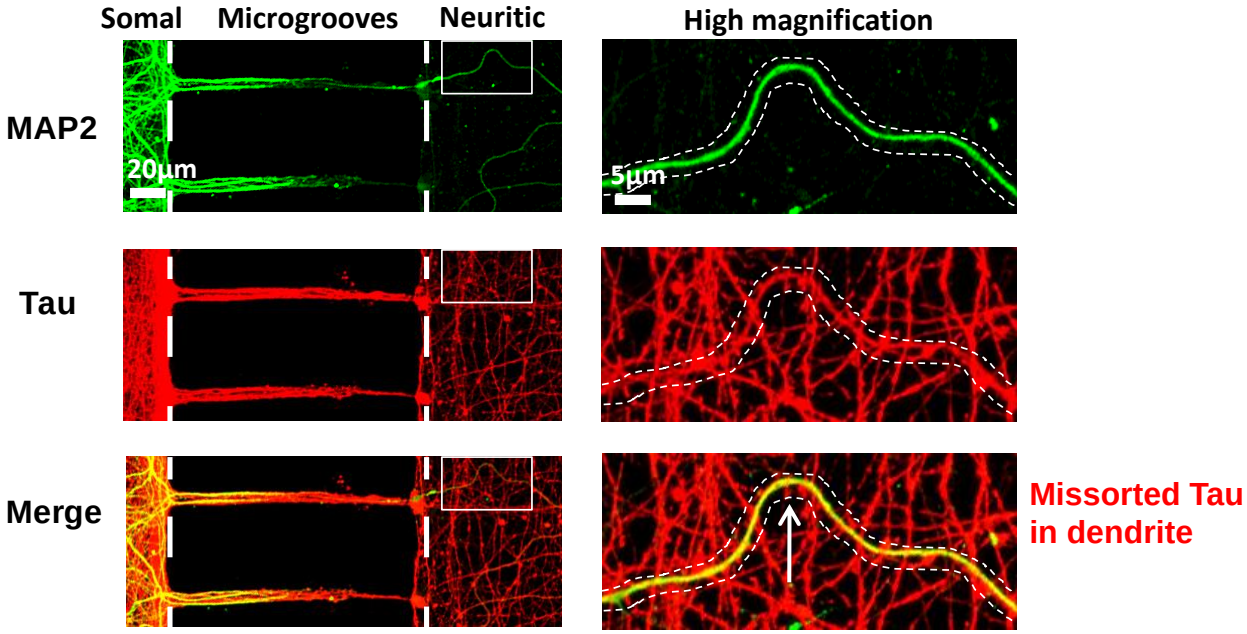

Treatment on the neuritic side for 24h with the proteasomal inhbitor - lactacystin (b).
(b) In cultures treated with lactacystin (b, 0.5µM, 24hrs), the fraction of dendrites with Tau increases strongly (see quantification in 3.7a) where a clear colocalization of Tau with MAP2 (merged images at the bottom in b, indicated by arrow) could be seen. Scale bars in the main images = 20µm, in insets = 5µm.

Fig 3.7 a. Quantification of dendrites with Tau missorting induced by protein degradation inhibitors

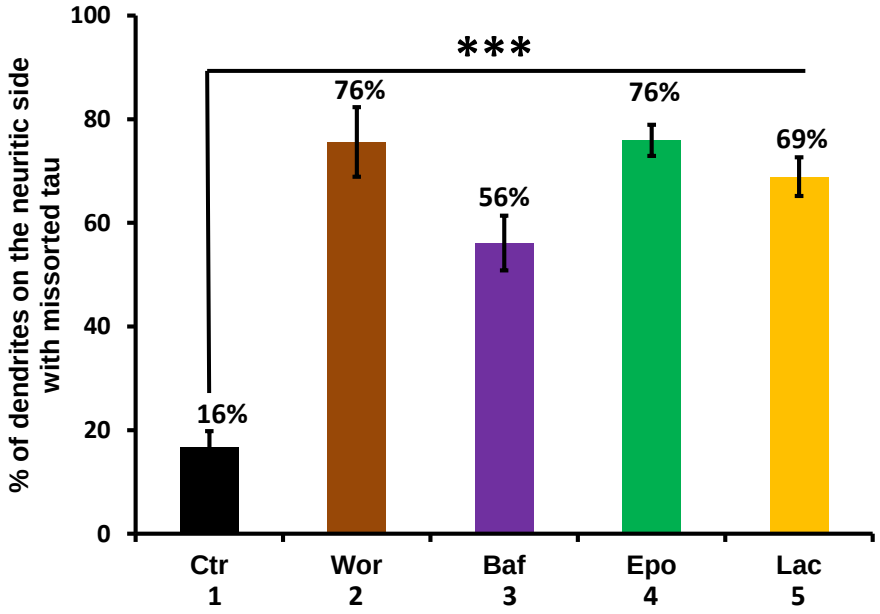

(a) Quantification of dendrites on the neuritic side showing co-localization of Tau with MAP2 following treatment with DMSO (Ctr, bar 1) or with the autophagy (bars 2 & 3) or proteasomal (bars 4 & 5) inhibitors. Error bars, SEM from *n* = 100 to 150 dendrites from 3-4 chambers in each condition. ****p* < 0.005 using student's t-test.

In order to examine the efficacy and specificity of the protein degradation inhibitors, the dendrites were monitored after treatment with the autophagy substrate - p62 or with the proteasomal substrates - ubiquitinated proteins. Missorting of Tau into the dendrites was monitored with MAP2 and Tau antibodies. Compared to the control neurons treated with vehicle (DMSO) **(Fig. 3.8a,** 2.1±0.27**)**, wortmannin **(Fig. 3.8b)** significantly increased p62 level (20.3±1.47**)** while epoxomicin **(Fig. 3.9b)** elevated the amount of ubiquitinated substrates in the dendrites on the neuritic side (36.7±1.08**)**, as revealed by immunofluorescence, suggesting the successful suppression of autophagy **(quantification in Fig. 3.8c)** and the proteasome **(quantification in Fig. 3.9c).** Overall, the inhibition of autophagy or the proteasome resulted in a significant increase in the percentage of dendrites with Tau missorting suggesting a role of the protein degradation pathways in the sorting of Tau.

Fig 3.8: The protein degradation inhibition by autophagy is specific and lead to Tau missorting

a. Vehicle ctr (DMSO, <0.1%)

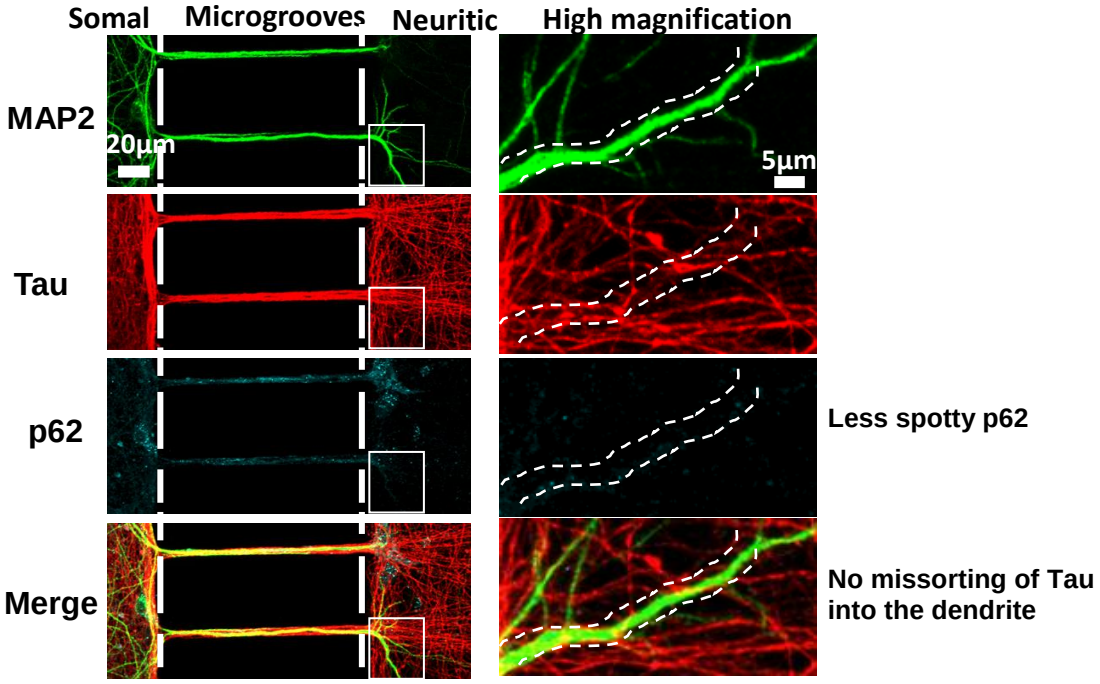

Rat hippocampal neurons (DIV 21-25) cultured in microfluidic devices were treated on the neuritic side for 24 h with DMSO (control, a). The dendrites were stained with MAP2 antibody (green) and total Tau with K9JA antibody (red). The anti-p62 antibody (cyan) was used to monitor the level of the autophagy substrate - p62. Magnified images of the insets are shown on the right with a pair of eye-guiding dotted lines to highlight a dendrite with or without Tau.
(a) In the vehicle-treated control (DMSO, <0.1%), Tau is predominantly localized to the axons (see merged images at the bottom in a). Only a small fraction of dendrites colocalizes with Tau. The level of p62 remains low. Scale bars in the main images = 20µm, in insets = 5µm

Fig 3.8: The protein degradation inhibition by autophagy is specific and lead to Tau missorting

b. Wortmannin treatment (Autophagy inhibitor - 1µM), 24hrs, neuritic side

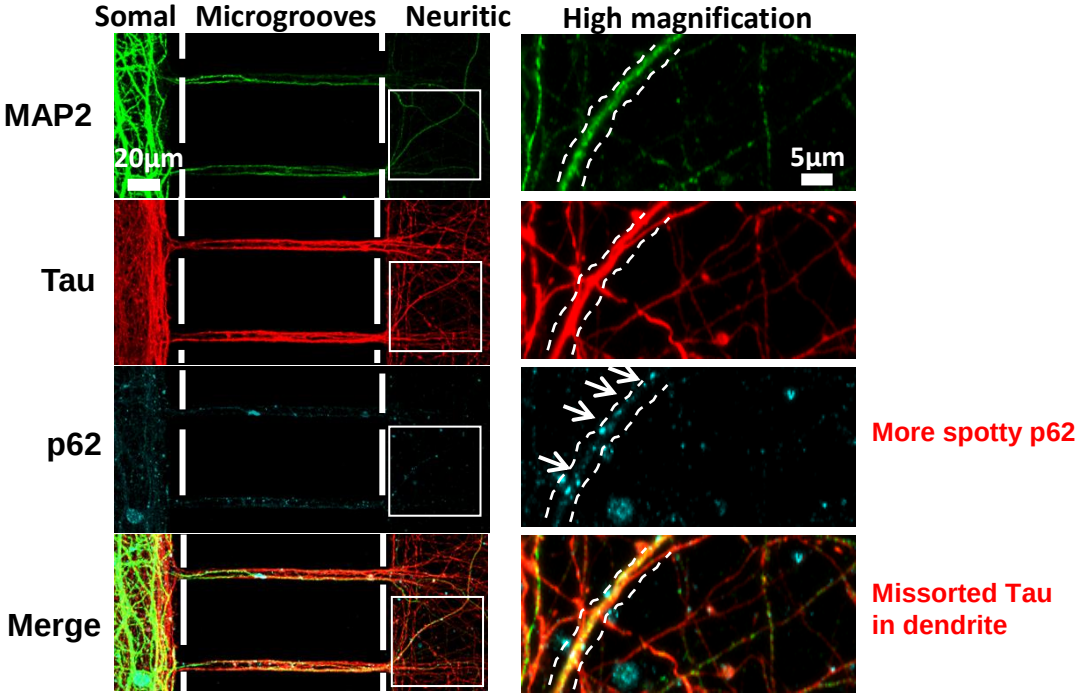

Treatment on the neuritic side for 24h with the autophagy inhbitor - wortmannin (b).
(b) In cultures treated with wortmannin (1µM, 24hrs), the fraction of dendrites with Tau increases strongly where it colocalizes with MAP2 (merged images at the bottom in b) and the dendrites with Tau localization also show an elevated level of p62 as indicated by arrows (compare high magnification of a and b to see an increase in p62). Scale bars in the main images = 20µm, in insets = 5µm.

c. Quantification of the number of p62 puncta in the dendrites on the neuritic side after inhibition of autophagy

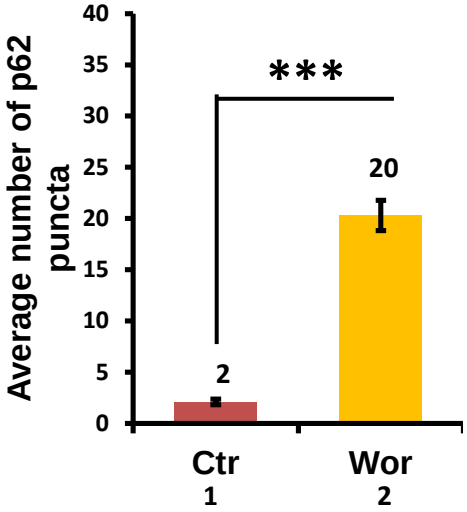

(c) Quantification of the average number of the p62 puncta per 100µm length of each dendrite on the neuritic side of the control (bar 1) and wortmannin (bar 2) treated cultures. Error bars, SEM from *n* = 15 – 20 dendrites from 3 chambers in each condition. ***$p < 0.005$ using Student's *t* test.

Fig 3.9: The protein degradation inhibition by the proteasome is specific and lead to Tau missorting

a. Vehicle ctr (DMSO, <0.1%)

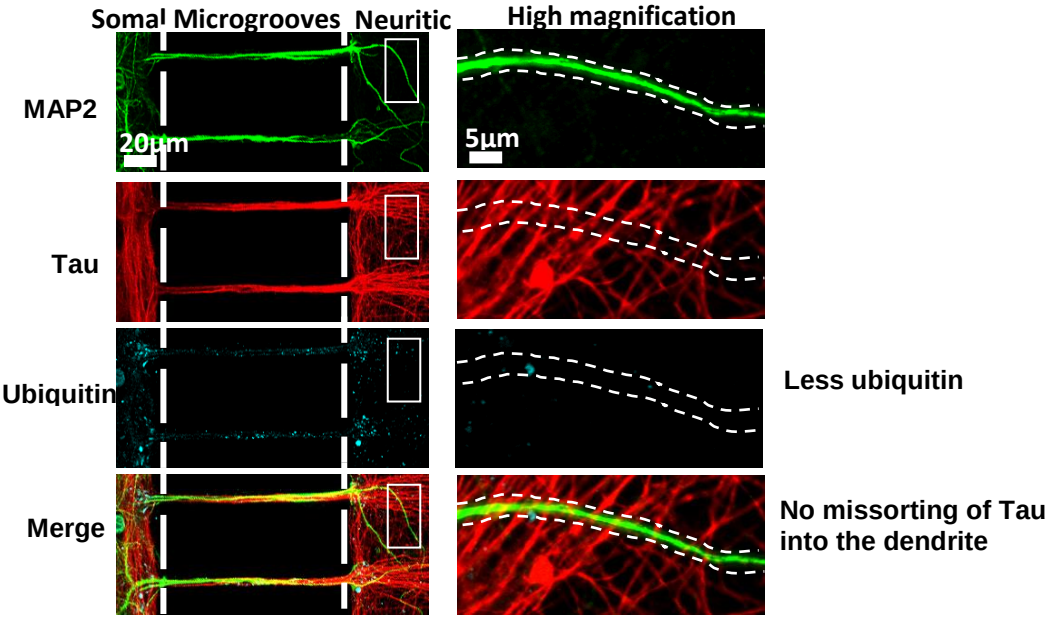

Rat hippocampal neurons (DIV 21-25) cultured in microfluidic devices were treated on the neuritic side for 24 h with DMSO (control, a). The dendrites were stained with MAP2 antibody (green) and total Tau with K9JA antibody (red). The anti-ubiquitin antibody (cyan) was used to monitor the level of ubiquitin. Magnified images of the insets are shown on the right with a pair of eye-guiding dotted lines to highlight a dendrite with or without Tau.

(a) In the vehicle-treated control (DMSO, <0.1%), Tau is predominantly localized to the axons (see merged images at the bottom in a). Only a small fraction of dendrites colocalizes with Tau. The level of ubiquitin remains low. Scale bars in the main images = 20µm, in insets = 5µm.

b. Epoxomicin treatment (Proteasome inhibitor – 0.2µM), 24hrs, neuritic side

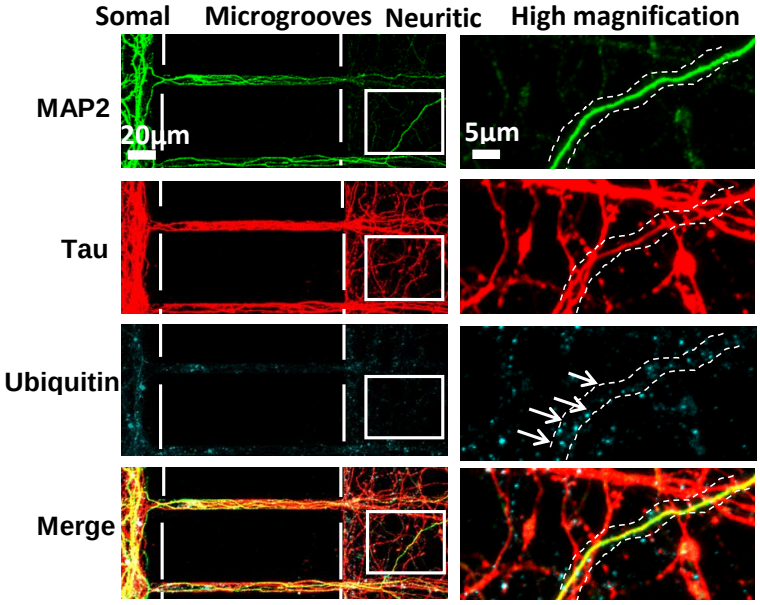

c. Quantification of ubiquitin puncta in the dendrites on the neuritic side after inhibition of the proteasome

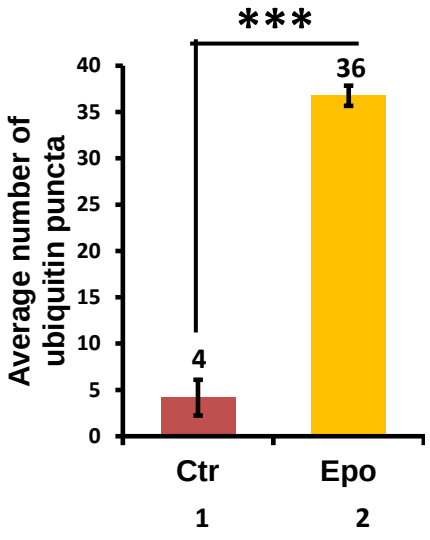

Treatment on the neuritic side for 24h with the proteasome inhbitor - epoxomicin (b).

(b) In cultures treated with epoxomicin (0.2µM, 24hrs), the fraction of dendrites with Tau increases strongly where it colocalizes with MAP2 (merged images at the bottom in b) and the dendrites with Tau localization also show an elevated level of ubiquitin as indicated by arrows (compare high magnication of a and b to see an increase in ubiquitin). Scale bars in the main images = 20µm, in insets = 5µm.

(c) Quantification of the average number of the ubiquitin puncta per 100µm length of each dendrite on the neuritic side of the control (bar 1) and epoxomicin (bar 2) treated cultures. Error bars, SEM from *n* = 15 – 20 dendrites from 3 chambers in each condition. ***$p < 0.005$ using Student's *t* test.

3.2.6 Differential phosphorylation states of dendritic and axonal Tau

Tau in AD and other Tauopathies is hyperphosphorylated (Kopke et al., 1993) and the hyperphosphorylation has been proposed to drive the missorting of Tau. Indeed, the diffusion barrier at the axonal initial segment cannot restrain phosphorylated Tau within axons (Li et al., 2011). In addition, it has been reported that in cultured neurons, Aβ oligomers induce Tau missorting into the somatodendritic compartment and the missorted Tau is phosphorylated mainly at the 12E8 and AT8 sites (Zempel et al., 2010). These observations prompted us to examine the phosphorylation status of the dendritic Tau induced by inhibition of protein degradation. We analyzed the phosphorylation state of Tau protein accumulating in the dendrites after inhibition of protein degradation, with phosphorylation-dependent antibodies - 12E8, PHF1 and AT8. Missorted dendritic Tau showed phosphorylation mainly at the 12E8 sites (pS262/pS356) upon treatment with either the autophagy inhibitor - wortmannin (in 66.9±5.6% dendrites) or the proteasomal inhibitor - epoxomicin (in 68.5±4.81% dendrites) **(Fig. 3.10, a-c & quantification in Fig. 3.11a)**, but not at the AT8 (pS202/pT205) **(Fig. 3.10, d-f)** and the PHF1 (pS396/pS404) **(Fig. 3.10, g-i)** sites. On the other hand, the axonal Tau exhibited phosphorylation at all these sites. Thus, the dendritic and axonal Tau are differentially phosphorylated. Based on this observation, we can conclude that the dendritic Tau degraded by the autophagy and the proteasomal pathways is phosphorylated mainly at the 12E8 site.

Fig 3.10: Tau in dendrites is phosphorylated predominantly at the 12E8 site

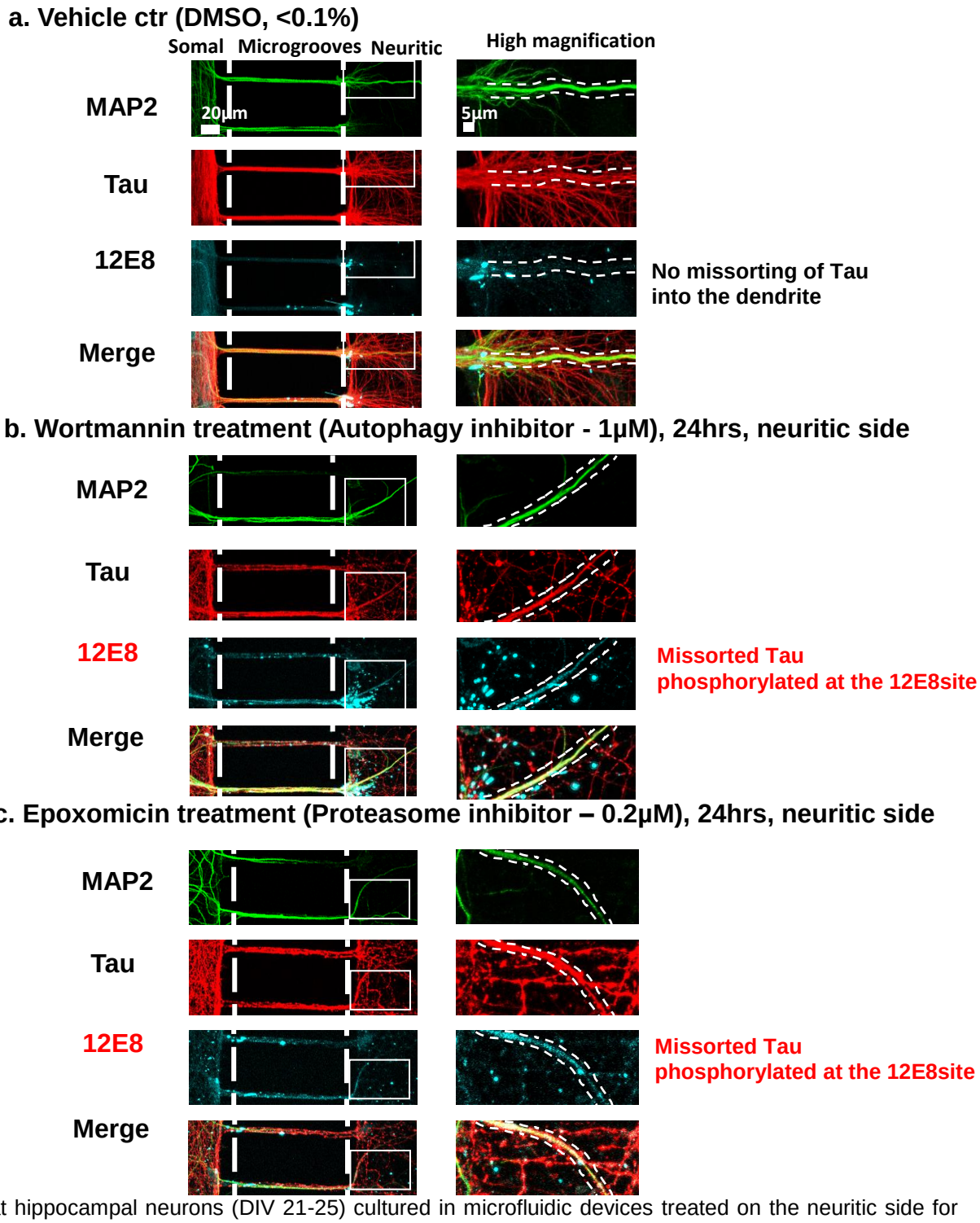

Rat hippocampal neurons (DIV 21-25) cultured in microfluidic devices treated on the neuritic side for 24 h either with DMSO (control, a), or with the autophagy inhibitor, wortmannin (b) or proteasomal inhibitor, epoxomicin (c). Phosphorylation-dependent Tau antibody - 12E8 (cyan) was used to probe the phosphorylation state of Tau at S262/S356 residues. All stainings were done in combination with the Tau antibody - K9JA (red) to indicate total Tau and the MAP2 antibody (green) to indicate dendrites. Magnified images of the insets are shown on the right with pairs of eye-guiding dotted lines in each image to highlight dendrites with or without colocalization with phospho Tau and total Tau.
(a-c) In the vehicle treated control (DMSO, <0.1%), Tau sorts mainly to the axons (a). Treatment with wortmannin (1µM, 24hrs) or epoxomicin (0.2µM, 24hrs) on the neuritic side causes an increase in the accumulation of Tau in the dendrites (indicated by K9JA staining) which is phosphorylated at the 12E8 site (b,c, quantification in 3.11a). The magnified insets of wortmannin and epoxomicin treated cultures on the right of (b) and (c) represent a clear colocalization of MAP2 with 12E8 Tau and total Tau. Scale bars in all main images = 20µm, in all the insets = 5µm.

Fig 3.10: Tau in dendrites is not phosphorylated at the AT8 site

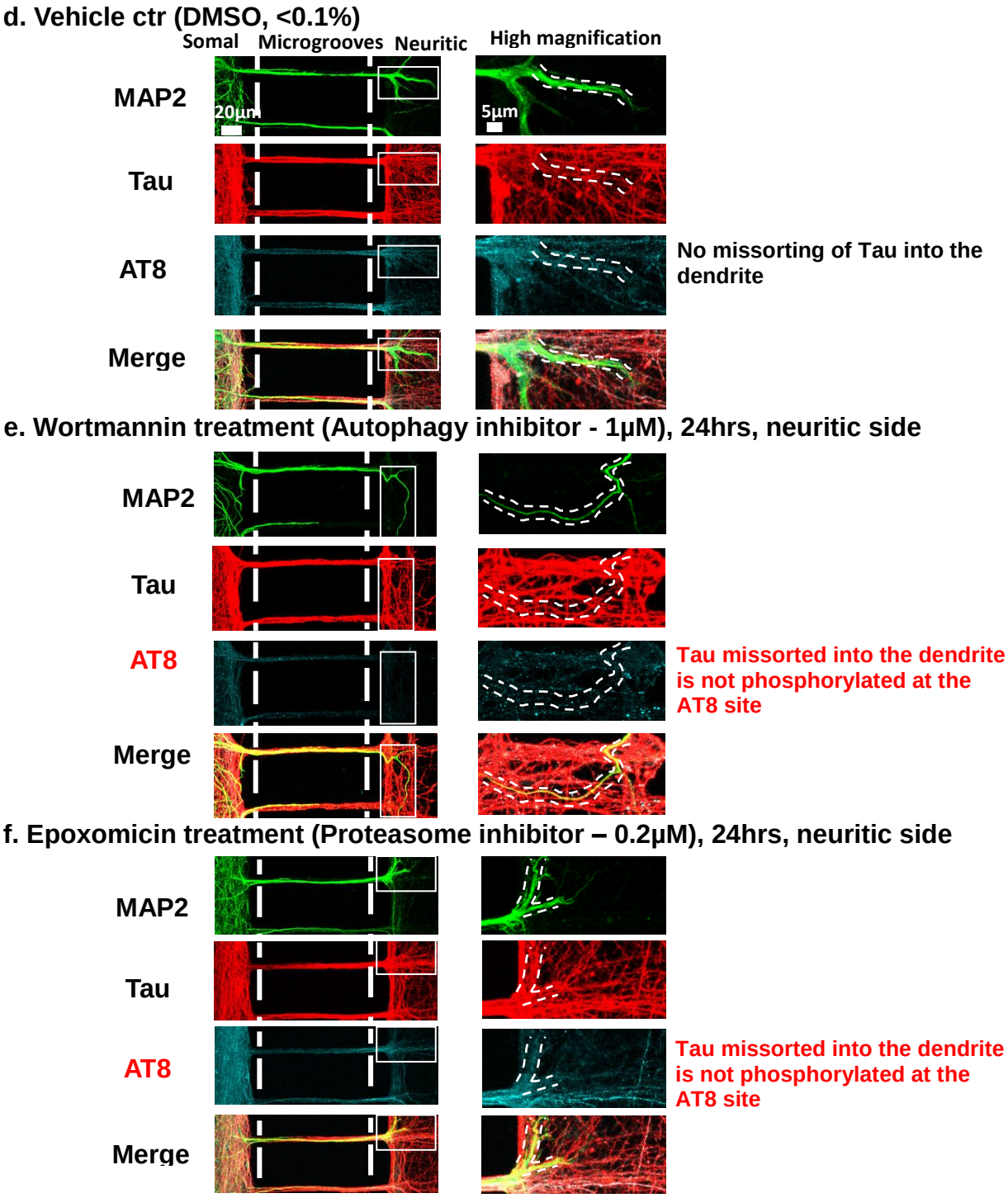

Treatment on the neuritic side for 24h with either DMSO (d) or with the autophagy inhibitor – wortmannin (e) or with the proteasomal inhibitor – epoxomicin (f). Staining was done with the phosphorylation-dependent Tau antibody – AT8 (cyan) to probe the phosphorylation state of Tau at S202/T205 residues in combination with the Tau antibody - K9JA (red) to indicate total Tau and the MAP2 antibody (green) to indicate dendrites.

(d-f) In the vehicle treated control (DMSO, <0.1%), Tau sorts mainly to the axons (d). Treatment with wortmannin (1µM, 24hrs) or epoxomicin (0.2µM, 24hrs) on the neuritc side did not result in an increase in the accumulation of phospho Tau (AT8 site) in the dendrites (e, f, quantification in 3.11a) although an accumulation in total Tau levels (missorting of Tau) was found. The magnified insets of wortmannin and epoxomicin treated cultures on the right of (e) and (f) represent a clear colocalization of MAP2 with total Tau and not with AT8 Tau. Scale bars in all main images = 20µm, in all the insets = 5µm.

Fig 3.10: Tau in dendrites is not phosphorylated at the PHF1 site

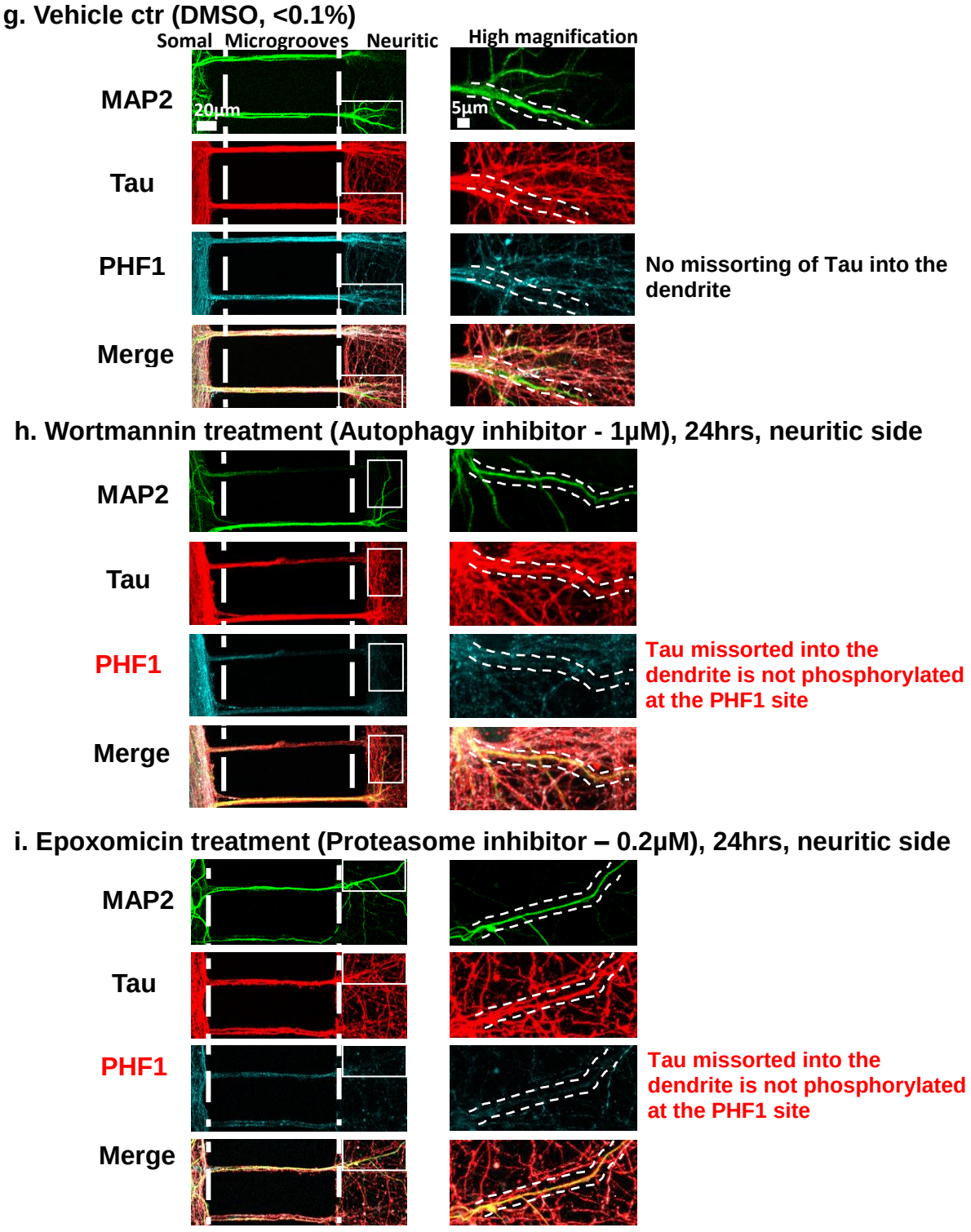

Treatment on the neuritic side for 24h with either DMSO (g) or with the autophagy inhibitor – wortmannin (h) or with the proteasomal inhibitor – epoxomicin (i). Staining was done with the phosphorylation-dependent Tau antibody – PHF1 (cyan) to probe the phosphorylation state of Tau at S396/S404 residues in combination with the Tau antibody - K9JA (red) to indicate total Tau and the MAP2 antibody (green) to indicate dendrites.

(g-i) In the vehicle treated control (DMSO, <0.1%), Tau sorts mainly to the axons (g). Treatment with wortmannin (1µM, 24hrs) or epoxomicin (0.2µM, 24hrs) on the neuritic side did not result in an increase in the accumulation of phospho Tau (PHF1 site) in the dendrites (h, i, quantification in 3.11a) although an accumulation in total Tau levels (missorting of Tau) was found. The magnified insets of wortmannin and epoxomicin treated cultures on the right of (h) and (i) represent a clear colocalization of MAP2 with total Tau and not with PHF1 Tau. Scale bars in all main images = 20µm, in all the insets = 5µm.

Fig 3.11. a. Quantification of dendrites with missorted phosphorylated Tau induced by protein degradation inhibitors

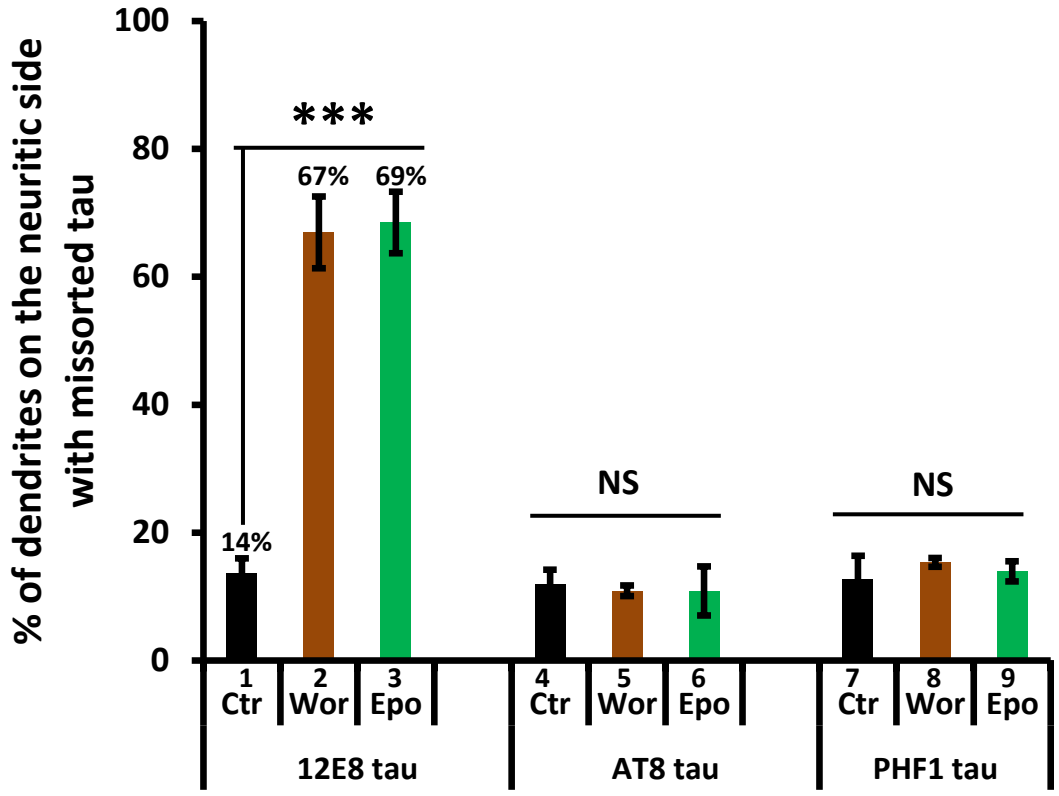

(a) Quantification of dendrites on the neuritic side shows co-localization of MAP2 with phospho-Tau species – 12E8 (bars 1-3), AT8 (bars 4-6) and PHF1 (bars 7-9) following different treatments. Error bars, SEM from *n* = 50 to 100 dendrites from 3 chambers in each condition. ***$p < 0.005$ using Student's *t* test. NS- not significant.

3.2.7 Isoforms of Tau degraded in dendrites by autophagy and the proteasome

The human brain expresses 6 isoforms of Tau, while the rat or mouse brain expresses mainly 3 isoforms of the 4R Tau. The different isoforms of Tau may have different functions, as the impairment of the ratio between 4R and 3R Tau isoforms (Lee et al., 2001, Gong et al., 2005) induced by Tau mutations can cause Tauopathies, and the generation of Tau isoforms is developmentally regulated. Recent studies showed that the different Tau isoforms may distribute in different subcellular compartments in neurons. It has been reported that the 1N isoform of Tau was found to be localized mainly to the nucleus but absent in axons whereas the 0N and 2N isoforms were found to be localized to the cell bodies and axons (Liu and Gotz, 2013). Thus, we further analyzed the isoform composition of the missorted dendritic Tau induced by the inhibition of protein degradation. Indeed, the two N-terminal inserts of Tau play an important role in its subcellular distribution. As rat

brain mainly expresses 4R Tau, we used antibodies against the N terminal inserts of Tau to differentiate between the different isoforms. For instance, we used an antibody against the first insert of Tau to detect the 1N Tau isoforms. The dendrites were monitored with anti-MAP2 antibody. Compared with the DMSO-treated control **(Fig. 3.12a)**, which showed missorting of Tau in ~14% (13.8±0.95%) of dendrites, the autophagy inhibition with wortmannin **(Fig. 3.12b,** in 62.8±3.12% dendrites**)** or the proteasomal inhibition with epoxomicin **(Fig. 3.12c**, in 72.8±2.2% dendrites**)** significantly elevated the missorting of the 1N Tau into the dendrites **(quantification in Fig. 3.12d)**. The localization of 0N and 2N Tau isoforms in the dendrites remains still to be elucidated.

Fig 3.12: 1N isoform of Tau is degraded by autophagy and the proteasome in dendrites

a. Vehicle ctr (DMSO, <0.1%)

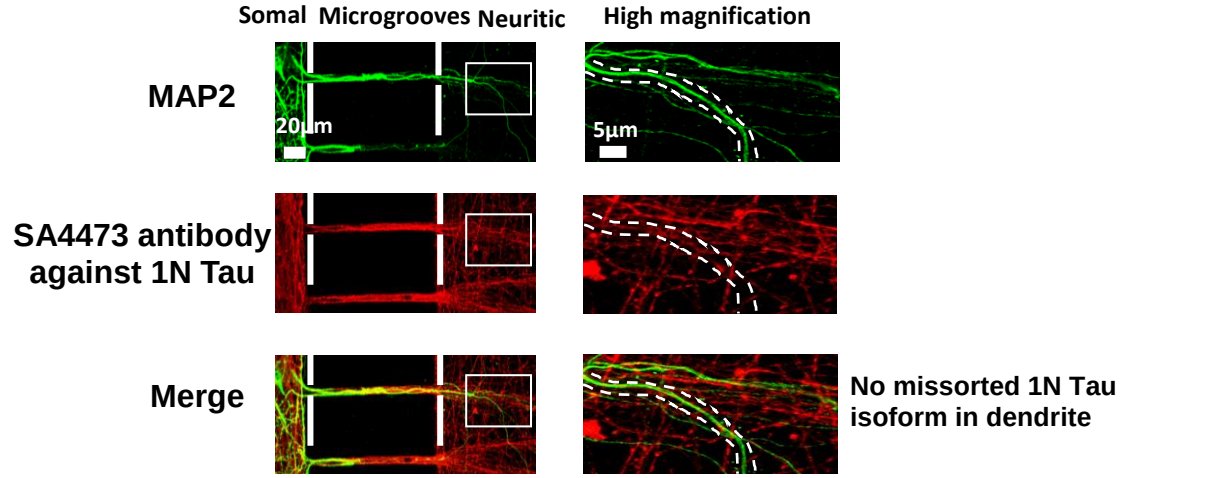

b. Wortmannin treatment (Autophagy inhibitor – 1µM), 24hrs, neuritic side

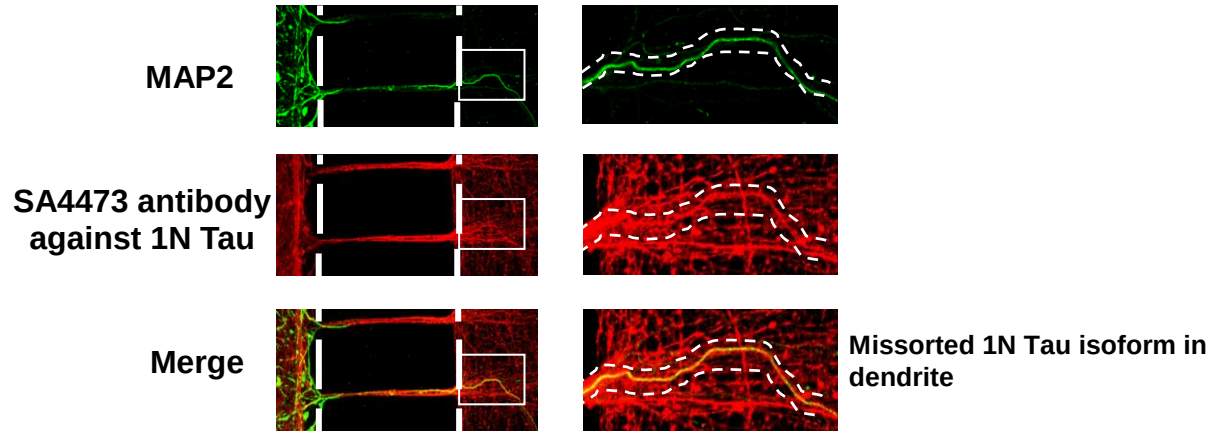

c. Epoxomicin treatment (Proteasome inhibitor – 0.2µM), 24hrs, neuritic side

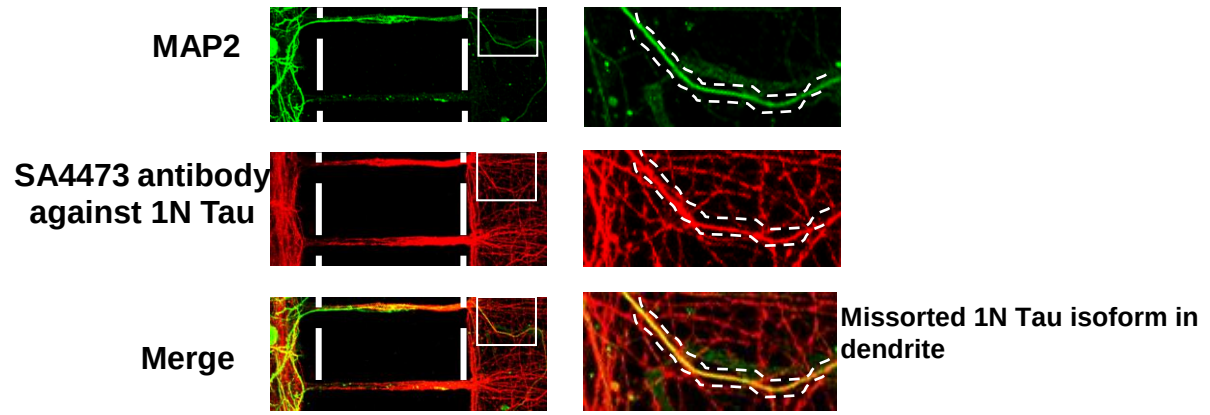

Rat hippocampal neurons (DIV 21-25) cultured in microfluidic devices were treated on the neuritic side for 24 h either with DMSO (control, a) or with the autophagy inhibitor - wortmannin (b) or with the proteasomal inhibitor - epoxomicin (c). Staining was done with MAP2 antibody (green) for dendrites and SA4473 antibody (red) against the 1N Tau isoforms. Magnified images of the insets are shown on the right with a pair of eye guiding dotted lines to highlight a dendrite with or without Tau.
(a) In the vehicle-treated control (DMSO, <0.1%), Tau is predominantly localized to the axons [see merged images at the bottom in (a)]. Only a small fraction of dendrites colocalizes with Tau.
(b, c) In cultures treated with wortmannin (b, 1µM, 24hrs) or with epoxomicin (c, 0.2µM, 24hrs), the fraction of dendrites with 1N Tau isoform increases strongly (see quantification in d) where a clear colocalization of 1N Tau with MAP2 (merged images at the bottom in b & c) could be seen. Scale bars in the main images = 20µm, in insets = 5µm.

Fig 3.12. d. Quantification of dendrites with 1N Tau isoform missorting induced by protein degradation inhibitors

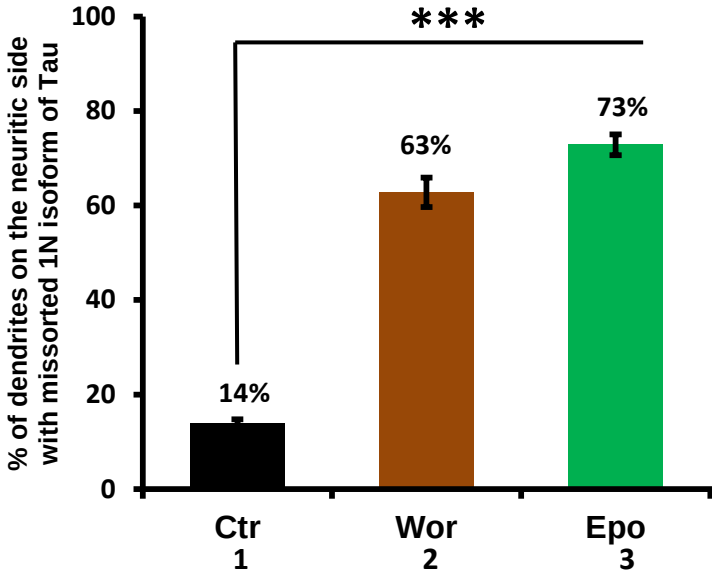

(d) Quantification of dendrites on the neuritic side showing co-localization of 1N Tau with MAP2 following different treatments. Error bars, SEM from *n* = 50 to 100 dendrites from 3 chambers in each condition. ****p* < 0.005 using Student's *t* test.

3.2.8 Enhancement of the activity of autophagy or of the proteasome reduces Tau missorting

To further validate that the protein degradation systems are involved in the sorting of Tau, we tested an alternative approach - stimulating the degradation systems instead of suppressing them, since stimulation of the protein degradation systems has been suggested to be of therapeutic potential for Tauopathies. We noticed that even under physiological conditions, ~15% of the dendrites showed missorting of Tau. We therefore asked whether stimulation of the autophagy or of the proteasome system can reduce the basal amount of Tau missorting. Our previous study had shown that trehalose induces autophagy (Kruger et al., 2012) in primary neurons and in an N2a cell model of Tauopathy and efficiently reduces the level of Tau and Tau aggregation. Since trehalose is free of toxic effects even at higher concentrations (Rodriguez-Navarro et al., 2010), we used a concentration of 150mM for treatment of neurons in microfluidic devices. We applied trehalose (150mM) on the neuritic side for 24hrs **(Fig. 3.13a)** with sucrose (150mM)-treatment serving as control. Trehalose treatment indeed supressed missorting of Tau, as only 3.4% (3.4±0.15%) of dendrites showed the presence of Tau, which is far below the control level (missorting in ~15%

dendrites) **(quantification in Fig. 3.13b).** These results thereby confirm the role of autophagy in degrading dendritic Tau.

Similar to the activation of autophagy, we wanted to enhance the proteasome activity in neurons in microfluidic chambers. A recent study showed that rolipram could enhance the cAMP-PKA activity leading to phosphorylation of the proteasomal subunits and thereby enhance its proteolytic activities in mice (Myeku et al., 2016). We first tested the concentration at which rolipram efficiently reduced the amount of ubiquitin conjugates in cultured primary neurons. We found that rolipram enhances the proteasomal activity at a concentration of 10μM at which the amount of ubiquitin conjugates were significantly lower than in the vehicle-treated control **(Fig. 3.14a & quantification in Fig. 3.14b)**. We applied rolipram (10μM) on the neuritic side for 24hrs **(Fig. 3.14c)** with vehicle (DMSO) (<0.1%) - treatment serving as control. Rolipram treatment indeed supressed missorting of Tau (in 4.3±0.57% dendrites) far below the control level (in 13.8±2.32% dendrites) **(quantification in Fig. 3.14d)** thereby confirming the role of the proteasome in degrading dendritic Tau.

The above two findings indeed confirm the role of the protein degradation pathways – autophagy and the proteasome as a prerequisite for the polarity development of the neuron.

Fig 3.13: Enhancement of the activity of autophagy by trehalose reduces Tau missorting into the dendrites

a. Trehalose (autophagy enhancer – 150mM), 24hrs, neuritic side, reduces Tau missorting into the dendrite

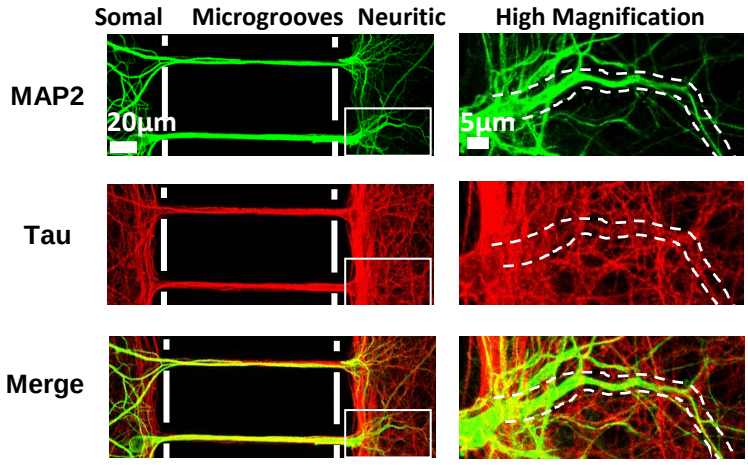

b. Trehalose reduces Tau missorting into the dendrites

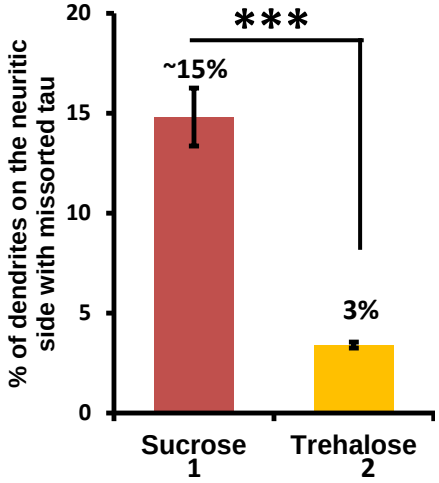

Rat hippocampal neurons (DIV 21-25) cultured in microfluidic chambers were treated on the neuritic side for 24h with Sucrose (150mM, as control) or with Trehalose (150mM), an enhancer of autophagy (a). The dendrites were stained with MAP2 antibody (green) and total Tau with K9JA antibody (red). Magnified images of the insets are shown on the right of (a) with a pair of eye guiding dotted lines to highlight a dendrite with or without Tau.

(a) In cultures treated with trehalose (150mM, 24hrs) on the neuritic side, the fraction of dendrites with Tau decreases strongly (see quantification in b) and a more stringent localization of Tau to the axons is seen. The magnified insets of the dendrites on the right of (a) represent reduced colocalization of Tau with MAP2. Scale bars in the main images = 20µm; in all the insets = 5µm.

(b) Quantification of dendrites on the neuritic side showing co-localization of Tau with MAP2. Although treatment with sucrose (150mM, 24hrs, bar 1) still resulted in a small fraction of dendrites with missorted Tau (as seen in DMSO treated cultures), treatment with trehalose (150mM, 24hrs, bar 2) resulted in a significantly reduced missorting of Tau. Error bars, SEM from n = 100 to 250 dendrites from 3 chambers in each condition. ***$p < 0.005$, using Student's t test.

Fig 3.14: Enhancement of the activity of the proteasome by rolipram reduces the level of ubiquitin conjugates

a. Western blot analysis of the ubiquitin conjugates following treatment of neurons with rolipram, a proteasome enhancer

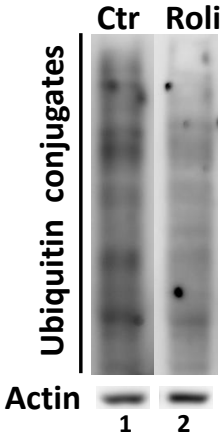

b. Quantification of the blot of (a) of ubiquitin conjugates after treatment with rolipram

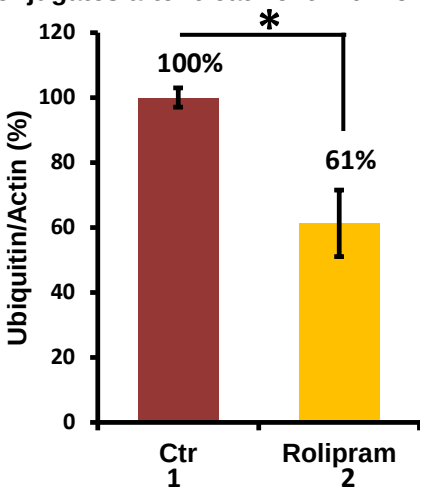

(a) Hippocampal neurons were treated with DMSO (<0.1%) or rolipram (10 µM) for 24h and the samples were collected and western blots were carried out using the antibody for ubiquitinated proteasomal substrates. Treatment with rolipram lead to a decreased level of ubiquitin conjugates (compare lanes 1 and 2).

(b) Quantification of the blot of (a) shows a decrease in the ubiquitin conjugates after treatment with rolipram (compare bars 1 and 2). Error bars, SEM from 3 independent experiments. *$p < 0.05$, using Student's t test.

Fig. 3.14: Enhancement of the activity of the proteasome by rolipram reduces Tau missorting into the dendrites

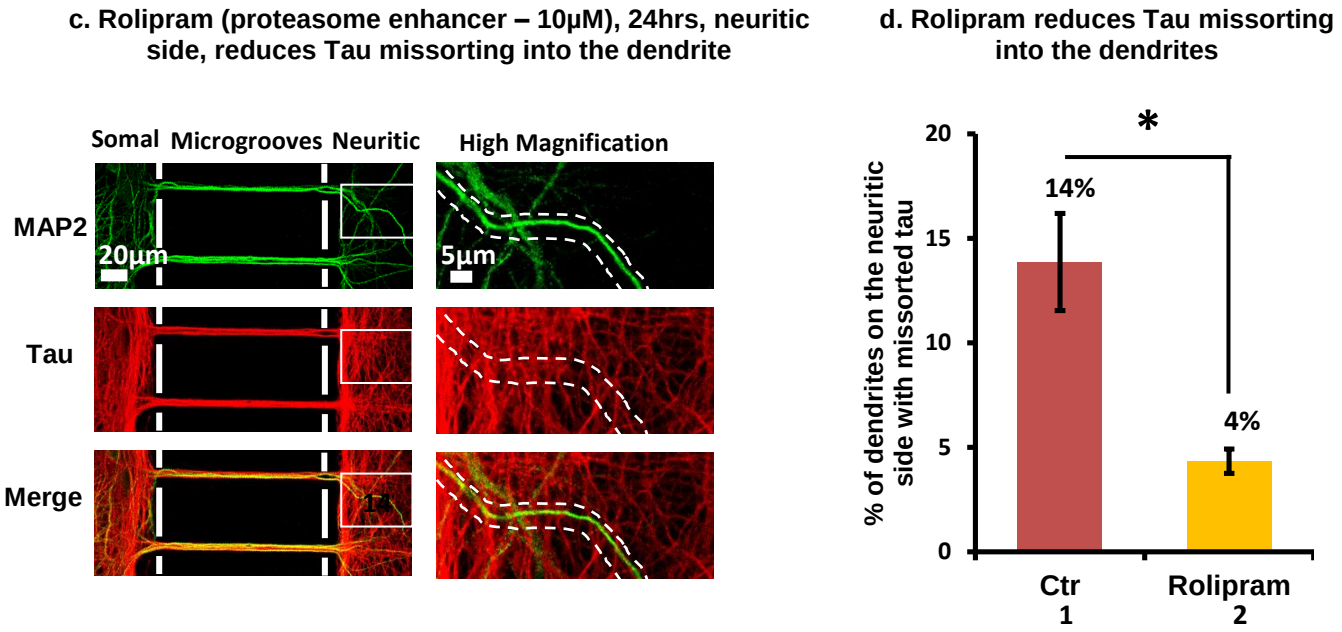

(c) In cultures treated with rolipram (10μM, 24hrs) on the neuritic side, the fraction of dendrites with Tau decreases strongly (see quantification in d). The magnified insets of the dendrite on the right of (c) represent reduced colocalization of Tau with MAP2. Scale bars in the main images = 20μm; in all the insets = 5μm.
(d) Quantification of dendrites on the neuritic side showing co-localization of Tau with MAP2 following different treatments. Although treatment with DMSO (<0.1%, 24hrs, bar 1) still resulted in a small fraction of dendrites with missorted Tau, treatment with rolipram (10μM, 24hrs, bar 2) significantly reduced missorting of Tau. Error bars, SEM from *n* = 100 to 250 dendrites from 3 chambers in each condition. *$p < 0.05$, using Student's *t* test.

3.2.9 Accumulation of Tau protein in dendrites via the inhibition of protein degradation systems results in loss of spines

Previous studies showed that the missorting of Tau into dendrites can cause loss of spines (Thies and Mandelkow, 2007, Zempel et al., 2010). By analogy, we wanted to examine if the accumulation of Tau in the dendrites induced by inhibition of the protein degradation systems could lead to spine loss as well.

Therefore we applied the autophagy inhibitor – wortmannin (1μM) **(Fig. 3.15b)** or the proteasomal inhibitor – epoxomicin (0.2μM) **(Fig. 3.15c)** on the neuritic side of microfluidic chambers for 24hrs. For controls we treated neurons with DMSO (<0.1%, vehicle control) on the neuritic side **(Fig. 3.15a)**. We labeled spines using phalloidin-actin staining. Whereas Tau-free dendrites in DMSO-treated controls had a spine density of ~17 per 20μm (17.32±0.98/20μm) length, there was approximately a two-fold decrease in the spine density in the Tau-containing dendrites in neurons treated

with wortmannin (7.56±0.21/20µm) or epoxomicin (6.6±0.75/20µm) **(quantification in Fig. 3.15d)**. To further elucidate whether the missorting of Tau is essential for the spine loss induced by the inhibition of protein degradation, we treated neurons from Tau-knockout mice cultured in microfluidic chambers on the neuritic side with the protein degradation inhibitors. No spine loss was observed in neurons treated with wortmannin or epoxomicin. This result suggests that the missorting of Tau into dendrites after application of inhibitors of the protein degradation systems causes spine loss.

Fig 3.15: Local treatment with protein degradation inhibitors suppresses protein degradation and lead to dendritic Tau mislocalization and spine loss

a. Vehicle control (DMSO, <0.1%)

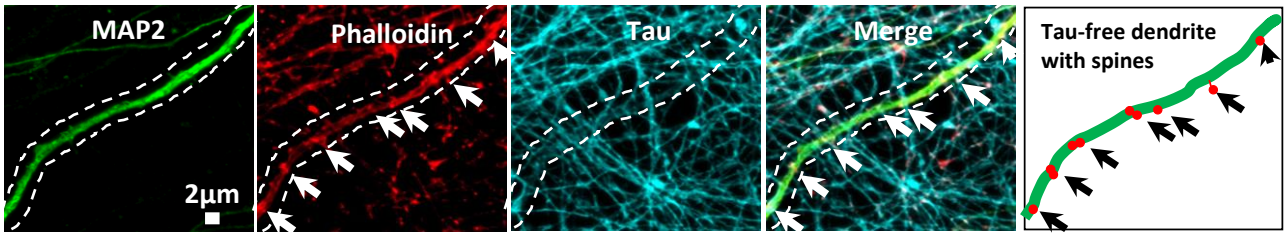

b. Wortmannin treatment (Autophagy inhibitor – 1µM), 24hrs, neuritic side

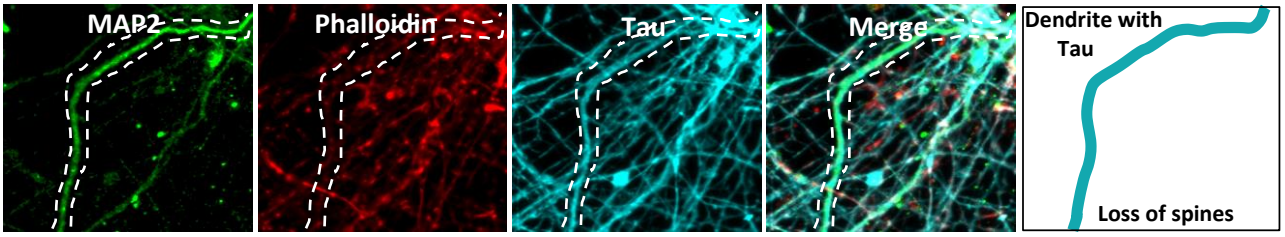

c. Epoxomicin treatment (Proteasome inhibitor – 0.2µM), 24hrs, neuritic side

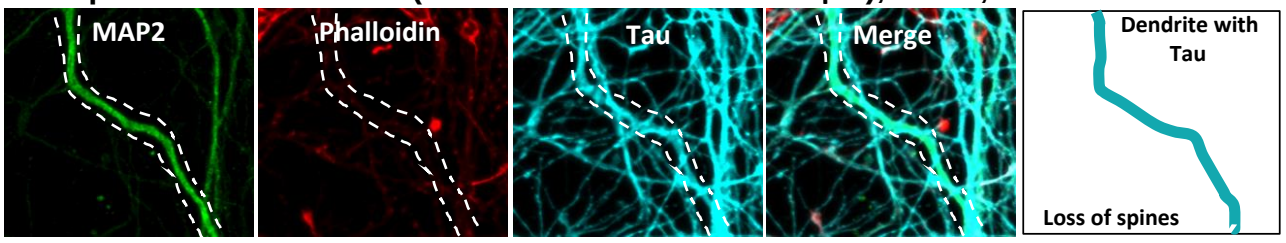

Rat hippocampal neurons (DIV 21-25) cultured in microfluidic devices were treated on the neuritic side for 24h either with DMSO (control, a) or with the autophagy inhibitor - wortmannin (b) or with the proteasomal inhibitor - epoxomicin (c). The dendrites were stained with MAP2 antibody (green), total Tau with K9JA antibody (cyan) and F-actin with phalloidin (red) to indicate spines.
(a) In the vehicle-treated control (DMSO, <0.1%), Tau is predominantly localized to the axons and not present in dendrites and the dendrites have a normal spine distribution (arrows).
(b, c) In cultures treated with wortmannin (b, 1µM, 24hrs) or with epoxomicin (c, 0.2µM, 24hrs), Tau can be observed in dendrites and in these cases the spine number is dramatically reduced (see quantification in d, bars 2 and 3). Scale bar = 2µm.

Fig 3.15: Local treatment with protein degradation inhibitors suppresses protein degradation and lead to dendritic Tau mislocalization and spine loss

d. Quantification of the dendritic spine density on the neuritic side after treatment with protein degradation inhibitors

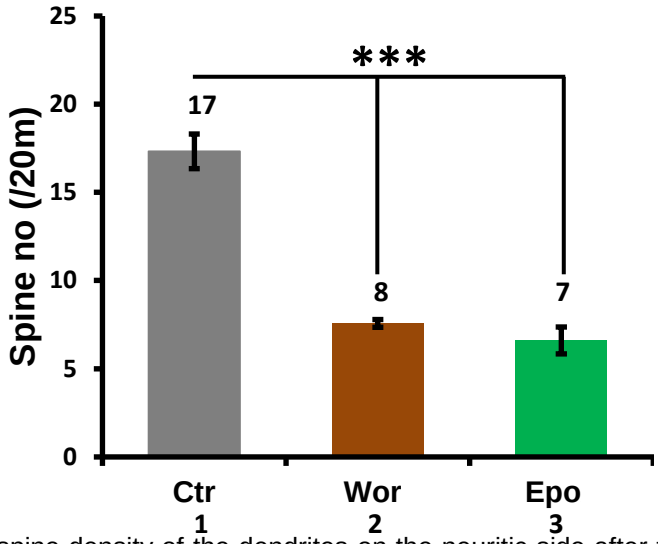

(d) Quantification of the spine density of the dendrites on the neuritic side after treatment with DMSO (ctr, bar 1) or with protein degradation inhibitors (wor and epo, bars 2 and 3). Error bars, SEM from *n* = ~20 dendrites from 3-4 chambers in each condition. ****p* < 0.005 using Student's *t* test.

3.2.10 Tau protein is locally synthesized in dendrites

Next we sought to figure out the source of the dendritic Tau. There could be two potential origins of dendritic Tau: (1) it could originate from the cell body or axons due to diffusion/transport; or (2) it could be locally synthesized in the dendrites. The local translation of Tau in the axons driven by the mTOR signaling pathway (Morita and Sobue, 2009) has been identified. By analogy, we asked whether the dendritic Tau could be produced by local synthesis as well. We tested if blocking local protein synthesis could prevent Tau missorting induced by the inhibition of protein degradation. Neurons cultured in microfluidic devices were treated on the neuritic side with protein translation inhibitors - cycloheximide (Kleiman et al., 1993) or anisomycin (Ghirardi et al., 2004) together with the protein degradation inhibitors - wortmannin or epoxomicin for 24 hours. As described above, axons and dendrites were monitored with Tau antibody - K9JA and with anti-MAP2 antibody respectively.

Treatment with cycloheximide together with wortmannin **(Fig. 3.16b)** or with epoxomicin **(Fig. 3.16c)** profoundly reduced Tau missorting [CHX+Wort: in 11.8±1.07% dendrites, CHX+Epox: in 19.7±8.72% dendrites] to a level comparable to that in vehicle-treated controls (DMSO: in 13.5±3.64% dendrites) **(Fig. 3.16a, quantification in Fig. 3.16h)**. We confirmed this observation by using another protein translation inhibitor – anisomycin together with wortmannin **(Fig. 3.16d)** or

with epoxomicin **(Fig. 3.16e).** Similar results were obtained as cycloheximide treatment [Ani+Wort: in 19.8±4.36% dendrties, Ani+Epox: in 21.2±5.03% dendrites]. These results indicate that the dendritic Tau induced by inhibition of protein degradation is derived from local synthesis.

As we showed above, missorting of Tau was observed in ~15% of dendrites under physiological conditions **(quantification in Fig. 3.16h, bar 1)**. When we treated neurons in microfluidic chambers on the neuritic side with protein translation inhibitors - cycloheximide (10µM) **(Fig. 3.16f)** or anisomycin (10µM) **(Fig. 3.16g)** alone for 24hrs, no missorting of Tau was detected. In addition, we have shown that stimulation of protein degradation can reduce missorting of Tau to a level lower than that under physiological conditions **(Fig. 3.13 & 3.14)**. Collectively, these data suggests that the local synthesis of Tau in dendrites occurs physiologically, and the compromise of the degradation systems in some dendrites (~15% dendrites) may result in Tau missorting.

Fig 3.16: Protein translation inhibitors prevent Tau missorting

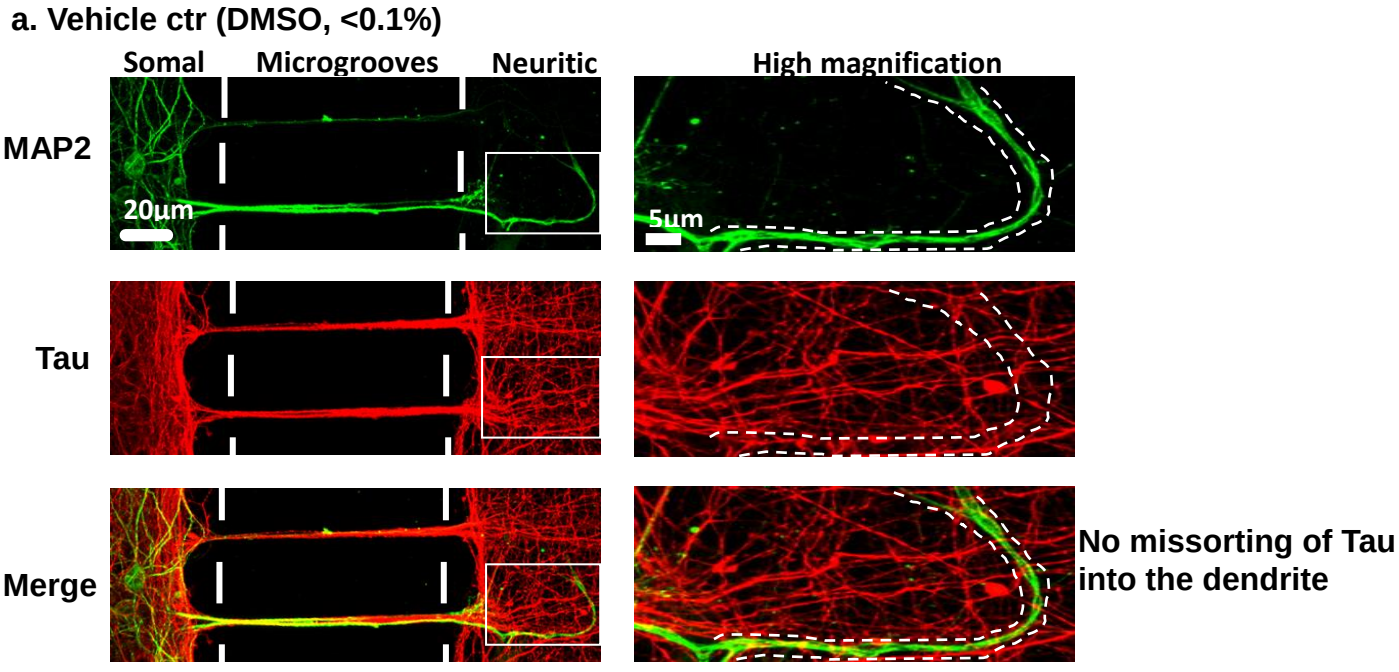

Rat hippocampal neurons (DIV 21-25) cultured in microfluidic chambers were treated on the neuritic side for 24h with DMSO (control, a). The dendrites were stained with MAP2 antibody (green) and total Tau with K9JA antibody (red). Magnified images of the insets are shown on the right with a pair of eye guiding dotted lines to highlight a dendrite with or without Tau missorting.
(a) In the vehicle-treated control (DMSO, <0.1%), Tau is predominantly localized to the axons (see merged images at the bottom in a). Only a small fraction of dendrites colocalizes with Tau (~15%). Scale bars in the main images = 20µm; in all the insets = 5µm.

Fig 3.16: Protein translation inhibitors prevent Tau missorting

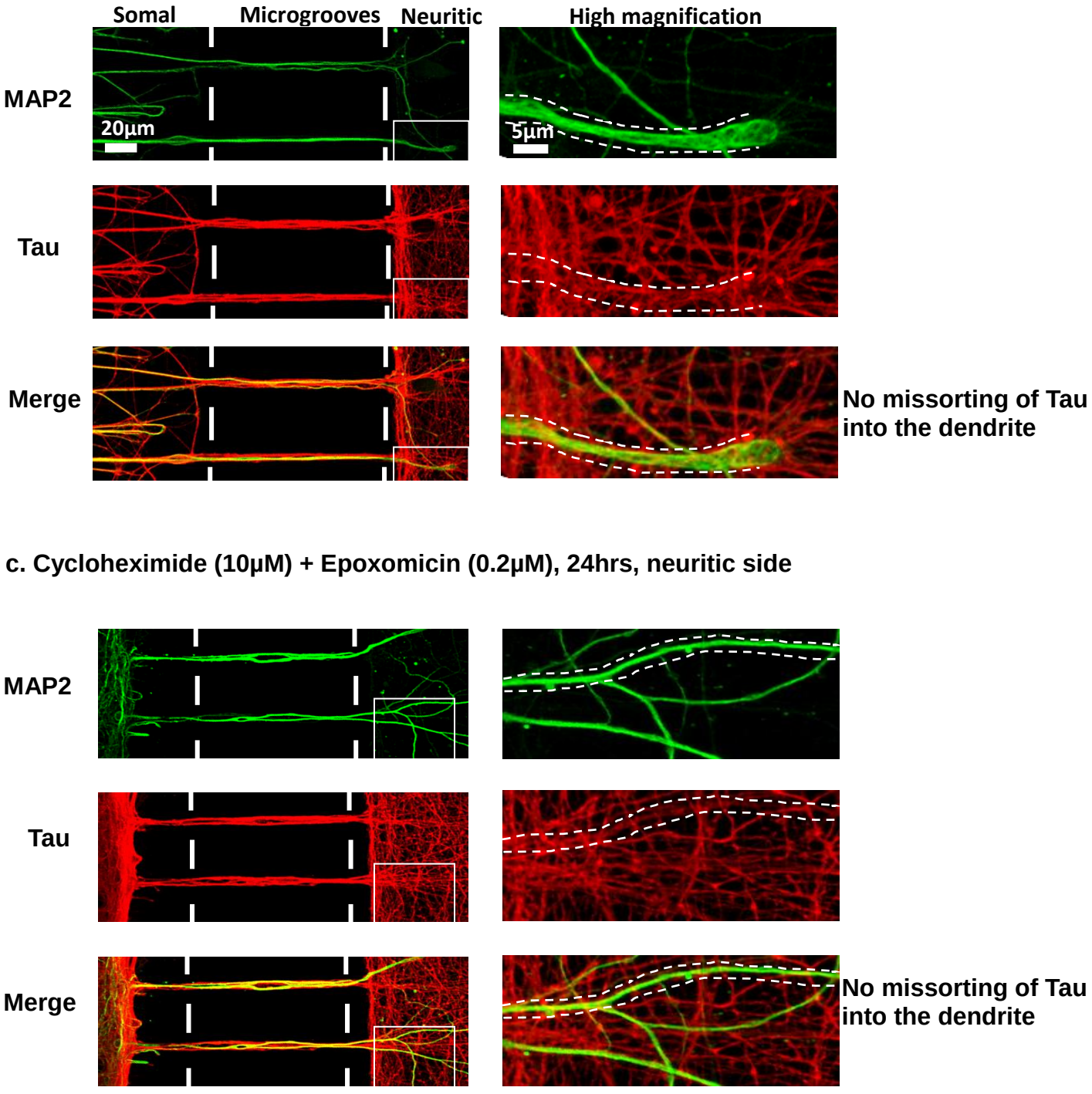

Treatment on the neuritic side for 24h with the protein translation inhibitor - cycloheximide combined either with the autophagy inhibitor - wortmannin (b) or with the proteasomal inhibitor - epoxomicin (c).
(b, c) When the neurons were treated with cycloheximide (10μM) together with wortmannin (1μM) (b) or with epoxomicin (0.2μM) (c) for 24hrs, there was no significant increase in the dendritic accumulation of Tau seen and the percentage of dendritically mislocalized Tau remains as low as in the control (quantification in h, see bars 5 and 7). Scale bars in the main images = 20μm; in all the insets = 5μm.

Fig 3.16: Protein translation inhibitors prevent Tau missorting

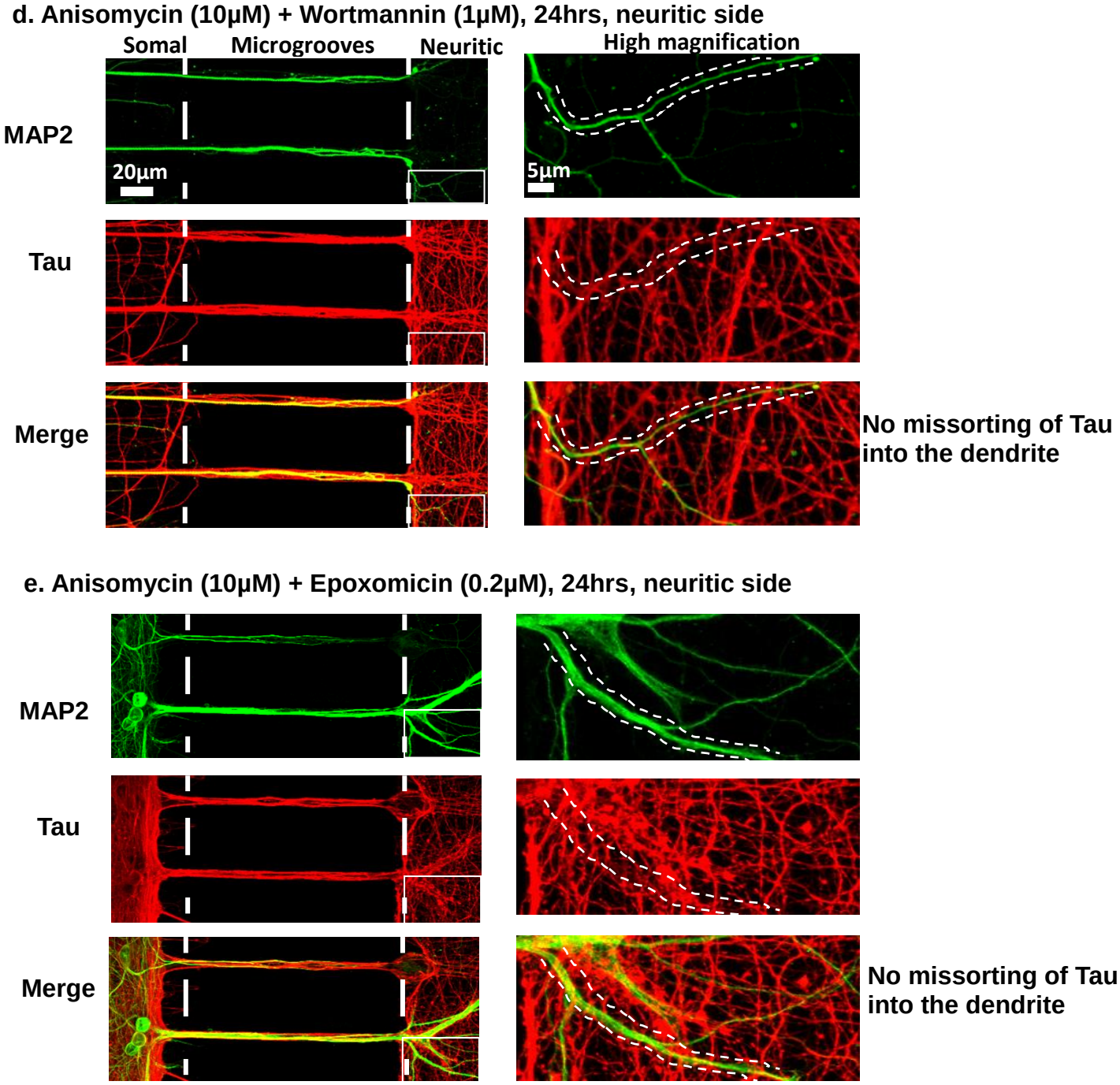

Treatment on the neuritic side for 24h with the protein translation inhibitor - anisomycin combined either with the autophagy inhibitor - wortmannin (d) or with the proteasomal inhibitor - epoxomicin (e).
(d, e) When the neurons were treated with anisomycin (10μM) together with wortmannin (1μM) (d) or with epoxomicin (0.2μM) (e) for 24h, there was no increase in the accumulation of Tau seen and the percentage of dendritically mislocalized Tau remains as low as in the control (quantification in h, see bars 9 and 11). Scale bars in the main images = 20μm; in all the insets = 5μm.

Fig 3.16: Protein translation inhibitors prevent Tau missorting

f. Cycloheximide (Protein translation inhibitor - 10µM), 24hrs, neuritic side

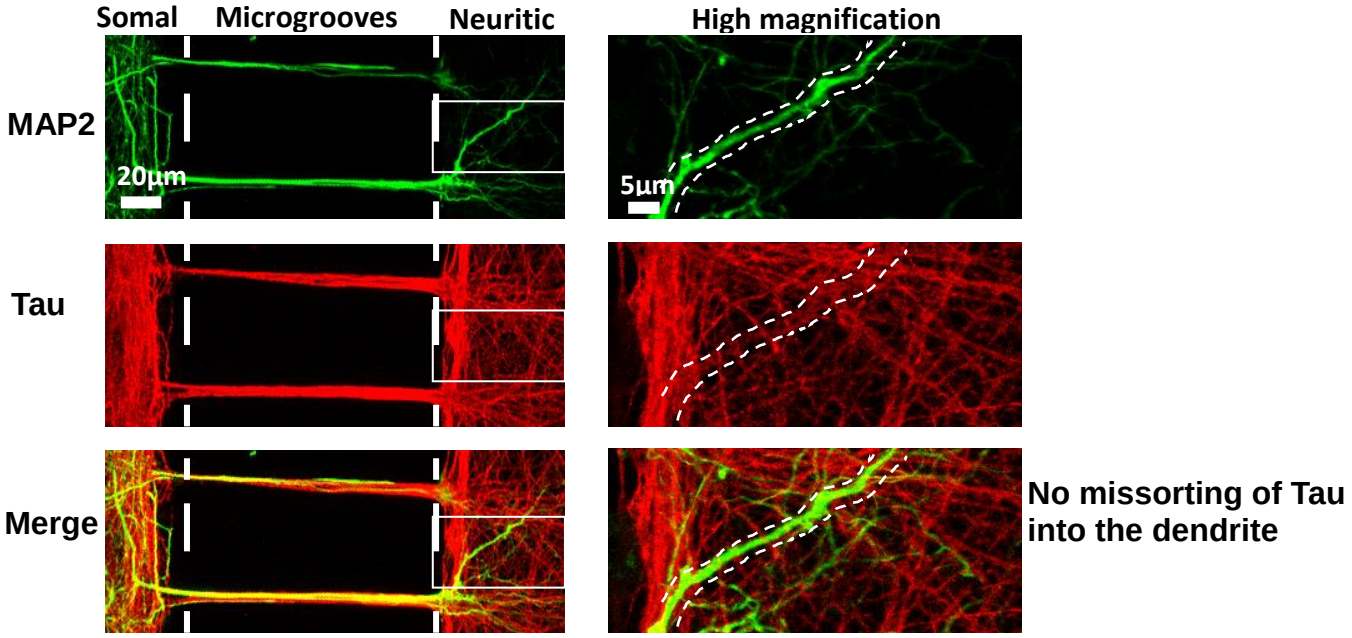

g. Anisomycin (Protein translation inhibitor - 10µM), 24hrs, neuritic side

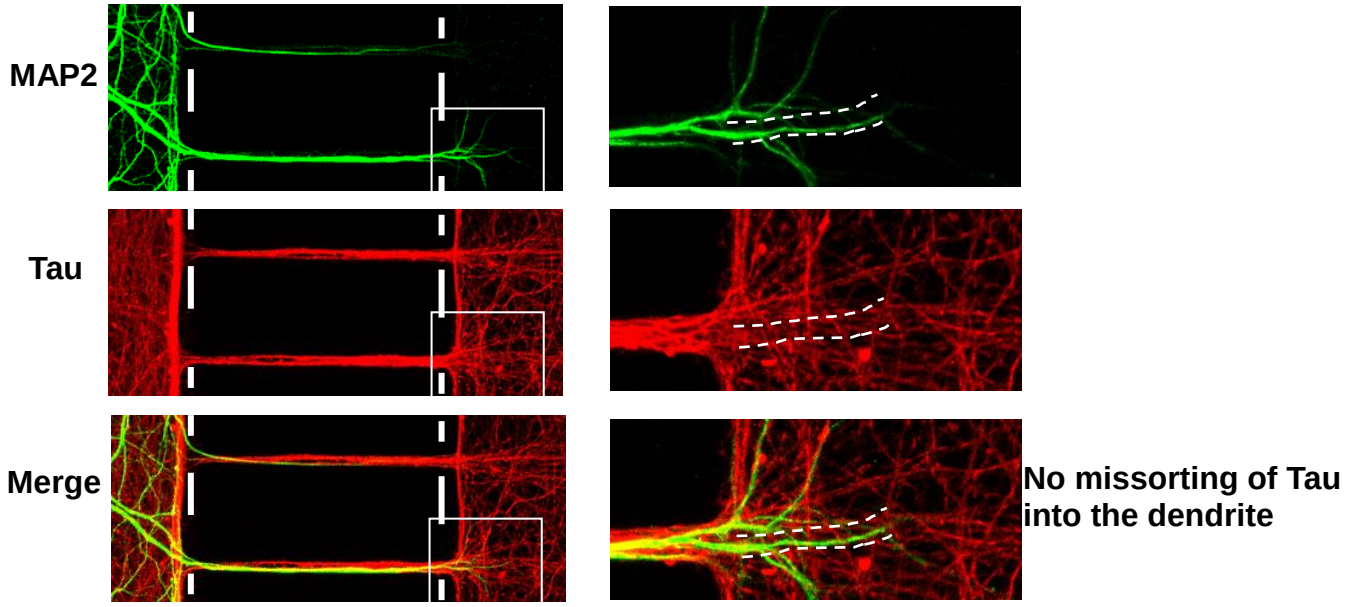

Treatment on the neuritic side for 24h with just cycloheximide (f) or with anisomycin (g).
(**f, g**) When the neurons were treated with cycloheximide (10µM) alone (f) or with anisomycin (10µM) alone (g) for 24hrs, there was no accumulation of Tau in the dendrites on the neuritic side seen (quantification in h, see bars 2 and 3). Scale bars in the main images = 20µm; in all the insets = 5µm.

Fig 3.16: Protein translation inhibitors prevent Tau missorting

h. Quantification of dendrites with Tau missorting after treatment with protein translation inhibitors alone or together with protein degradation inhibitors

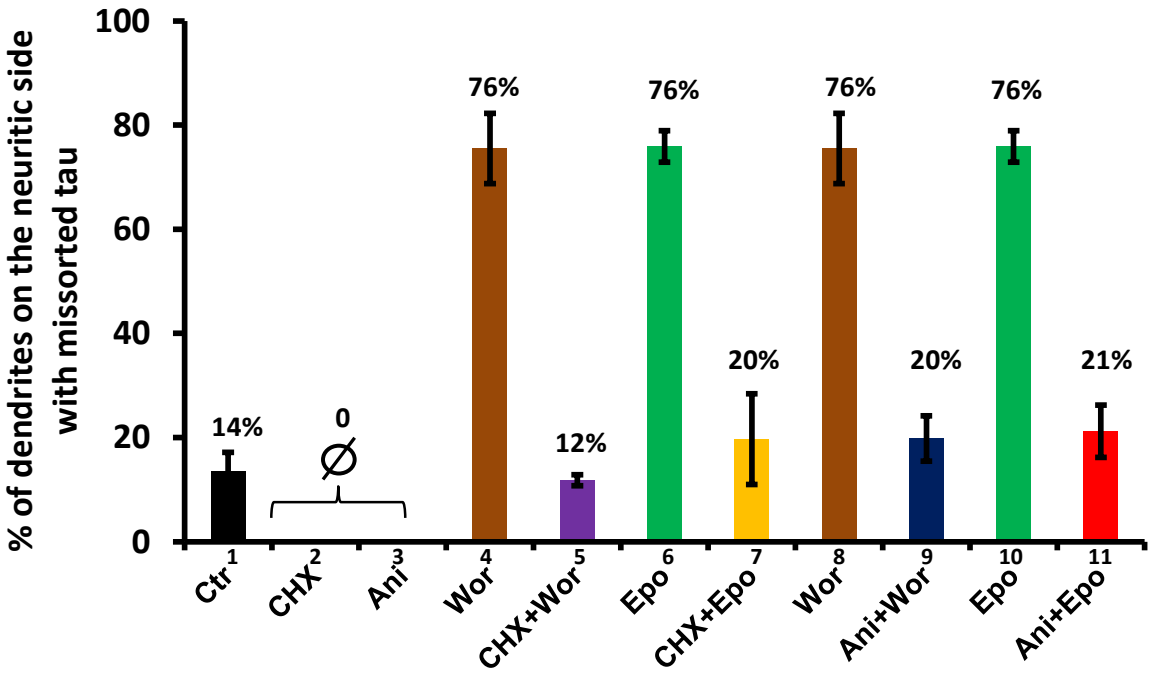

(**h**) Quantification of dendrites on the neuritic side showing co-localization of Tau with MAP2 following different treatments. Error bars, SEM from *n* = 100 – 150 dendrites from 3-4 chambers in each condition. No significant difference between Ctr (bar 1), CHX+Wor (bar 5), CHX+Epo (bar 7), Ani+Wort (bar 9) and Ani+Epox (bar 11). Protein translation inhibitors – cycloheximide (bar 2) and anisomycin (bar 3) prevent Tau missorting.

3.2.11 Tau mRNA distributes to the dendrites, axons and cell bodies

Since we showed that missorted Tau in the dendrites was derived from local synthesis, the distribution of Tau mRNA in dendrites was no surprise. However, up to date, the subcellular distribution of Tau mRNA in neurons remains an issue under debate. While it was demonstrated that Tau mRNA only localizes to the cell body and the proximal region of the axon (Litman et al., 1993), the other study argued that it distributes to proximal dendrites as well (Kosik et al., 1989). Thus, to clarify this issue, we performed fluorescence in situ hybridization assays to assess the distribution of Tau mRNA in cultured rat hippocampal neurons. The rat Tau mRNA probe we used was around 1135 base pairs long covering the entire coding region of Tau mRNA and could detect all the isoforms of Tau mRNA.

The in situ hybridization process was followed by immunostaining with the somatodendritic marker MAP2 and the axonal marker - Tau (K9JA antibody) **(Fig.**

3.17a). Although Tau mRNA predominantly distributes into the cell body (180.36±21.66 Tau mRNA puncta/cell body), a small amount of Tau mRNA was detected in dendrites as well (19.9±3.48 Tau mRNA puncta/50-100µm length of a dendrite; **Fig. 3.17, a & quantification in Fig. 3.17b, bars 1 and 2**). To rule out the possibility of non-specificity of the probe used, staining without probe was also done in parallel. No positive signal for mRNA was observed **(Fig. 3.17c)**. This observation together with the above finding that the dendritic Tau was due to local synthesis, confirms our result that Tau mRNA is present in the dendrites and is actively translated.

Fig 3.17. a. Fluorescence insitu hybridization reveals Tau mRNA across all compartments of the neuron

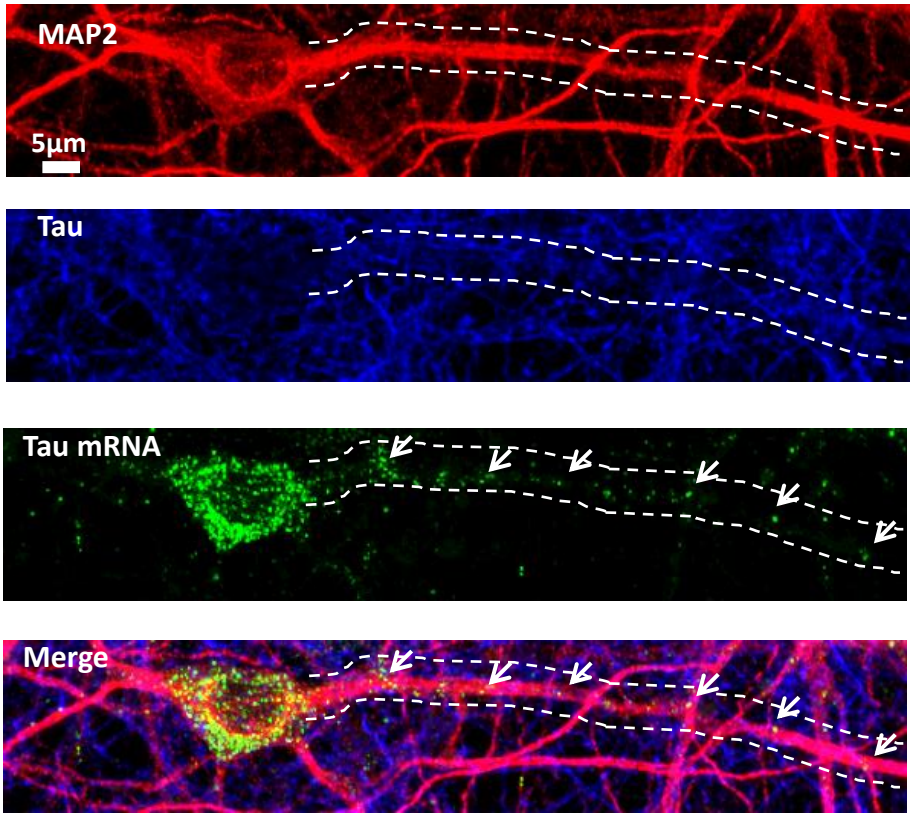

(a) Tau mRNA in cultured rat hippocampal neurons (DIV 21-25) monitored by fluorescence in situ hybridization with a rat Tau mRNA probe. Axons and dendrites were visualized by immunostaining with pan-Tau antibody K9JA (blue) and anti-MAP2 antibody (red), respectively following the insitu hybridization procedure. First panel shows staining with MAP2 antibody for dendrites and cell bodies, second panel shows staining with K9JA antibody for Tau, highlighting axons, followed by the third panel indicating Tau mRNA localization (green puncta). Note that Tau mRNA is present across all compartments of the neuron. The dendrites also contain a sparse distribution of Tau mRNA as indicated by white arrows. Scale bar = 5µm.

Fig 3.17: Fluorescence insitu hybridization reveals Tau mRNA across all compartments of neurons

b. Quantification of the number of Tau mRNA puncta in cell body and dendrites

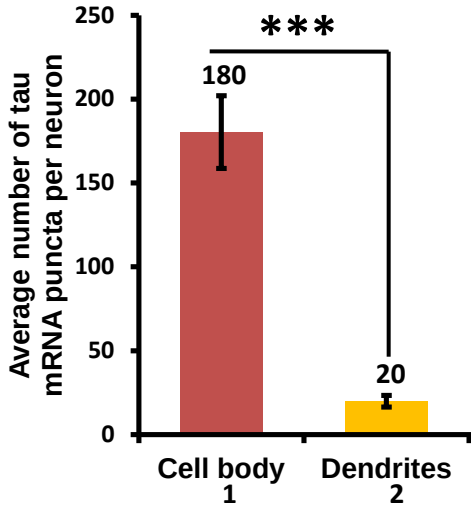

c. No probe - negative control

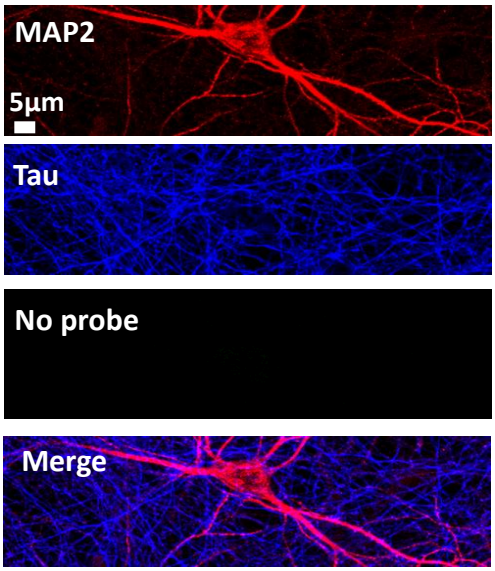

(b) Quantification of the average number of Tau mRNA puncta in the cell body (bar 1) v.s dendrites (bar 2). Error bars, SEM from *n* = 50 - 60 dendrites from 3 individual experiments. ****p* < 0.005 using Student's *t* test.
(c) Tau mRNA in cultured rat hippocampal neurons (DIV 21-25) monitored by fluorescence in situ hybridization without adding Tau mRNA probe. Axons and dendrites were visualized by immunostaining with pan-Tau antibody K9JA (blue) and anti-MAP2 antibody (red), respectively following insitu hybridization procedure. First panel shows staining with MAP2 antibody for dendrites and cell bodies, second panel shows staining with K9JA antibody for Tau, highlighting axons. Since no probe was used in the analysis the third panel is blank showing the absence of mRNA puncta which indicate the specificity of the probe used in the Fluorescence insitu hybridization (FISH) analysis. Scale bar = 5µm.

3.3 Impact of experimental manipulations on the missorting of Tau protein

Tau is mainly in the axons of mature neurons under physiological conditions (Zempel and Mandelkow, 2014), but surprisingly, the missorting of Tau in the majority of mature cultured neurons was often observed (Migheli et al., 1988, Papasozomenos and Binder, 1987, Mondragon-Rodriguez et al., 2012, Dotti et al., 1987). The cause of the missorting in these studies has not been addressed.

The role of fixation in the physiological localization of Tau protein has been studied in human fibroblasts (Rossi et al., 2008) although only a few fixation methods were used and a confirmatory study in neurons was lacking which could lead to erroneous interpretations. By analogy, the fixation protocols might be responsible for the observed missorting of Tau in cultured neurons in other studies.

We therefore investigated the role of fixation protocols in the sorting of endogenous Tau in mature neurons in culture, in order to figure out an ideal protocol that can result only in a basal level of Tau missorting. We tested a variety of fixation protocols used widely in the literature to study Tau missorting. We focused on the influence of the fixative, fixation temperature and fixation time on the distribution of Tau. In addition, in some protocols sucrose was added to the fixation solution in order to preserve the native state of tubulin (Morejohn and Fosket, 1984). Thus we also examined the impact of sucrose on Tau distribution.

Neurons fixed with formaldehyde together with sucrose at 37°C for 30 minutes (Deshpande et al., 2008) resulted in only ~15% of neurons with Tau missorting **(Fig. 3.18a, i & quantification in Fig. 3.18b)** although fixing neurons with formaldehyde for 30 minutes at 37°C (Mann et al., 1987) in the absence of sucrose resulted in around 25% of neurons with Tau missorting **(Fig. 3.18a, ii)**. Fixation with glutaraldehyde (Weber et al., 1978) for 30minutes at 37°C resulted in all cells with missorted Tau irrespective of the presence or absence of sucrose **(Fig. 3.18a, iii, iv & quantification in Fig. 3.18b)**. Fixing neurons with formaldehyde in combination with sucrose (Kusser and Randall, 2003) for 15 minutes at room temperature **(Fig. 3.18a, v)** resulted in around 25% of neurons with missorted Tau. On the other hand, fixing neurons with formaldehyde at room temperature for 15minutes (Mondragon-Rodriguez et al., 2012) in the absence of sucrose **(Fig. 3.18a, vi)** resulted in around 60% of neurons with Tau missorting. All neurons in cultures showed missorting of Tau when fixed with glutaraldehyde at room temperature for 15minutes irrespective of the presence or absence of sucrose **(Fig. 3.18a, vii & viii)**. Interestingly, while fixation with cold methanol (-20°C) (Dotti et al., 1987) resulted in around 60% neurons with Tau missorting **(Fig. 3.18a, ix)**, fixation with acetone (Alshammari et al., 2016) also resulted in missorting of Tau in a significantly higher percentage of neurons (around 80%) **(Fig. 3.18a, x & quantification in Fig. 3.18b).** Overall, the optimal procedure to ensure proper sorting of Tau to the axonal compartment, would be to fix neurons with formaldehyde together with sucrose for 30minutes at 37°C **(Fig. 3.18a, i and bar1 circled in orange in Fig. 3.18b)**. This is because the fast penetrance of formaldehyde in combination with the protein preserving nature of sucrose and 37°C enable the analysis of proteins in its native form and localization.

Fig 3.18. a. Tau redistributes into the somatodendritic compartment after experimental manipulations

i. Formaldehyde (FA)/Sucrose, 30‘, 37degrees **~ 15% neurons with Tau missorting**

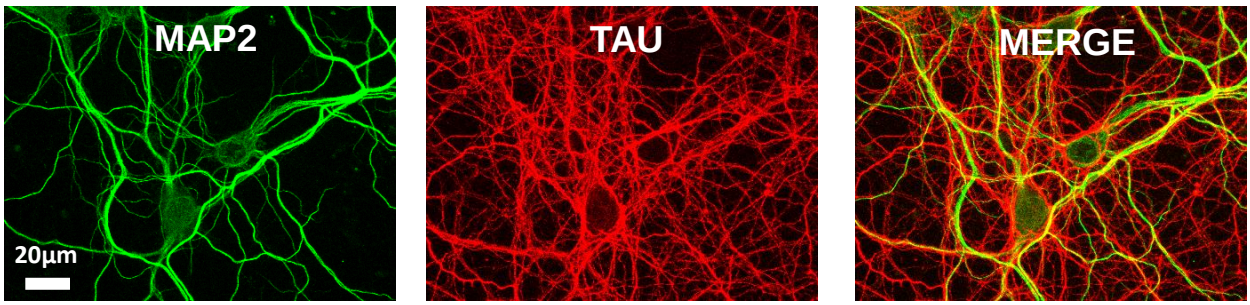

ii. Formaldehyde (FA), 30‘, 37degrees **~ 25% neurons with Tau missorting**

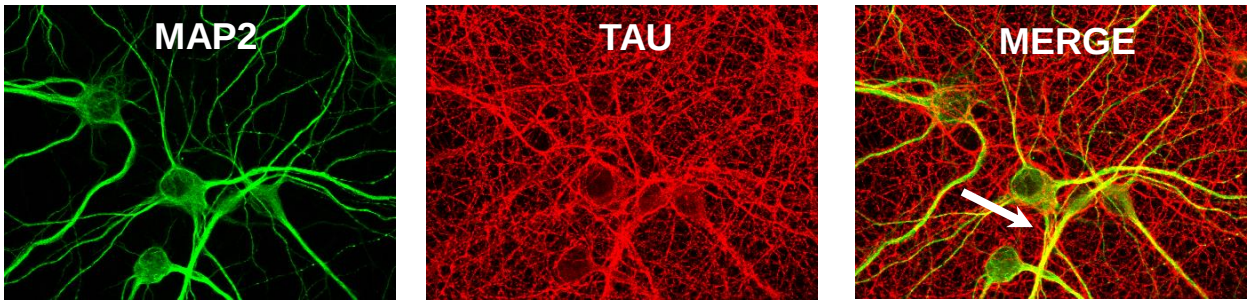

iii. Glutaraldehyde (Glu), 30‘, 37deg **100% neurons with Tau missorting**

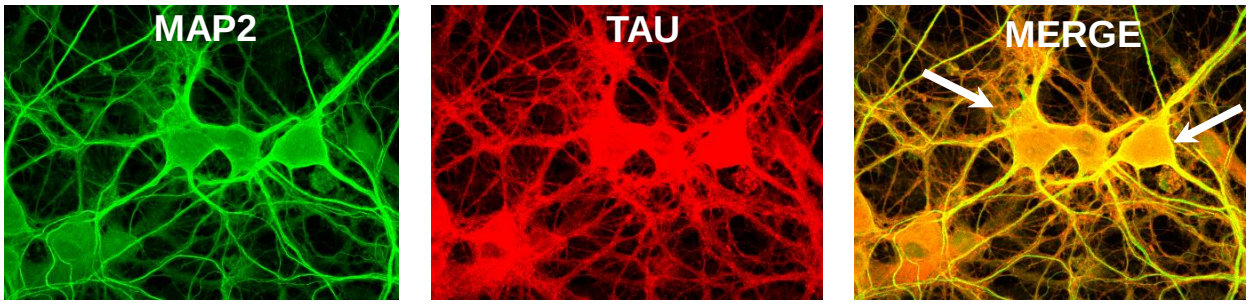

iv. Glutaraldehyde (Glu)/Sucrose, 30‘, 37deg **100% neurons with Tau missorting**

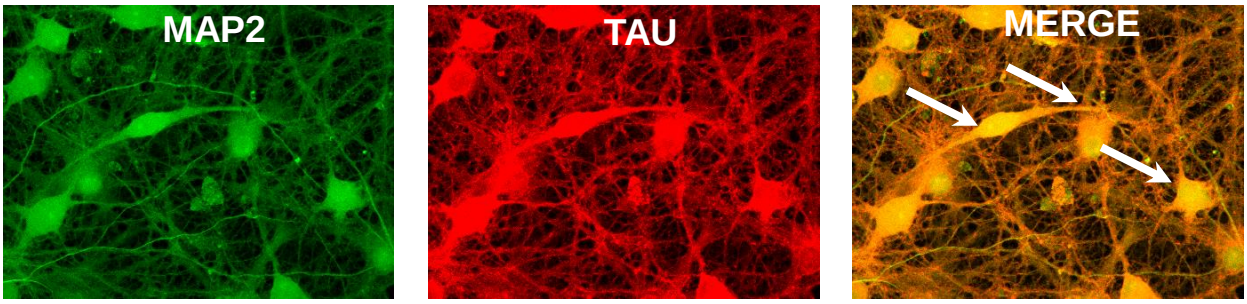

Rat hippocampal neurons (DIV 21) cultured conventionally on coverglasses in 24-well plates and fixed with different fixation procedures and stained. Each figure represents a double immunostaining for Tau (red) and MAP2 (green).
(a, i-iv) Neurons fixed with Formaldehyde and sucrose for 30minutes at 37degrees show a basal level of Tau missorting (i, ~15% neurons with Tau missorting) whereas when fixed with Formaldehyde alone for 30minutes at 37degrees a little higher level of missorting was seen (arrow in ii, ~25% neurons with Tau missorting). When neurons were fixed with glutaraldehyde with or without sucrose for 30minutes at 37 degrees (iii & iv, 100% neurons with Tau missorting) all neurons in the culture showed mislocalization of Tau (indicated by arrows, quantification in b). Scale Bar = 20µm.

Fig 3.18. a. Tau redistributes into the somatodendritic compartment after experimental manipulations

v. Formaldehyde (FA)/Sucrose, 15‘, Room temperature

~ 25% neurons with Tau missorting

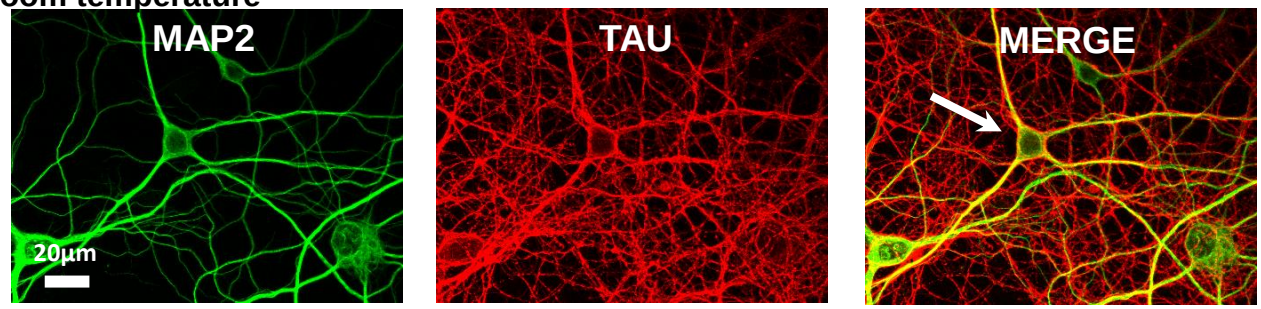

vi. Formaldehyde (FA), 15‘, Room temperature

~ 60% neurons with Tau missorting

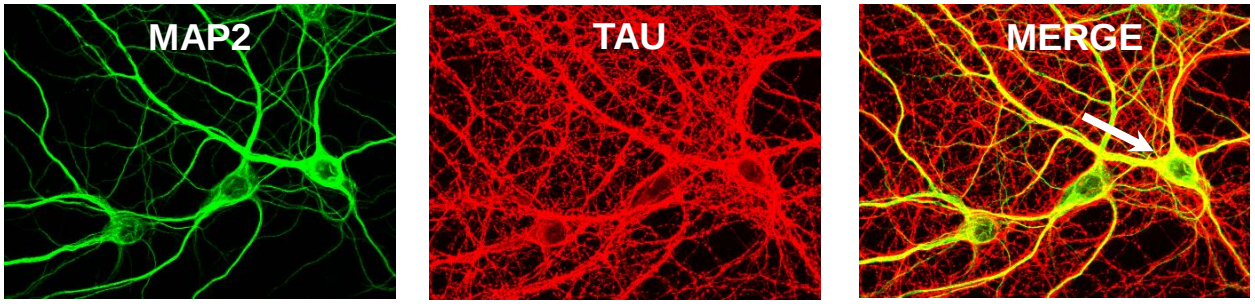

vii. Glutaraldehyde (Glu), 15‘, Room temperature

100% neurons with Tau missorting

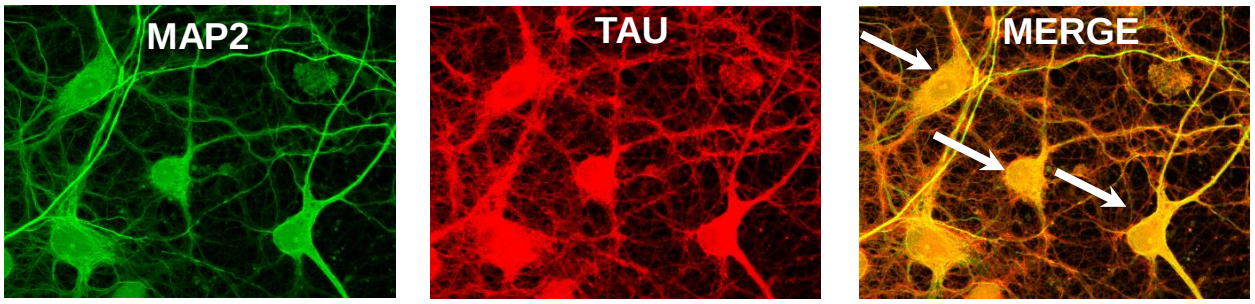

viii. Glutaraldehyde (Glu)/Sucrose, 15‘, Room temperature

100% neurons with Tau missorting

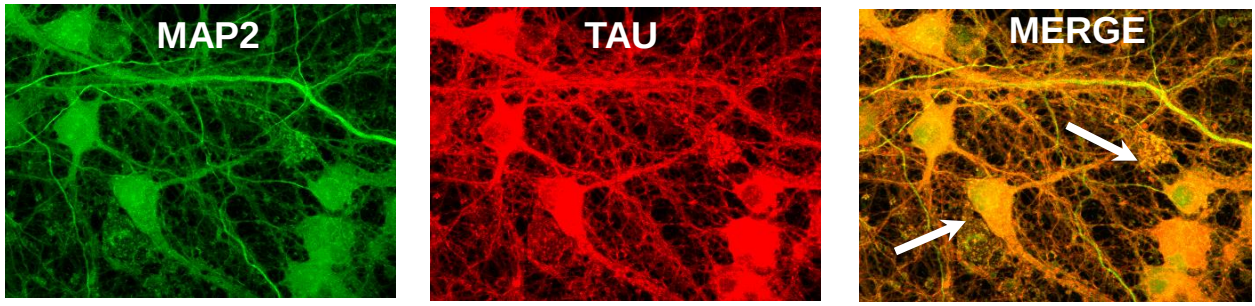

(a, v-viii) Missorting of Tau was also observed when neurons were fixed with Formaldehyde and sucrose for 15minutes at room temperature (v, ~25% neurons with Tau missorting) although a little higher than the basal level (~15% neurons with Tau missorting). Tau missorting was significantly higher when neurons were fixed with Formaldehyde for 15 minutes at room temperature (vi, ~60% neurons with Tau missorting). When neurons were fixed with glutaraldehyde with or without sucrose for 15minutes at room temperature (vii & viii, 100% neurons with Tau missorting), all neurons showed mislocalization of Tau (indicated by arrows, quantification in b). Scale Bar = 20µm.

Fig 3.18. a. Tau redistributes into the somatodendritic compartment after experimental manipulations

ix. Ice-cold methanol,10', Room temperature **~ 60% neurons with Tau missorting**

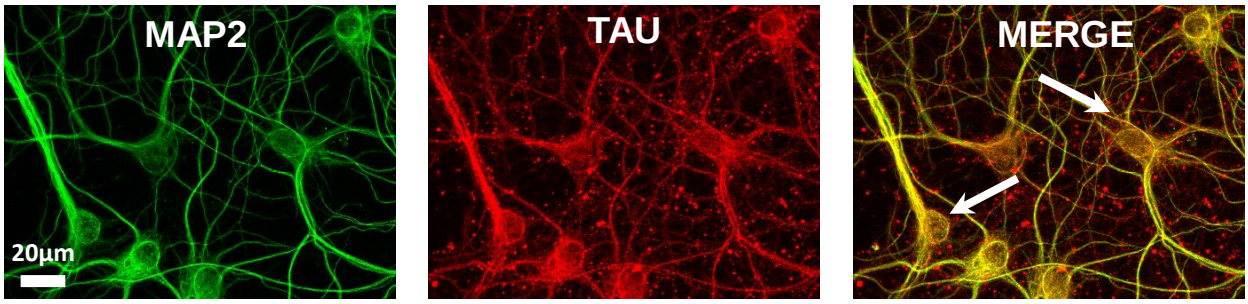

x. Ice-cold acetone, 10', Room temperature **~ 80% neurons with Tau missorting**

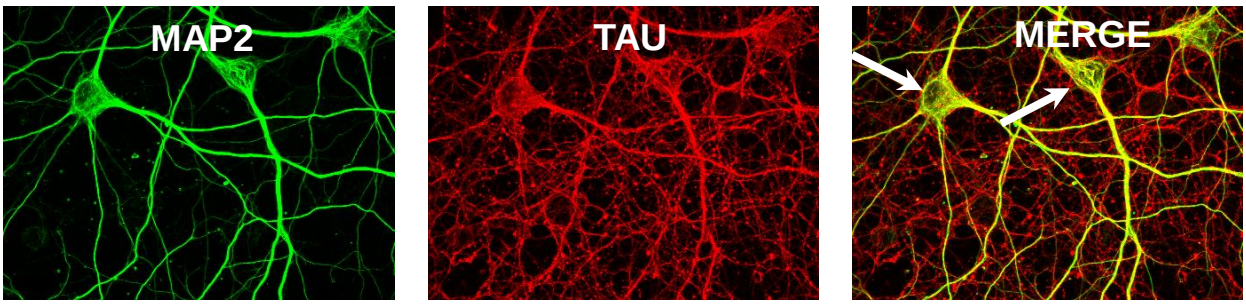

(a, ix & x) Tau missorting was significantly higher when neurons were fixed with ice-cold methanol for 10minutes at room temperature (ix, ~60% neurons with Tau missorting) and with ice-cold acetone for 10minutes at room temperature (x, ~80% neurons with Tau missorting) as indicated by arrows. Scale Bar = 20µm.

b. Quantification of neurons with Tau missorting following fixation with different protocols

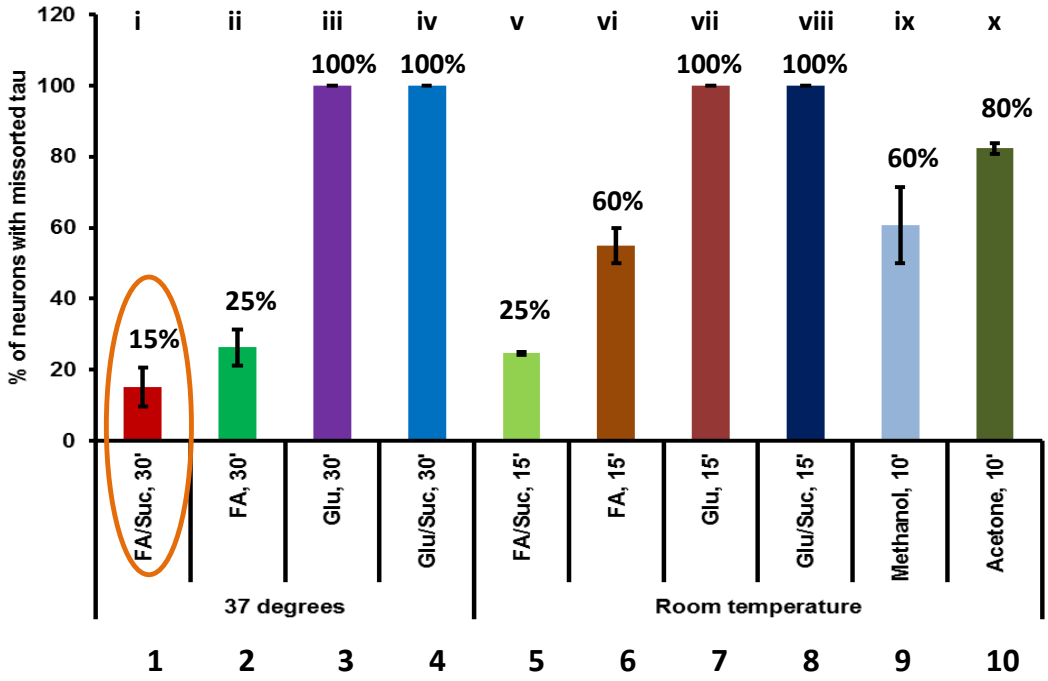

(b) Quantification of neurons with Tau missorting following fixation with different fixation procedures. Error bars, SEM from *n* = 50-80 neurons from 3 independent cultures in each condition.

3.4 Spreading of Tau via exosomes

Having delineated the mechanisms for Tau sorting to the axons, we next investigated the spreading of Tau protein from one neuronal population to another. Given the load of Tau protein in the axons, one could predict that it could possibly spread to the adjacent neurons (Zempel and Mandelkow, 2014) to exert its toxic effects and might continue to spread further. Although several mechanisms have been proposed, one of the important modes of Tau spreading across different neuronal populations could be via exosomes since exosomes are released by neurons (Faure et al., 2006) and were found to contain Tau (Polanco et al., 2016). The mechanism of Tau spreading across neurons via exosomes remains still elusive. It could be either that the exosomes are released from one neuron and then taken up by the adjacent neuron or the exosomes containing Tau could get transmitted across neurons via synapses although the evidence for this mechanism is still missing.

Since endogenous Tau can be released via exosomes, we examined whether exosomes can act as carriers to mediate the transmission of Tau between cells. In order to directly monitor Tau-containing exosomes, we prepared exosomes from N2a cells transiently over-expressing human Tau tagged with GFP at the N-terminus (longest isoform in CNS, 2N4R or hTau40, for short - Tau^{GFP}). To investigate the neuron-to-neuron transmission of exosomal Tau, we took advantage of microfluidic devices since it allows the culture of two populations of neurons in two separate chambers connected by microgrooves, enabling the direct observation of the transfer of exosomal Tau from neurons on one side (somal side) to neurons on the other side (neuritic side) **(schematic in Fig. 3.19,b and d)**. One caveat is that the uptake of exosomes can occur both at the somatodendritic and axonal compartments of neurons (Fruhbeis et al., 2013). Thus even though exosomes were added to the somal side of the chamber, some neurons on the neuritic side projecting through microgrooves might obtain exosomes via direct axonal uptake, independently of the transfer of exosomes from neurons seeded on the somal side. To solve this issue, we seeded the 1^{st} order neurons on the somal side two weeks earlier than the 2^{nd} order neurons on the neuritic side, anticipating that the projections from the 1^{st} order neurons occlude the microgrooves and thus eliminate axons and dendrites from the 2^{nd} order neurons to project through microgrooves to the other side.

To test whether indeed only the 1st order neurons project through the microgrooves, we selectively stained either the 1st order neurons on the somal side **(Fig. 3.19c)** or the 2nd order neurons on the neuritic side **(Fig. 3.19a)** with DiI and monitored the staining of cells by live imaging. When the 2nd order neurons were stained with DiI, the cell bodies of some of the 1st order neurons on the somal side were also positive for DiI, because their neurites projected through microgrooves into the neuritic side **(arrowhead in Fig. 3.19a)**. By contrast, when the 1st order neurons were stained with DiI, no cell bodies of the 2nd order neurons were positive for DiI, although neurites from the 1st order neurons that projected through microgrooves into the neuritic side were labeled by DiI **(Fig. 3.19c)**. These results confirm that only the 1st order neurons projected through the microgrooves. Accordingly, when the 1st order neurons were treated with Tau^{GFP} exosomes, any Tau^{GFP} found in the neurites or cell bodies of the 2nd order neurons would indicate its transmission from the 1st order neurons.

Treatment of the 1st order neurons on the somal side at DIV25 with Tau^{GFP} exosomes resulted in the transmission of Tau^{GFP} across neurites in microgrooves **(Fig. 3.19e, left panels)**, indicating the uptake and transmission of Tau^{GFP} exosomes by the 1st order neurons on the somal side. In addition, in ~4% (4.3±0.4%) of the 2nd order neurons (DIV11), the accumulation of Tau^{GFP} puncta in cell bodies was observed **(Fig. 3.19e, right panels)**, suggesting the transmission of Tau^{GFP} from the 1st order neurons to the 2nd order neurons. The Tau^{GFP} in 2nd order neurons was visible in flotillin positive vesicles, likely exosomes **(Fig. 3.19f)**. Such Tau^{GFP} puncta in 2nd order neurons may come from two sources: (1) from Tau^{GFP} exosomes internalized by the 1st order neurons; (2) from newly synthesized exosomes in the 1st order neurons which contain Tau^{GFP} released by the internalized exosomes. To distinguish between these two possibilities, we pre-treated 1st order neurons with spiroepoxide (5µM) to block the biogenesis of exosomes (Li et al., 2013) before treatment with Tau^{GFP} exosomes. The spiroepoxide treatment does not affect the transmission of Tau^{GFP}, as Tau^{GFP} puncta were observed in ~4% of the 2nd order neurons **(Fig. 3.19g)**. This rules out novel synthesis (option 2) and indicates that Tau^{GFP} exosomes can be taken up by 1st order neurons and then directly be transmitted to 2nd order neurons (option 1). As a second line of investigation, we sought to test whether Tau^{GFP} exosomes internalized by the 1st order neurons can be directly transmitted to the 2nd order neurons (option 1). To this end, we isolated exosomes from N2a cells

co-transfected with Flotillin^{GFP} and RFP-Tau (Tau^{RFP}). We utilized 3-chamber devices, as they allow the observation of the transmission of exosomes to an additional population of neurons in the 3rd chamber. We reasoned that if puncta in the 2nd or 3rd order neurons contain both Tau^{RFP} and Flotillin^{GFP}, they would represent the exosomes internalized by the 1st order neurons, as it is unlikely that the newly synthesized exosomes in the 1st or 2nd order neurons encapsulate both Tau^{RFP} and Flotillin^{GFP} released by the internalized exosomes. As shown in **Fig. 3.19h**, when the 1st order neurons were treated with Tau^{RFP} and Flotillin^{GFP} exosomes, majority of puncta in the 2nd order neurons were positive for both Tau^{RFP} and Flotillin^{GFP}. In addition, puncta containing Tau^{RFP} and Flotillin^{GFP} were also observed in the 3rd order neurons. These results suggest that exosomes can indeed be directly transmitted between neurons.

Fig. 3.19: Transmission of Tau^{GFP} exosomes from one neuronal population to the other in microfluidic chambers

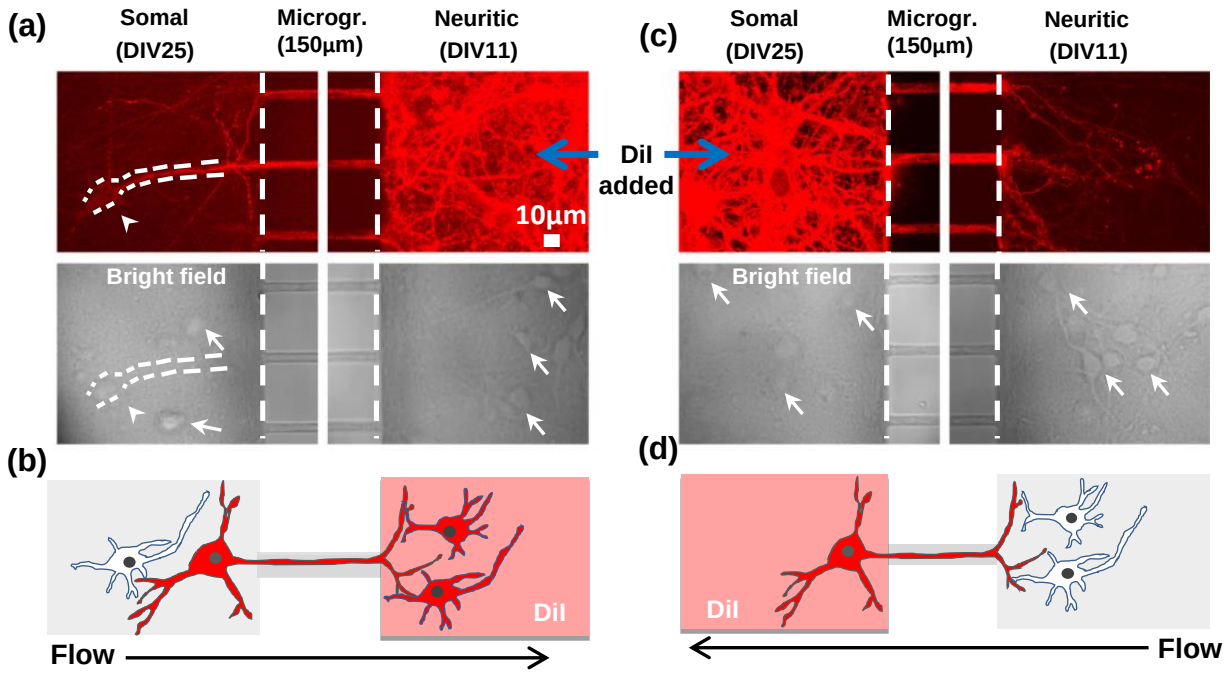

(a-d) The 1st order hippocampal neurons were seeded on the somal side (left) of the microfluidic chamber. Fourteen days later, the 2nd order hippocampal neurons were seeded on the neuritic side (right) and cultured for additional 10-11 days. Neurons were treated on the neuritic side (a) or somal side (c) with DiI for 2h to 3h. The living cells were then imaged using fluorescence microscopy. When the 2nd order neurons on the neuritic side were treated with DiI (a, top right panel), cell bodies of the 1st order neurons whose neurites projected through microgrooves to the neuritic side were positive for DiI staining (arrowhead in a, top left panel), by contrast, cell bodies of neurons that do not project to the neuritic side were not positive for DiI staining (arrows in a, bottom left panel). When the 1st order neurons on the somal side were treated with DiI (c, top left panel), their processes that projected through microgrooves to the neuritic side were stained by DiI (c, top right panel). However, no cell bodies of the 2nd order neurons (arrows in c, bottom right) were positive for DiI staining, indicating that the 2nd order neurons do not project through microgrooves to the somal side. The result of a and c is illustrated by b and d respectively. The flow of the conditioned medium (indicated by arrow) prevents the diffusion of added DiI from treated side to the opposite side. Scale bar = 10µm.

Fig. 3.19: Transmission of Tau^{GFP} exosomes from one neuronal population to the other in microfluidic chambers

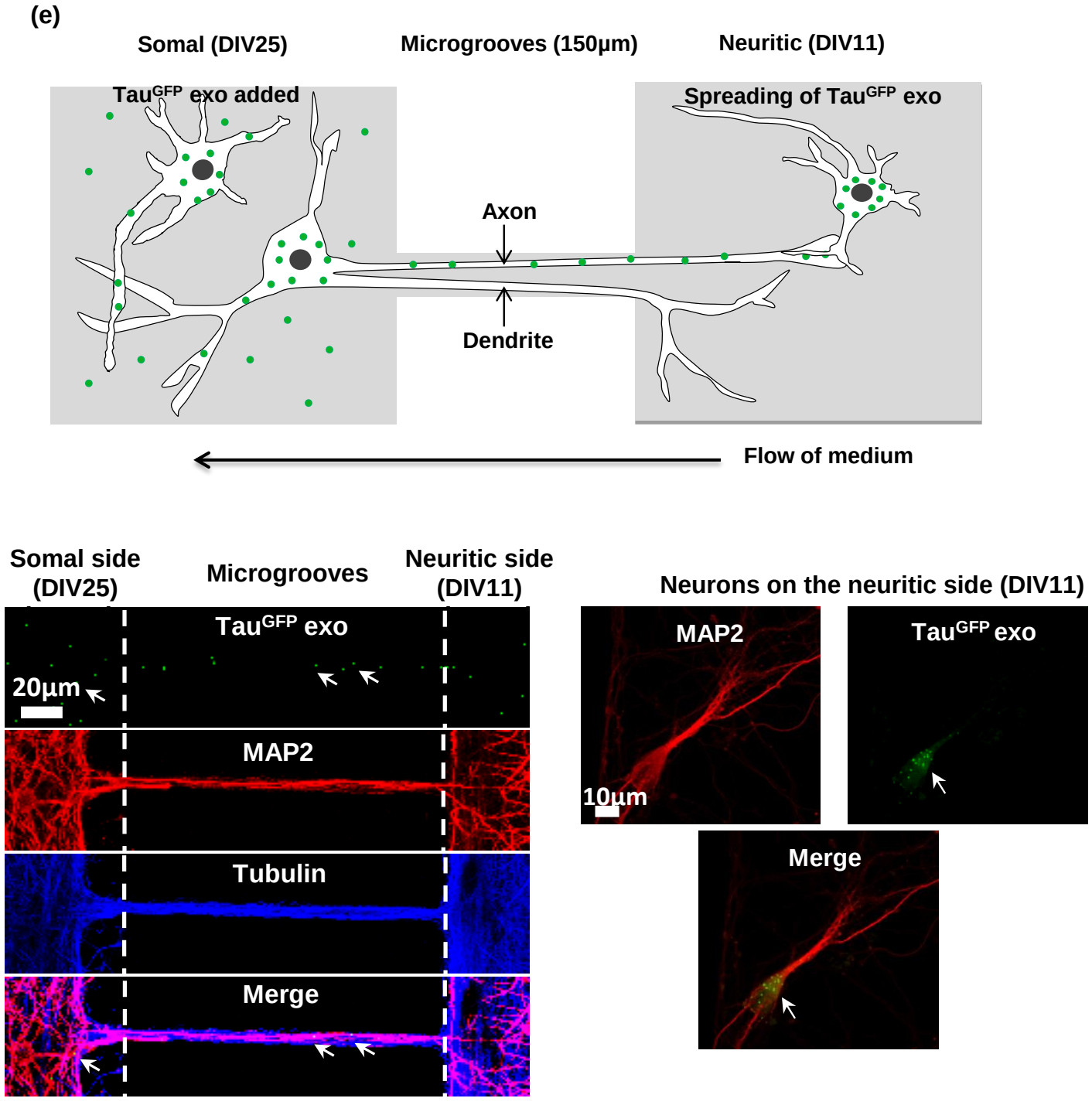

(e) Uptake and transmission of Tau^{GFP} by neurons cultured in microfluidic chambers with short microgrooves (150µm). The 1st order neurons were treated with Tau^{GFP} exosomes at DIV25 for 24 hours, when the 2nd order neurons were at DIV11. Neurons were stained with antibodies against MAP2 (red) and tubulin (blue). Arrows indicate Tau^{GFP} positive vesicles. Note that Tau^{GFP} puncta were detected in the microgrooves (left panel) and also in the 2nd order neurons on the neuritic side (right panels) that was not treated with Tau^{GFP} exosomes, indicating the uptake and the transmission of Tau^{GFP} via exosomes between the two populations of neurons. Scale bar in Left panels = 20µm; right panels = 10µm.

Fig. 3.19: Transmission of Tau^{GFP} exosomes from one neuronal population to the other in microfluidic chambers

(f) **Neurons on the neuritic side (DIV11)**

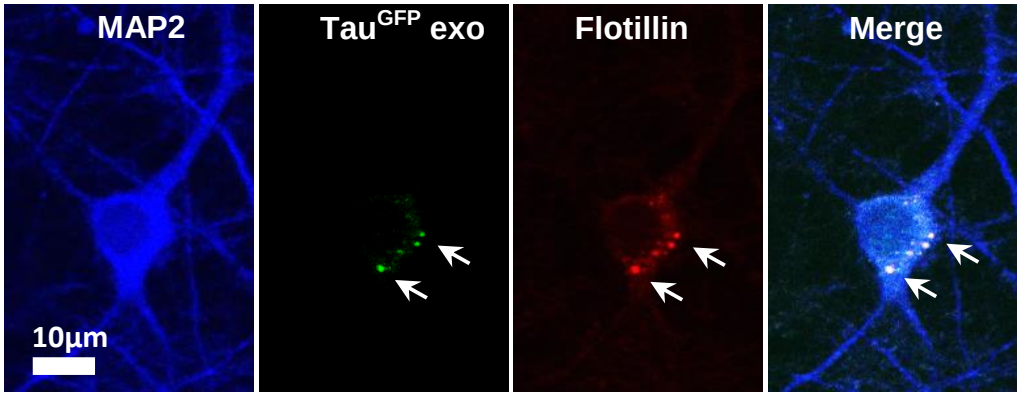

(f) The direct transmission of exosomes from 1st order neurons to the 2nd order neurons in microfluidic chambers. Neurons were treated as described in (e). Neurons were stained with antibodies against MAP2 (blue) and Flotillin (red). Arrows indicate Tau^{GFP} exosomes. The colocalization of Tau^{GFP} with Flotillin indicate that Tau is indeed located in the exosomes. Scale bar = 10µm.

(g) **Somal side (DIV25)** **Microgrooves** **Neurons on the neuritic side (DIV11)**

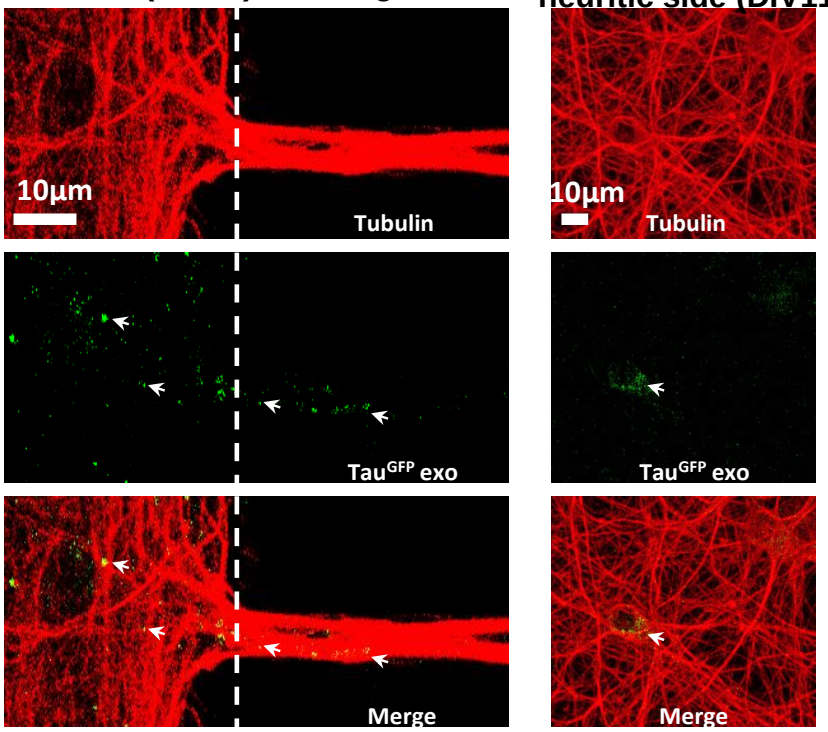

(g) Inhibition of the synthesis of exosomes does not affect the transmission of Tau^{GFP} mediated by exogenous exosomes. The 1st order neurons cultured in microfluidic chambers with short microgrooves (150µm) were treated first with the exosome synthesis inhibitor, spiroepoxide (5µM) for 2 hours and subsequently with Tau^{GFP} exosomes for 24 hours at DIV25, when the 2nd order neurons were at DIV11. Neurons were stained with an antibody against tubulin (red). Arrows indicate Tau^{GFP} positive vesicles. Note that Tau^{GFP} puncta were detected in the microgrooves (left panel) and also in the 2nd order neurons on the neuritic side (right panels) that was not treated with Tau^{GFP} exosomes. This indicates the uptake and the transmission of exogenously added Tau^{GFP} via exosomes between the two populations of neurons and rules out the possibility for the transmission of newly biosynthesized exosomes. Scale bar in left and right panels = 10µm.

Fig. 3.19: Transmission of Tau^{GFP} exosomes from one neuronal population to the other in microfluidic chambers

(h) (i)

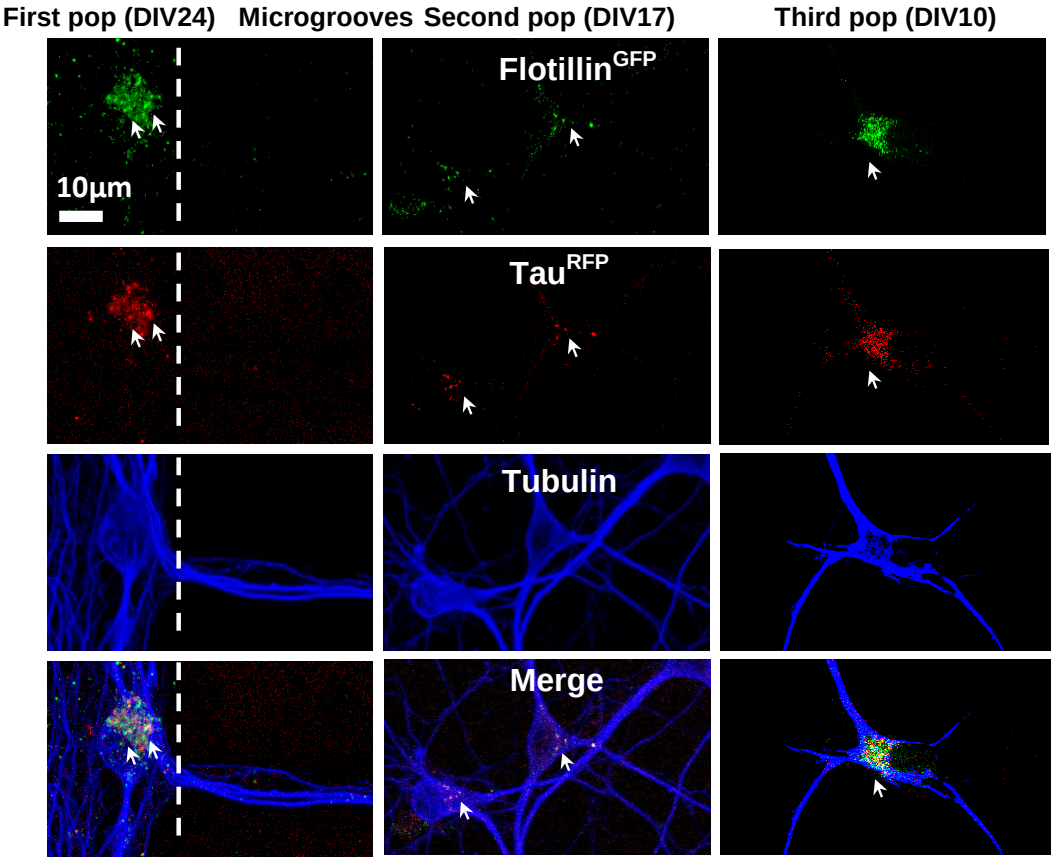

(i) Direct transmission of exosomes from 1st order (or 1st population) neurons to the 2nd and 3rd order (or 2nd and 3rd population) neurons in microfluidic chambers. The 1st order neurons were treated with Tau^{RFP} and Flotillin^{GFP} positive exosomes (20µg) at DIV24 for 24 hours, when the 2nd and 3rd order neurons were at DIV17 and DIV10 respectively. Neurons were stained with an antibody against tubulin (blue). Arrows indicate Tau^{RFP} and Flotillin^{GFP} positive vesicles. Note that Tau^{RFP} and Flotillin^{GFP} positive puncta were detected in the 2nd and 3rd order neurons that were not treated with exosomes, indicating the uptake and the transmission of exosomes between the three populations of neurons. Scale bar = 10µm.

(h) (ii) Quantification of Tau^{RFP} and Flotillin^{GFP} colocalized puncta

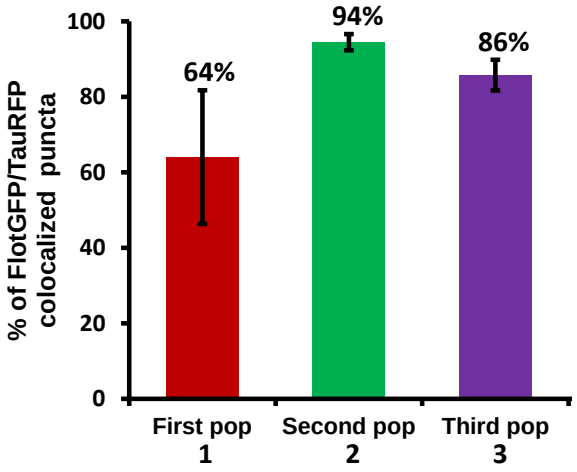

(ii) Quantification of colocalized Flotillin^{GFP} and Tau^{RFP} puncta in the three populations of neurons. Majority of the puncta in 2nd (bar 2, 94.5±3.7% of 220 puncta in 3 different microfluidic chambers) and 3rd populations (bar 3, 85.7±7.1% of 105 puncta in 3 different microfludic chambers) of neurons were positive for both Tau^{RFP} and Flotillin^{GFP}. Error bars, SEM from *n* = 100 - 220 puncta counted from 3 chambers.

3.4.1 Transmission of Tau^{GFP} exosomes can occur via axons

The microfluidic devices with short microgrooves (~150µm) used in the above experiments allow axons and dendrites of the 1st order neurons to reach the neuritic side, enabling the potential transfer of Tau^{GFP} exosomes to 2nd order neurons. To distinguish between axons and dendrites, we performed experiments in microfluidic devices with long microgrooves (~900µm) that prevent dendrites to project to the neuritic side. Tau^{GFP} puncta were detected in both microgrooves and 2nd order neurons **(Fig. 3.20)**, indicating that transmission of Tau^{GFP} can occur through axons.

Fig. 3.20: Transmission of Tau^{GFP} exosomes from one neuronal population to the other can occur via axons

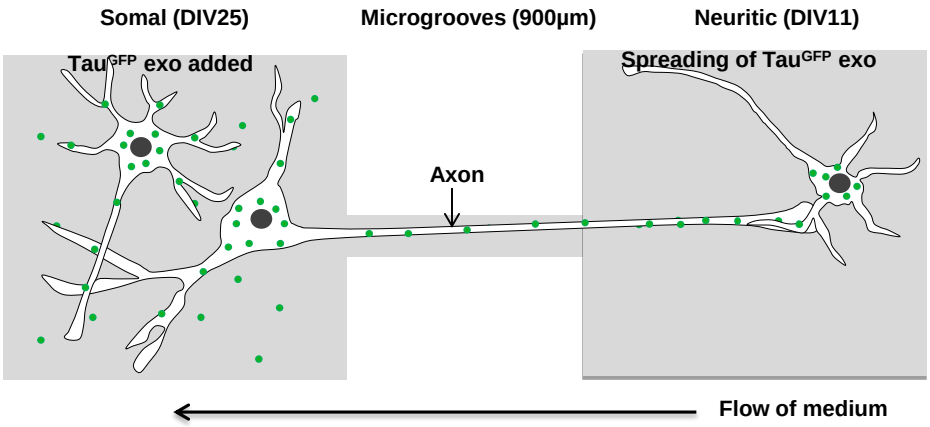

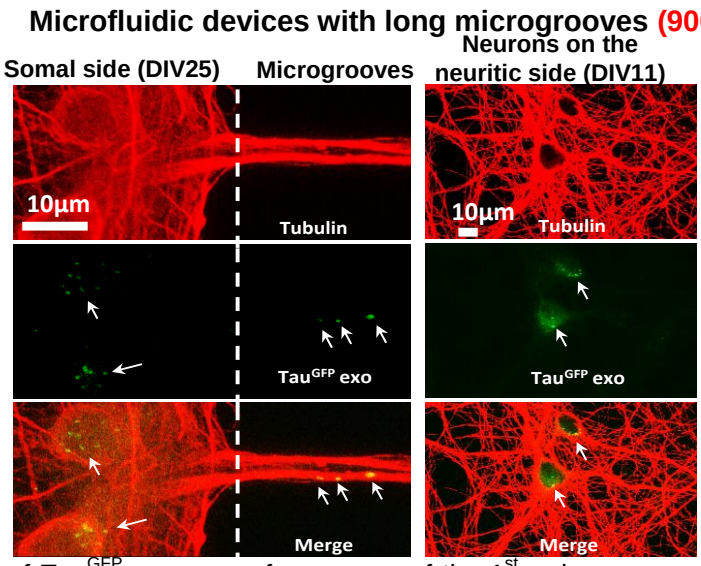

The transmission of Tau^{GFP} exosomes from axons of the 1st order neurons to the 2nd order neurons cultured in microfluidic chambers with long microgrooves (900µm). The 1st order neurons were treated with Tau^{GFP} exosomes at DIV25 for 24 hours, when the 2nd order neurons were at DIV11. Neurons were stained with an antibody against tubulin (red). Arrows indicate Tau^{GFP} positive exosomes. Note that Tau^{GFP} puncta were detected in the microgrooves (left panel) and also in the 2nd order neurons on the neuritic side (right panels) that was not treated with exosomes. Since no dendrites project through the long microgrooves (900µm) to the neuritic side, the transmission of Tau^{GFP} exosomes occurs through axons of the 1st order neuron to the 2nd order neurons. Scale bars in left and right panels=10µm.

3.4.2 Synaptic contacts are required for exosome-mediated transmission of Tau

Since recent studies have suggested that the spreading of Tau occurs by a trans-synaptic mechanism (de Calignon et al., 2012, Dujardin et al., 2014b, Liu et al., 2012), we sought to determine whether and how the transmission of Tau^{GFP} exosomes can occur from the axons of the 1st order neurons to the 2nd order neurons.

Two possible mechanisms may explain the exosome-mediated transmission of Tau. (i) Transmission takes place directly across trans-synaptic connections from 1st order to 2nd order neurons. (ii) Exosomes in 1st order neurons are released into the conditioned medium and then internalized by 2nd order neurons at extrasynaptic sites **(Fig. 3.21a)**. We analyzed the formation of synapses in 2nd order neurons (DIV11) on the neuritic side by examining the co-localization of the post-synaptic marker GluR1 (green) and the pre-synaptic marker synaptophysin (red) **(Fig. 3.21b)**. Mature synapses were observed in 2nd order neurons (DIV11) **(Fig. 3.21, b3)**, although at a lower density than in mature neurons (DIV 25 or DIV18) on the somal side **(Fig. 3.21, b1, b2 and quantification in b5)**. Thus, synaptic contacts may contribute to Tau^{GFP} transmission in this case.

To further determine the potential role of synaptic contacts in the transmission of Tau, we examined whether the transmission of Tau^{GFP} exosomes can occur when no synapses are present in 2nd order neurons. To this end, we selectively treated the 1st order neurons (DIV18) when the 2nd order neurons were at a very early stage (at DIV4). No synaptic contacts were detected in 2nd order neurons at DIV4 **(Fig. 3.21, b4)**. Notably, no Tau^{GFP} puncta were detected in the cell bodies of the 2nd order neurons at DIV4 (before synapse formation, **Fig. 3.21c, right panels**), although Tau^{GFP} puncta in microgrooves were detected as indicated by arrows **(Fig. 3.21c, left panels)**. This indicates that although Tau^{GFP} exosomes were taken up by the 1st order neurons on the somal side, they were not transmitted to 2nd order neurons. Taken together, these results suggest that synaptic contacts are necessary for the transmission of Tau by exosomes. The low transmission of Tau into young neurons (DIV4) could be explained either because these neurons have not yet developed an uptake mechanism for exosomes, or because the Tau^{GFP} exosomes were not released on the neuritic side by the 1st order neurons. To clarify this issue we

checked the uptake of Tau^{GFP} exosomes in young neurons (DIV4) by an immunofluorescence assay. Tau^{GFP} exosomes were detected in neurons **(arrows in Fig. 3.21d)**, indicating the internalization of exosomes. This result suggests that once Tau^{GFP} exosomes were internalized by the 1^{st} order neurons, they were rarely released into conditioned medium on the neuritic side by neurites of the 1^{st} order neurons. Thus the transmission of Tau^{GFP} from the 1^{st} order neurons to the 2^{nd} order neurons (DIV11) occurs through synaptic contacts: Tau^{GFP} exosomes are released by presynapses and taken up by postsynapses.

To highlight the importance of synaptic connections for the transmission of Tau by exosomes, we performed another set of experiments using 3-chamber devices. Neurons were seeded in the 1^{st} and 3^{rd} chambers, but not 2^{nd} chamber **(Fig. 3.21e)** of a triple chamber device. Thus the axons from the two populations of neurons projected to the 2^{nd} chamber, but no synapses were formed between them. Treatment of the neurons in the 1^{st} chamber with Tau^{GFP} exosomes resulted in the distribution of Tau^{GFP} puncta in microgrooves between 1^{st} chamber and 2^{nd} chamber **(Fig. 3.21e)**, indicating the uptake of Tau^{GFP} exosomes by neurons in the 1^{st} chamber. However, no Tau^{GFP} exosomes were detected in microgrooves between the 2^{nd} and 3^{rd} chamber and also in neurons in the 3^{rd} chamber. This means that no transmission of Tau^{GFP} occured between the two populations of neurons. On the contrary, when neurons were seeded in all the three chambers of the triple chamber devices, spreading of Tau^{GFP} exosomes was observed across the 2^{nd} and 3^{rd} chambers as well. A clear transmission of Tau^{GFP} exosomes from the 1^{st} to the 2^{nd} and to the 3^{rd} order neurons was observed **(Fig. 3.21f, i and ii)** confirming the role of synaptic connections in the transmission of Tau^{GFP} exosomes.

Collectively, these data argue that exosomes can mediate the trans-synaptic transmission of Tau. Notably, when the 1^{st} order neurons were treated with exosomes that were disrupted by sonication, no Tau^{GFP} puncta were detected in the microgrooves and the 2^{nd} order neurons, indicating that the integrity of exosomes is necessary for the transmission of Tau protein.

Fig 3.21: Synaptic contacts are required for exosome-mediated transmission of Tau^{GFP}

(a)

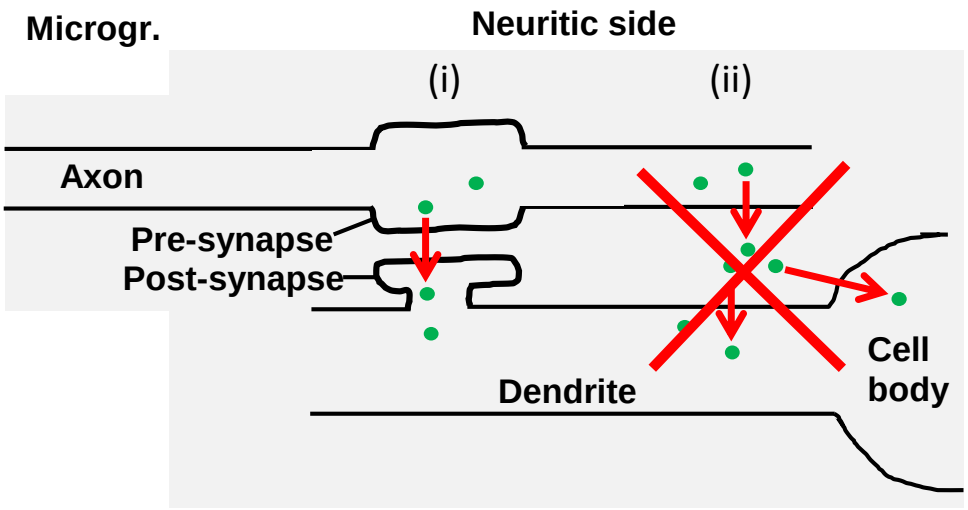

(a) Diagram illustrating the possible mechanisms underlying exosome-mediated Tau transmission. (i) Transmission occurs specifically through trans-synaptic connections from 1st order to 2nd order neurons. (ii) Exosomes in 1st order neurons are released into the conditioned medium and then internalized by the 2nd order neurons, although based on our observations, the exosomes containing Tau^{GFP} was found not to be released into the medium.

Fig 3.21: Synaptic contacts are required for exosome-mediated transmission of Tau^{GFP}

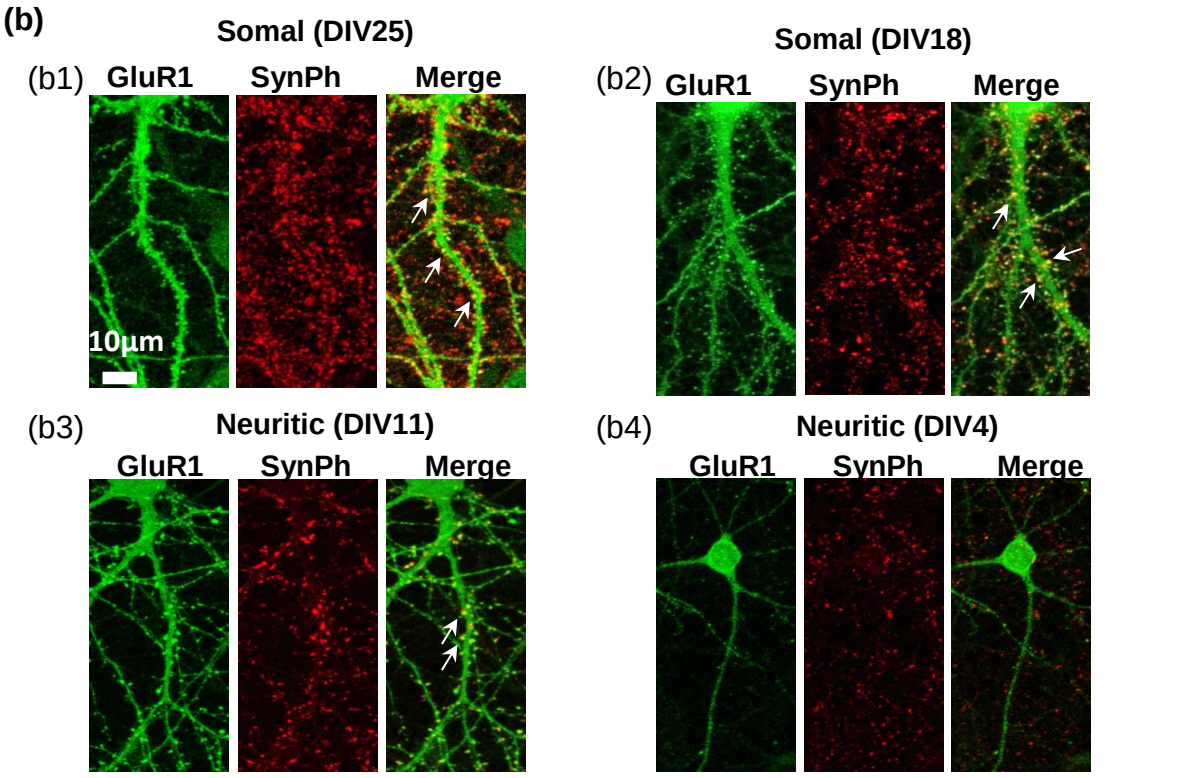

(b5) Quantification of synapse density in neurons cultured in microfluidic chambers

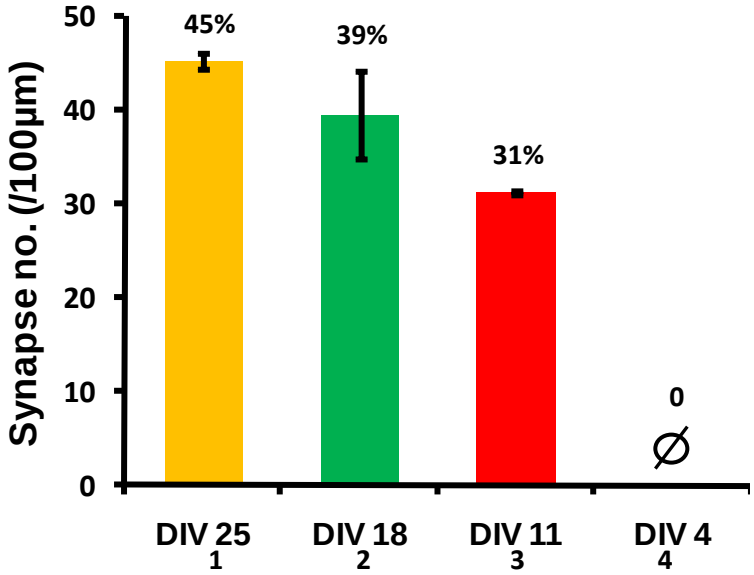

(b) Formation of synaptic contacts at different states of maturation. (b1 – b4) Neurons were stained for post-synaptic marker GluR1 (green) and pre-synaptic marker synaptophysin (SynPh) (red). The co-localization of GluR1 and synaptophysin indicates formation of synaptic contacts (white arrows in merged panels). Synaptic connections were formed in the 1st order mature neurons (DIV 25 or DIV18) on the somal side (b1, b2) and also in the 2nd order old neurons on the neuritic side (DIV11) (b3), but not in the 2nd order young neurons (DIV4) (b4). Scale bar = 10µm. (b5) Quantification of synapse density shown in b1-b4. Synapses are formed in neurons at DIV11 (bar 3), although the density is lower than that in mature neurons (DIV18, bar 2 and DIV25, bar 1). Notably, nearly no synapses are formed in young neurons at DIV4 (bar 4).

Fig 3.21: Synaptic contacts are required for exosome-mediated transmission of Tau^{GFP}

(c)

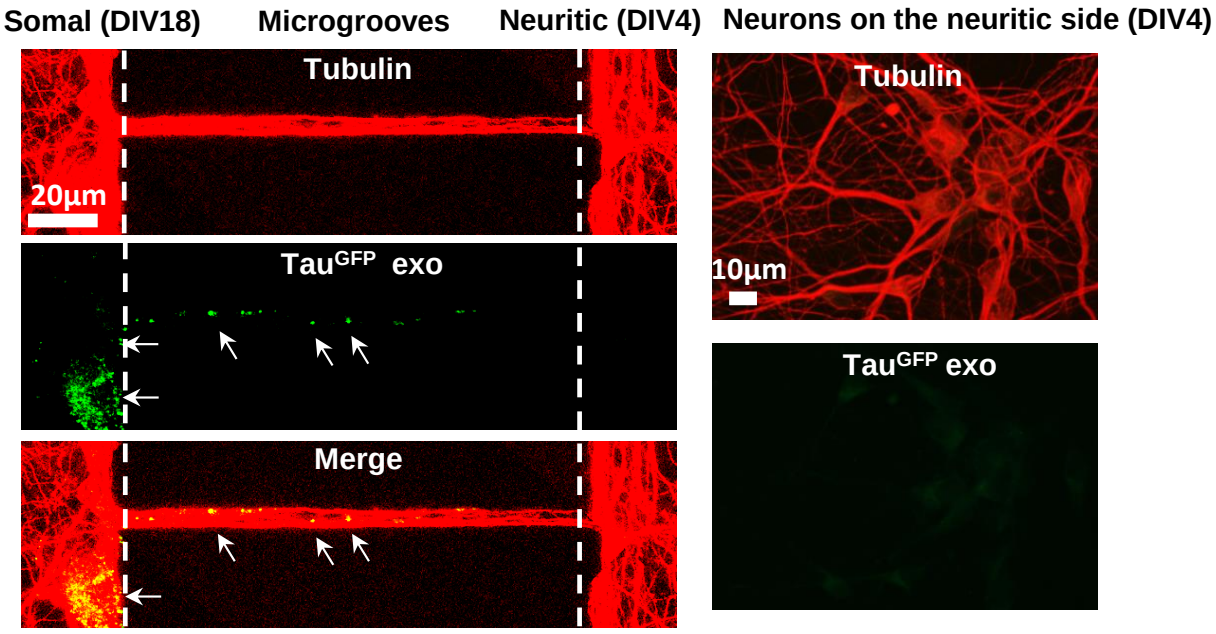

(c) No transmission of Tau^{GFP} exosomes from mature neurons (DIV18) to very young neurons (DIV4) cultured in microfluidic chambers. The 1st order neurons were treated with Tau^{GFP} exosomes at DIV18 for 24 hours, when the 2nd order neurons were at DIV4. Neurons were stained with an antibody against tubulin (red). Arrows indicate Tau^{GFP} positive exosomes in the microgrooves (left side, middle), but not in the 2nd order neurons on the neuritic side (right side, bottom) that was not treated with exosomes, indicating no transmission of Tau^{GFP} via exosomes between the two populations of neurons. Scale bar in the left panels = 20µm; in the right panels = 10µm.

(d) **Young neurons (DIV4)**

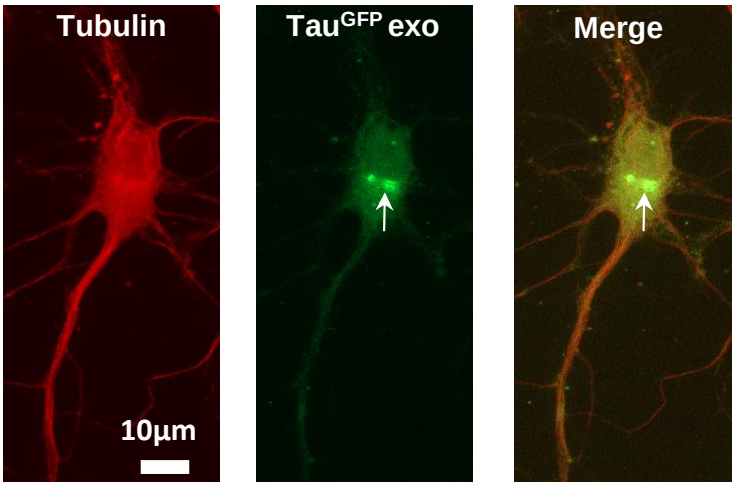

(d) The internalization of Tau^{GFP} exosomes by young neurons (DIV4). Young neurons (DIV4) were treated with Tau^{GFP} exosomes for 24 hours and then stained with an antibody against tubulin (red). Arrows indicate Tau^{GFP} positive exosomes. Note that Tau^{GFP} puncta are detected inside neurons, suggesting the uptake of Tau^{GFP} exosomes by young neurons from the medium. Scale bar=10µm.

Fig 3.21: Synaptic contacts are required for exosome-mediated transmission of Tau^{GFP}

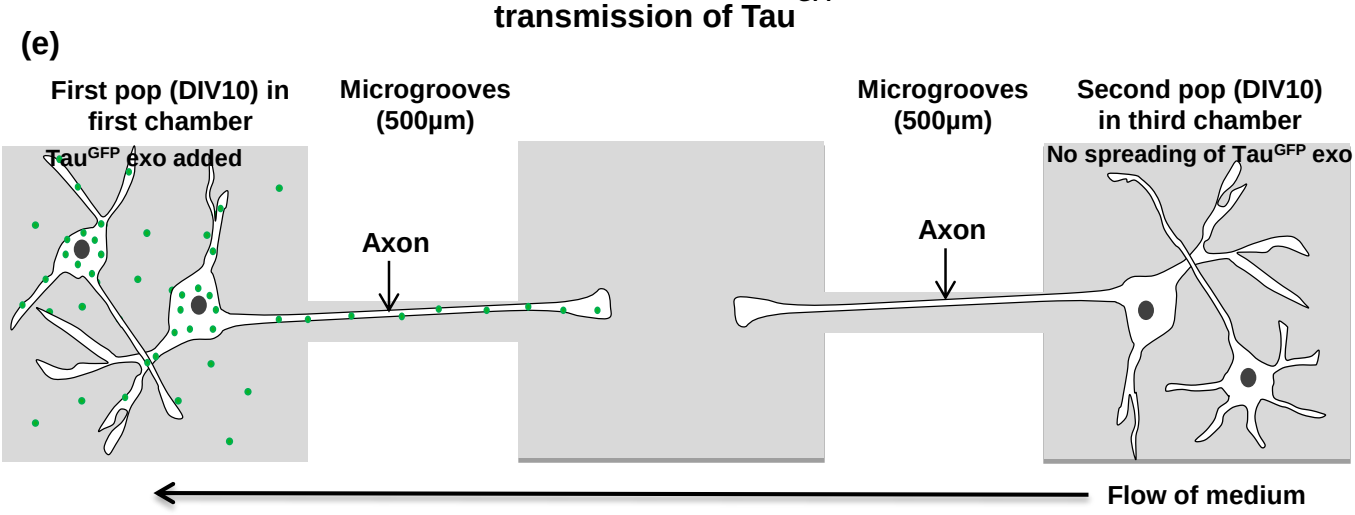

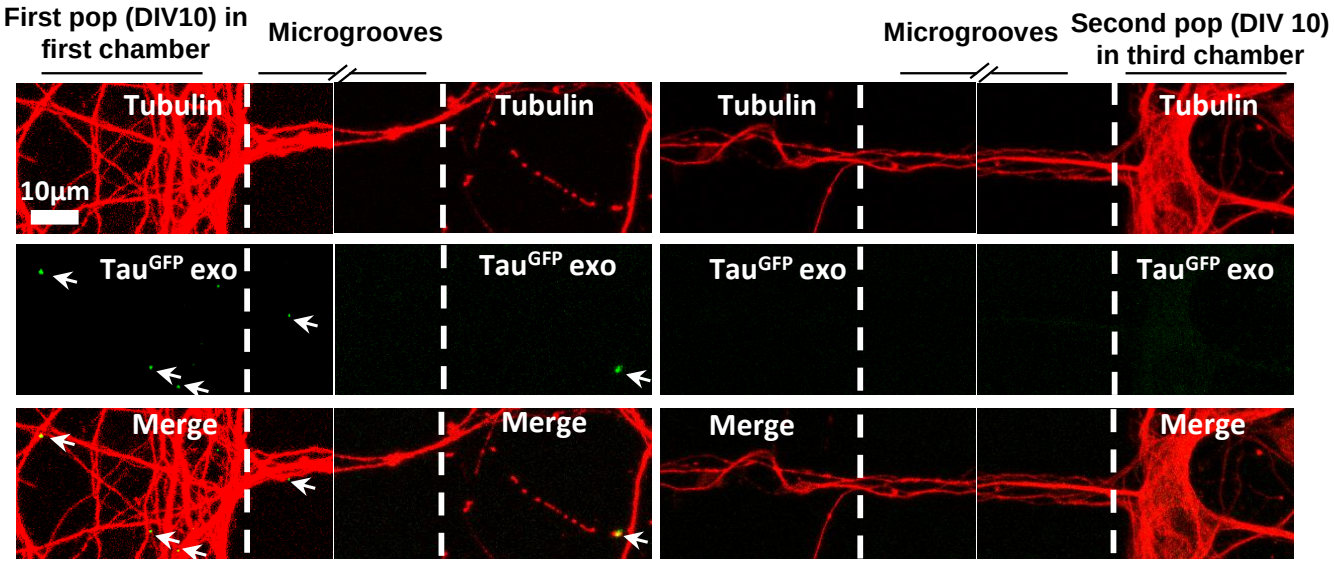

(e) No transmission of Tau^{GFP} exosomes from neurons cultured in 1st chamber (DIV10) to neurons cultured in 3rd chamber (DIV 10). The 1st order neurons were treated with Tau^{GFP} exosomes for 24 hours. Neurons were stained with an antibody against tubulin (red). Arrows indicate Tau^{GFP} positive exosomes in the first channel and in the axons projecting from the 1st order neurons. Note the absence of Tau^{GFP} positive exosomes in the third chamber indicating no transmission of Tau^{GFP} via exosomes between the two populations of neurons. Scale bar = 10µm.

Fig 3.21: Synaptic contacts are required for exosome-mediated transmission of Tau^{GFP}

(f) (i)

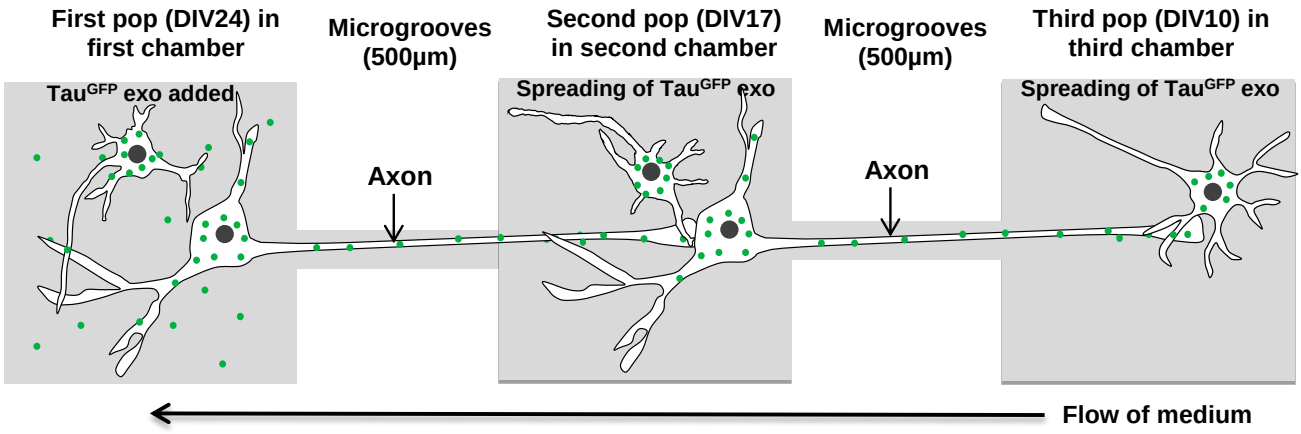

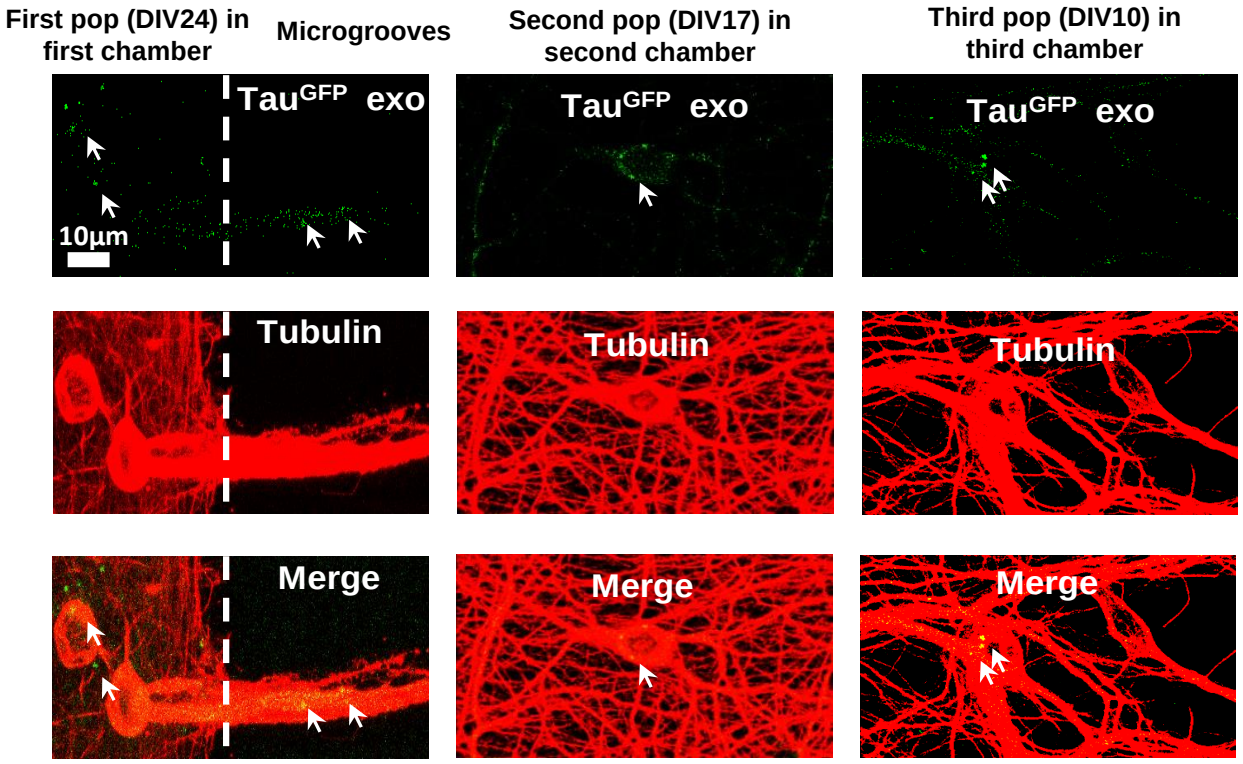

(i) Transmission of Tau^{GFP} exosomes from 1st order neurons in the first chamber to the 2nd and 3rd order neurons in the second and third chambers respectively. The 1st order neurons cultured in the 1st chamber were treated with Tau^{GFP} exosomes at DIV24 for 24 hours. Tau^{GFP} exosomes added to the 1st order neurons cultured in 1st chamber (DIV24) are transmitted to neurons cultured in the 2nd (DIV17) and to the 3rd (DIV10) chambers. Neurons were stained with an antibody against tubulin (red). Arrows indicate Tau^{GFP} positive exosomes . Note the presence of Tau^{GFP} positive exosomes in all the three populations of neurons indicating transmission of Tau^{GFP} via exosomes between the three different populations of neurons. Scale bars = 10µm.

Fig 3.21: Synaptic contacts are required for exosome-mediated transmission of Tau^{GFP}

(f) (ii) Quantification of neurons with Tau^{GFP} positive exosomes

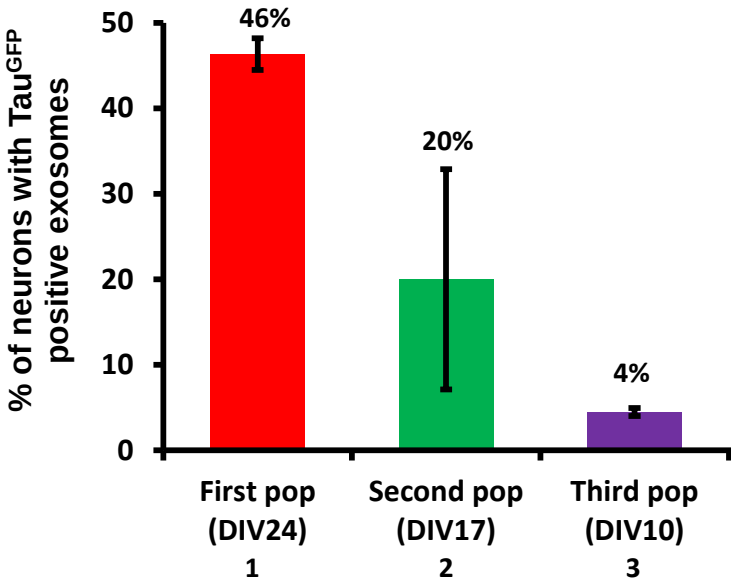

(ii) Quantification of neurons with Tau^{GFP} positive exosomes in all the three chambers. There is a clear transmission of Tau^{GFP} exosomes from the first to the second and the third populations of neurons. The decrease in the percentage of neurons with Tau^{GFP} exosomes in the third chamber (DIV10, bar 3) in comparison to the neurons in the first chamber (DIV24, bar 1), indicate the role of synapses in the transmission of Tau^{GFP} exosomes. Error bars, SEM from *n* = 200-300 neurons counted from 3 chambers.

3.4.3 Tau containing exosomes, independently of their origin, are transmitted across neuronal populations

To exclude the possibility that the transmission of exosomal Tau between neurons is only applied to exosomes derived from N2a cells, we treated neurons in microfluidic devices with exosomes derived from neurons infected with adeno-virus expressing CFP-Tau40 (Tau^{CFP}). Similar to treatment with N2a cell-derived exosomes, CFP puncta were observed in the 2nd order neurons **(arrows in Fig. 3.22, right panels)**, suggesting exosomes can indeed serve as a carrier to regulate the transfer of Tau between neurons independently of the origin of exosomes.

Fig 3.22: Tau containing exosomes are transmitted across neuronal populations independently of their origin

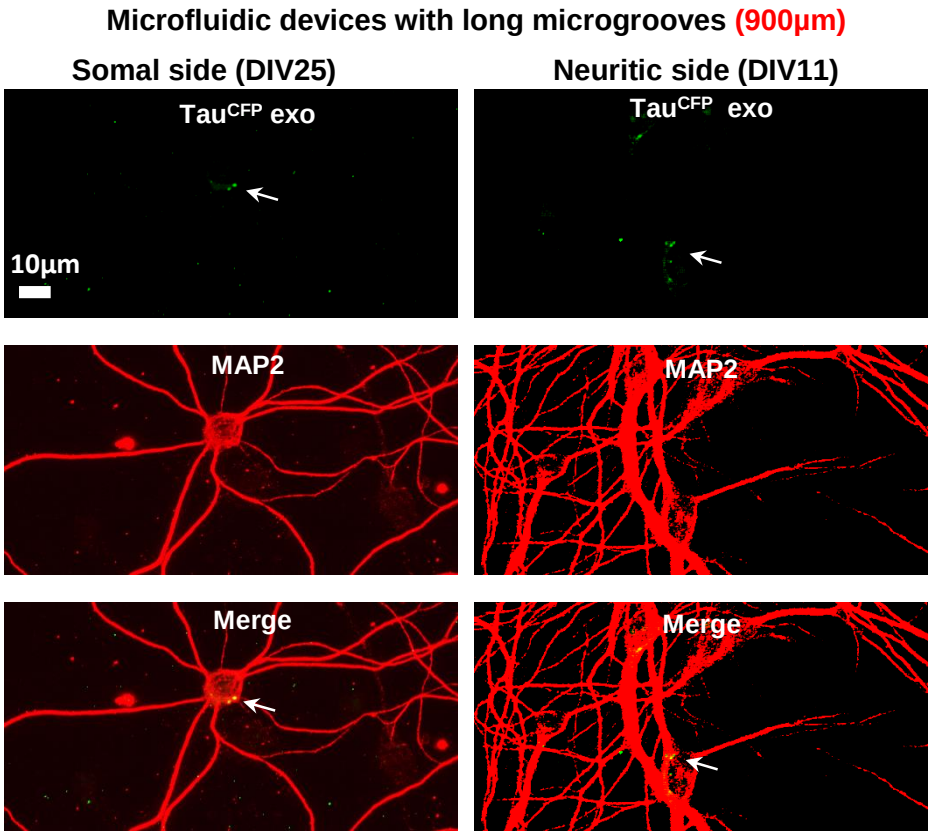

Uptake and transmission of Tau^{CFP} by cultured primary neurons via exosomes derived from cultured neurons. Uptake and transmission of exosomes containing Tau^{CFP} by neurons cultured in microfluidic chambers with long microgrooves (900µm). The 1st order neurons at DIV25 were treated for 24 hours with exosomes isolated from primary cortical neurons infected with adeno-virus expressing Tau^{CFP}, when the 2nd order neurons were at DIV11. Neurons were then fixed and stained with antibody against MAP2 (red). Arrows denote Tau^{CFP} exosomes. Note that Tau^{CFP} exosomes were detected in the 2nd order neurons on the neuritic side, indicating their uptake by 1st order neurons on the somal side, transport across the microgrooves, and synaptic transmission to the neurons on the neuritic side. Scale bar = 10µm.

4 Discussion

4.1 Sorting mechanisms of Tau protein

4.1.1 Developmental regulation of the distribution of Tau in neurons

Tau is a microtubule associated protein which is mainly expressed in neurons. In mature neurons, Tau occurs mostly in axons, but in young neurons, Tau distributes evenly into the cell body and neurites. The subcellular distribution of Tau appears to be strictly regulated during development (Zempel and Mandelkow, 2014). Early studies showed that the dominant axonal distribution of Tau emerges after seven to ten days in culture (DIV 7-10) (Mandell and Banker, 1995). Consistent with previous studies, we observed that Tau protein was distributed across all compartments of cultured neurons starting from DIV1 until DIV9. But at DIV10, a sudden decrease in the localization of Tau in the somatodendritic compartment occurred, leading to the dominant axonal distribution of Tau. Our results suggest that the sorting mechanisms of Tau are established at DIV10. However, the details of the sorting mechanisms of Tau, remains a matter of debate (Hirokawa et al., 1996).

4.1.2 Polarized distribution of Tau protein in neurons

Due to the dominant axonal distribution of Tau, it has been regarded as an axonal protein (Binder et al., 1985). However, several recent studies demonstrated that despite the minor amount of Tau in dendrites, the Tau protein distributing into the somatodendritic compartment may have important physiological functions, e.g. regulation of synaptic plasticity (Kimura et al., 2014, Regan et al., 2016) . Importantly, it is essential for Aβ-induced neurotoxicity (Ittner et al., 2010, Mondragon-Rodriguez et al., 2012) . Furthermore, the increase of dendritic Tau itself is sufficient to induce spine loss (Thies and Mandelkow, 2007). In addition, the mislocalization of Tau protein into the somatodendritic compartment is a hallmark of Alzheimer disease and other Tauopathies (Li et al., 2011). These observations prompted us to study the sorting mechanisms of Tau, as the breakdown of them could cause missorting of Tau in pathological situations. Multiple mechanisms have been proposed to underlie the axonal sorting of Tau (or conversely, the loss of Tau from the somatodendritic compartment) (Hirokawa et al., 1996, Litman et al., 1993, Morita and Sobue, 2009, Kanai and Hirokawa, 1995, Li et al., 2011).

4.1.3 The role of protein degradation systems in the axonal sorting of Tau protein

The following reasons prompted us to investigate the role of the protein degradation systems in Tau distribution. (1) It has been proposed that the differential turnover of Tau in axons versus in the somatodendritic compartment may play a role in Tau distribution. This proposal was based on the observation that Tau microinjected into primary neurons initially distributes through the whole neuron (cell body, axons and dendrites), but later persists only in axons (Hirokawa et al., 1996). It was assumed that the disappearance of exogenous microinjected Tau from the somatodendritic compartment was due to its degradation. In fact, since lysosomes (an essential component of autophagic degradation) are enriched in the somatodendritic compartment of neurons (Parton et al., 1992), it was speculated that a more efficient degradation of Tau would occur in dendrites. However, the disappearance of exogenous Tau can also be interpreted by the existence of a retrograde diffusion barrier of Tau at the axonal initial segment discovered in our lab recently (Li et al., 2011) as the diffusion barrier prevents axonal Tau from diffusing into the dendrites while it allows dendritic Tau to diffuse or get transported into the axons. More investigation is needed to clarify this issue. (2) If the differential turnover of Tau indeed contributes to axonal Tau sorting, then the incomplete degradation of Tau in dendrites would explain the physiological dendritic distribution of Tau. (3) We and other groups showed that autophagy plays a dominant role in Tau degradation in neurons (Wang et al., 2009, Brown et al., 2005, Feuillette et al., 2005, Kruger et al., 2012), but the involvement of the proteasome in Tau degradation is still unclear as the inhibition of the proteasome in primary neurons lead to the compensatory stimulation of autophagy. As the protein degradation inhibitors induce toxic effects in conventional neuronal cultures, we used in this study microfluidic chambers which compartmentalize neurons allowing the “local” treatment with different inhibitors.

Using microfluidic chambers we show here that the degradation of dendritic Tau occurs by both the proteasome and autophagy pathways, as suppressing these pathways dramatically increased the dendritic accumulation of Tau protein **(schematic in Fig. 4.1)**, in addition to increasing the substrates of these pathways – p62 **(Fig. 3.8)** and ubiquitinated substrates **(Fig. 3.9)**. Thus the impairment of the

protein degradation systems may be one of the major causes of Tau missorting. It is noteworthy that in AD, both the proteasome and autophagy pathways become compromised (Wang and Mandelkow, 2012), which could be one of the reasons for the missorting of Tau into the somatodendritic compartment.

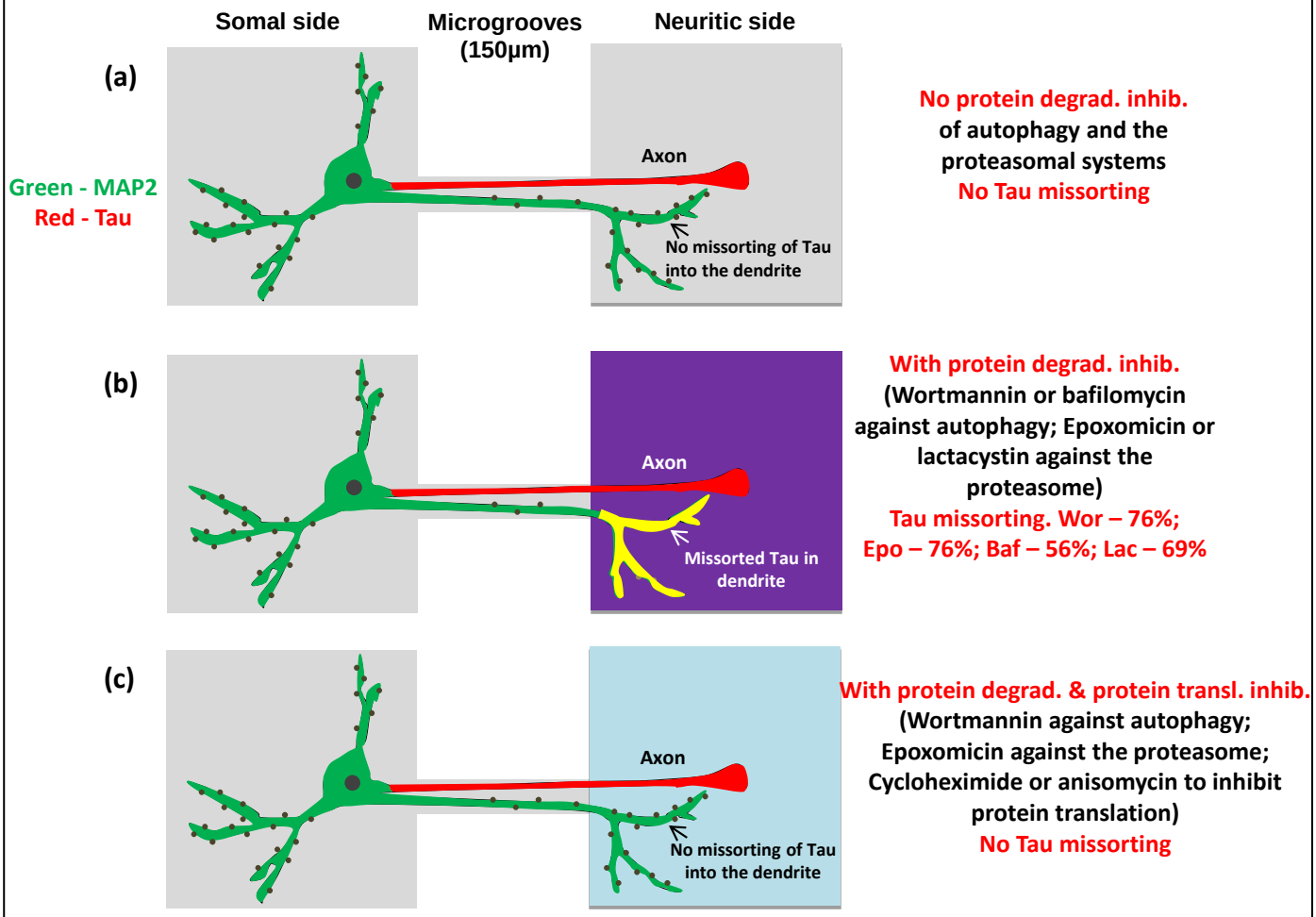

Fig 4.1. Schematic representation of the different treatments and its consequences in neurons cultured in microfluidic chambers. (a) In the absence of protein degradation inhibitors, Tau (red) sorts mainly into the axons and MAP2 (green) into the somatodendritic compartment. (b) When treated with the protein degradation inhibitors (wortmannin or bafilomycin against autophagy and epoxomicin or lactacystin against the proteasome; violet box) on the neuritic side, an increased number of dendrites with Tau accumulation (yellow) were observed indicating local inhibition of degradation of Tau in the dendrites. (c) In the presence of the protein degradation inhibitors (wortmannin or epoxomicin) and the protein translation inhibitors (cycloheximide or anisomycin; pale blue box), Tau sorts mainly into the axons indicating that local translation of Tau mRNA in the dendrites is necessary for Tau missorting.

We noticed that there is a basal level of Tau missorting (~16%) in the dendrites of cultured neurons even under physiological conditions **(Fig. 3.7a, bar 1)**. Stimulation of the autophagy with trehalose (Kruger et al., 2012) **(Fig. 3.13)** or the proteasome with rolipram (Myeku et al., 2016) **(Fig. 3.14)** significantly reduced such missorting, indicating that at least in part the basal level of Tau missorting is due to less active protein degradation systems in these dendrites. This result highlights the important role of protein degradation systems in maintaining the polarized distribution of Tau in neurons and suggests that reducing Tau missorting by enhancing the activity of the autophagy or proteasome system could serve as a valuable therapeutic strategy in AD and other tauopathies.

4.1.4 Protein degradation inhibition results in missorting of Tau with differential phosphorylation status and isoform distribution

Abnormal phosphorylation is known to be a hallmark of Tau pathology, and therefore we tested its relationship to Tau missorting (Zempel and Mandelkow, 2014). Indeed, after application of protein degradation inhibitors, missorted Tau in dendrites showed a different phosphorylation pattern compared to Tau in axons. While the axonal Tau was phosphorylated at the 12E8, PHF1 and AT8 sites, the dendritic Tau was mainly phosphorylated at the 12E8 site after inhibition of protein degradation **(Fig. 3.10 & schematic in Fig. 4.3)**. This suggested that there might be a polarized distribution of kinase or phosphatase activity towards Tau. This could be explained as follows:

(i) Possible role of phosphatases: PP2A, which is mainly present in axons (Zhu et al., 2010) cannot dephosphorylate Tau at the PHF-1 epitope (Qian et al., 2010) although it could dephosphorylate other sites of Tau such as S262, the 12E8 epitope. This could explain the enrichment of PHF-1 positive Tau and lower amount of 12E8 Tau in axons. On the other hand, PP2B, present mainly in dendrites, can dephosphorylate Tau at the PHF-1 epitope (Liu et al., 2005). This may explain why the dendritic Tau is phosphorylated at 12E8 sites, but not PHF1 and AT8 sites. Indeed, the localization of 12E8 Tau in dendrites has been observed (Kishi et al., 2005), in young neurons (~DIV7) where Tau sorting has not started yet.

(ii) Possible role of kinases: It is known that GSK3β which phosphorylates Tau at the AT8 and PHF1 sites shows preferential activity in dendrites (Jiang et al., 2005). However here we observed high AT8 and PHF1 phosphorylation of axonal Tau but

not dendritic Tau. This suggests that the axonal Tau may be phosphorylated by kinases other than GSK3β, while in the dendrites the activity of GSK3β toward Tau phosphorylation may be antagonized by the phosphatase activity. Another well-known kinase, MARK, phosphorylates Tau at S262 (Schneider et al., 1999), the 12E8 epitope. Although it has been reported that MARK2 phosphorylates MAP2 and leads to shortening of dendrites (Terabayashi et al., 2007), this effect could also be attributed to the phosphorylation of Tau at the 12E8 sites. This may explain the specific degradation of 12E8 positive Tau in dendrites.

In addition to identifying the phosphorylation status of Tau protein degraded in the dendrites, we also obtained information on the isoforms of Tau degraded in the dendrites. We found that the 1N isoforms of Tau (i.e. 1N3R and 1N4R) accumulate in the dendrites upon inhibition of both the autophagic and proteasomal degradation **(Fig. 3.12)**. This indicates the localization of the 1N isoform mainly in the axonal compartment whereas degradation takes place in the dendrites. This is contrary to the findings of Liu & Gotz who identified the 1N Tau isoform in the neuronal nucleus, cell bodies and dendrites but not in the axons (Liu and Gotz, 2013). The reason for this discrepancy could be the different neuronal culture systems used in both studies and the role of experimental manipulation in determining the localization of Tau (see later part of discussion).

4.1.5 Tau mRNA is present in the dendrites of neurons and is actively translated

Tau is generally considered to be produced in the cell body and proximal axons, where the mRNA is located (Litman et al., 1993). The localization of Tau mRNA in the proximal region of dendrites was also shown (Kosik et al., 1989) which was proposed to decline distally due to the reduction of ribosomes, but no direct evidence for the proximo-distal change of Tau mRNA distribution was shown. In our study, we showed that Tau mRNA, although it was abundantly localized in the soma, a sparse distribution in the dendrites and axons was also observed **(schematic in Fig. 4.2)**. The study of Kosik et al (1989) did not identify Tau mRNA beyond proximal dendrites which could be due to a lower sensitivity of the in situ hybridization technique used at that time. In our study, the fluorescence in situ hybridization technique gives 8000 fold amplification of fluorescence of every RNA molecule **(Fig. 3.17)**.

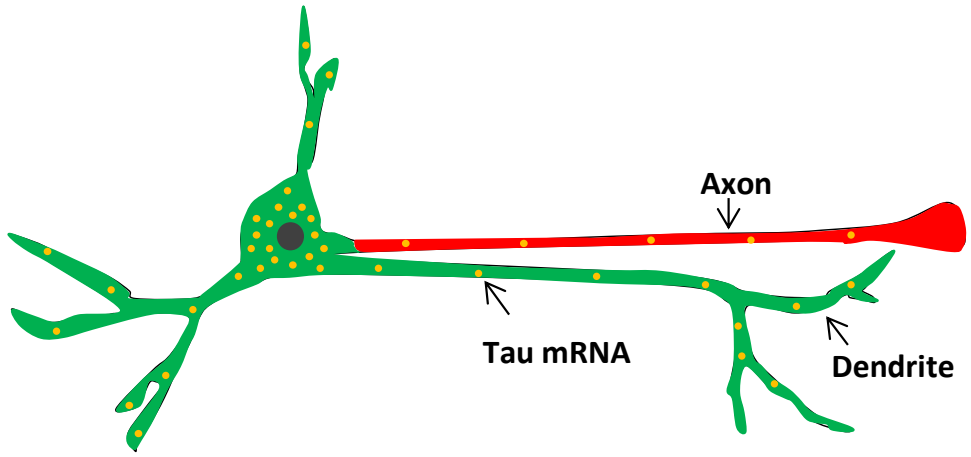

Fig. 4.2. Schematic representation of the distribution of Tau mRNA in a neuron. Fluorescence insitu hybridization revealed Tau mRNA (orange puncta) distribution mainly to the cell body (green) with a sparse distribution in the axon (red) and in the dendrite (green).

It is known that the local translation of proteins in dendrites and spines (Steward and Levy, 1982) is required for activity-dependent synaptic modifications (Steward and Schuman, 2003). Thus, the translational machinery such as polyribosomes exists in dendrites and spines. The distribution of Tau mRNA in dendrites indicates that Tau may be actively translated in dendrites. Indeed, suppression of protein translation dramatically reduces dendritic Tau suggesting that the active translation of Tau does occur in dendrites **(Fig. 3.16)**.

Local translation of Tau mRNA has been reported to occur in axons which appears to be controlled by the 5' TOP sequence in the 5' UTR of Tau mRNA (Morita and Sobue, 2009). It seems that the 5' TOP sequence in the UTR of tau mRNA also controls the translation in the dendrites. This evidence has not been investigated in detail so far. Our data clearly indicates that Tau mRNA is localized in the dendrites **(Fig. 3.17)** and is actively translated **(Fig. 3.16).** This resolves the debate on both the Tau mRNA localization and translation in dendrites.

Overall, our results argue that the minor amount of Tau in the somatodendritic compartment results from the balance of local synthesis and local protein degradation.

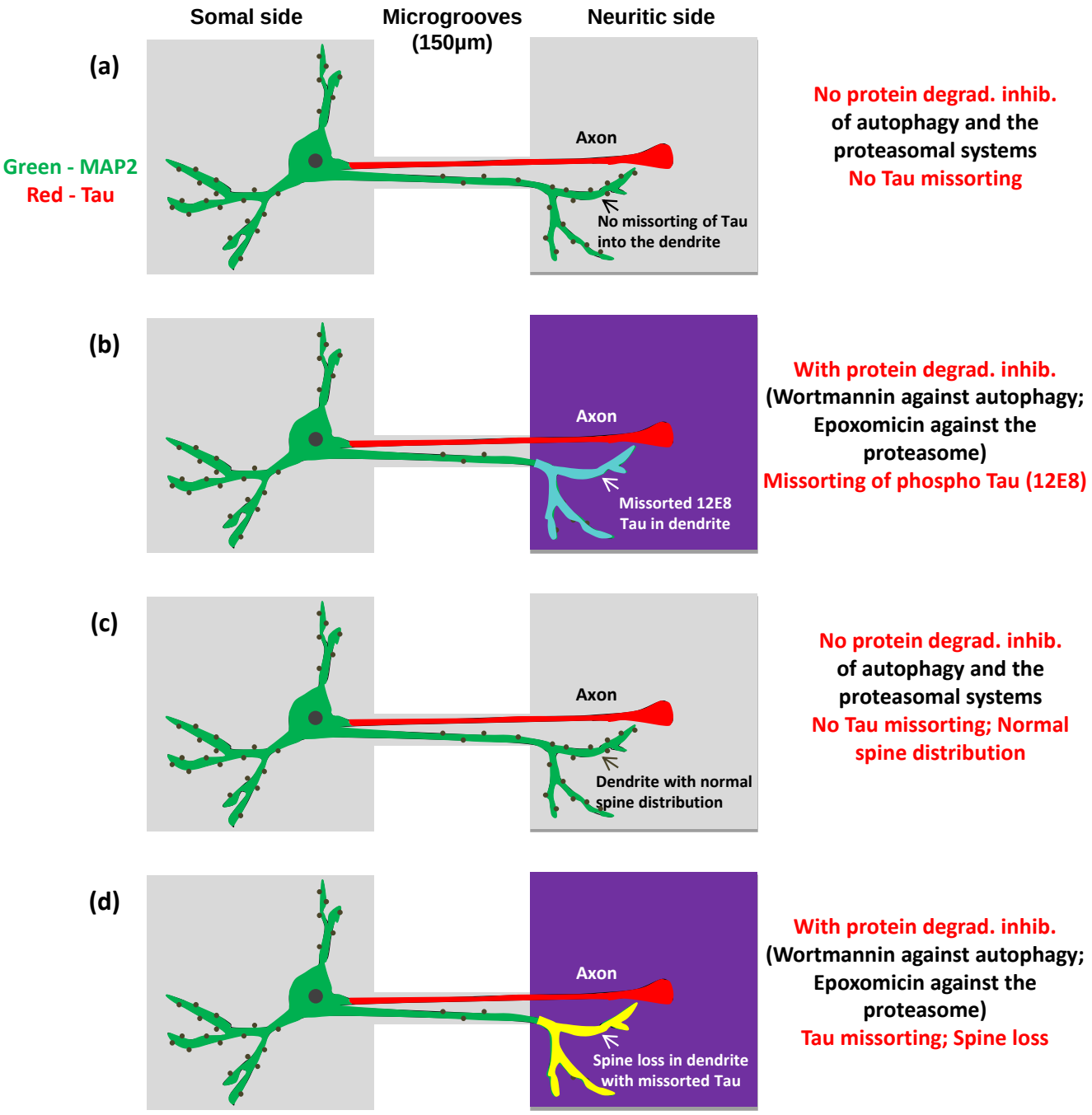

Fig. 4.3. Schematic representation of the different treatments and its consequences in neurons cultured in microfluidic chambers. (a) In the absence of protein degradation inhibitors, Tau (red) sorts mainly into the axons and MAP2 (green) into the somatodendritic compartment. (b) When treated with the protein degradation inhibitors (wortmannin against autophagy and epoxomicin against the proteasome; violet box) on the neuritic side, an increased number of dendrites with missorted Tau phosphorylated at the 12E8 site (cyan) were observed. (c) In the absence of Tau, the dendrites show a normal spine distribution (brown protrusions). (d) Loss of spines was observed in dendrites with missorted Tau after inhibition of the protein degradation systems.

4.1.6 Inhibition of protein degradation causes missorting of Tau into dendrites and spine loss

In line with previous observations of the loss of spines due to missorting of Tau (Zempel et al., 2010, Thies and Mandelkow, 2007), we found that Tau accumulation in the dendrites induced by protein degradation inhibition resulted in the loss of spines as well **(Fig. 3.15 & schematic in Fig. 4.3)**. Since protein degradation inhibition does not induce spine loss in Tau-knockout neurons, we conclude that the missorted Tau is the culprit of spine loss. The missorted Tau may cause spine loss via the following two mechanisms - (i) It could bind to microtubules in dendrites and thereby prevent the binding of motor proteins leading to the inhibition of mitochondrial transport, loss of ATP and eventually spine loss (Thies and Mandelkow, 2007), (ii) The missorting of Tau into the dendrites could result in the breakdown of microtubules in the dendrites by the sequential recruitment of TTLL6 and spastin (Zempel et al., 2013) which could eventually lead to loss of spines.

Although overexpression of Tau (Thies and Mandelkow, 2007) or hyperphosphorylation (Hoover et al., 2010) caused Tau to enter the spines and destroy them, we did not detect Tau protein in the spines after inhibition of protein degradation. This could be explained in two ways (i) the missorted endogenous Tau could cause spine loss much earlier and faster than the exogenous Tau or (ii) the amount of endogenous Tau is too low compared to exogenous Tau.

In conclusion, this study demonstrates that: (1) the degradation systems of the proteasome and the autophagy are responsible for the polarized distribution of Tau during differentiation; (2) dendritic Tau can be synthesized locally; (3) Tau mRNA is distributed across the entire neuron with the majority in the soma and minor fractions in the axons and dendrites; (4) the dendritic Tau protein is phosphorylated at the 12E8 site and is mainly in the form of the 1N isoform; (5) the inhibition of protein degradation results in the missorting of Tau into the dendrites and in the loss of spines.

4.1.7 Chemical fixation can lead to artefacts of Tau mislocalization

Although it is well accepted that Tau is mainly distributed into the axons, some studies observed nearly even distribution of Tau in all cellular compartments in

cultured neurons (Dotti et al., 1987, Mondragon-Rodriguez et al., 2012). The cause of such discrepancies has not been well addressed. Here we showed that the protocols used for fixation of neurons can dramatically affect the distribution of Tau and thus lead to artefacts. Factors such as the fixative, time of fixation and the temperature, notably the absence or presence of sucrose, can all lead to artefacts of Tau missorting. The best procedure turned out to be to fix cells with formaldehyde plus sucrose at 37°C, which minimized missorting of Tau **(Fig. 3.18)**.

As Tau binds to microtubules in axons, any fixation protocol that disrupts microtubules would accordingly affect the axonal localization of Tau, because (1) the high affinity of Tau with axonal microtubules (Kanai and Hirokawa, 1995) contributes to the axonal distribution of Tau, as it could retain Tau in axons; (2) the microtubule is essential for the diffusion barrier. Since the stability of microtubules is vulnerable to temperature changes, low or room temperature can quickly lead to disassembly of microtubules. Therefore, it is not surprising that the fixation at 37°C shows lowest missorting of Tau in protocols using different fixatives. Formaldehyde, due to its low molecular weight, can penetrate cells more quickly than glutaraldehyde and thereby can exert fixative effects faster than glutaraldehyde. This may account for the lower missorting using formaldehyde than using glutaraldehyde, when the other conditions are the same. In fact, we found that fixation with glutaraldehyde resulted in the missorting of Tau in all neurons irrespective of the fixation temperature or time, the presence or absence of sucrose. Thus, glutaraldehyde is not a suitable fixative to be used for investigating Tau distribution. In addition, fixing neurons with methanol or acetone resulted in a significant increase in Tau missorting in comparison with fixation using Formaldehyde **(Fig. 3.18)**. In line with our observation, fixation using methanol (Dotti et al., 1987) induced much higher missorting of Tau than fixation using formaldehyde supplemented with sucrose (Mandell and Banker, 1995).

It is worth to point out that although formaldehyde appears to be the best fixative of all tested, formaldehyde could detach proteins from microtubules (Rossi et al., 2008) and thereby potentially lead to microtubule breakdown. Of note, sucrose is well-known to preserve the native state of tubulin (Morejohn and Fosket, 1984). This may explain why the supplement of sucrose in the fixative can further reduce the observed missorting of Tau.

4.2 Trans-synaptic transmission of Tau protein via exosomes

Some recent studies proposed that Tau pathology can spread via a trans-synaptic mechanism along anatomical circuits (Dujardin et al., 2014b, Liu et al., 2012, de Calignon et al., 2012). However, direct evidence showing transmission of Tau from presynaptic to postsynaptic compartments, and the nature of the transmitted Tau, is difficult to obtain and still controversial. Microfluidic devices are excellent tools to study the transitions of Tau between cell compartments and across cells. By co-culturing neurons in microfluidic devices, we found that treatment of the 1st order neurons with exosomes containing Tau^{GFP}resulted in the transmission of Tau^{GFP} into the 2nd order neurons, indicating that exosomes can act as carriers to mediate the transmission of Tau **(Fig. 3.19e)**. The transmission of Tau is likely due to the direct transition of exosomes from the 1st order neurons to the 2nd order neurons, because (i) Tau^{GFP} colocalized with the vesicle marker – flotillin after transmission from the 1st order to the 2nd order neurons **(Fig. 3.19f)** (ii) In line with other observations pointing to the role of axonal trafficking of different Tau species (Wu et al., 2013), our study also indicates that Tau^{GFP} inside exosomes could be transmitted along the axons to other neuronal populations **(Fig. 3.20)**. Moreover, we found that it is specifically the exogenously added exosomes which get transmitted across synapses to the next neuronal population. We ruled out the role of “endogenous” exosomes by (i) inhibiting their synthesis in the 1st order neurons **(Fig. 3.19g)** (ii) adding exosomes containing markers for both flotillin and Tau **(Fig. 3.19h)** and still observed the occurrence of the transmission of the added exosomes.

The exosome-mediated transmission of Tau^{GFP} requires synaptic connections between the 1st order neurons on the somal side and 2nd order neurons on the neuritic side. This view is based on three observations. (1) No exosomes were detected in conditioned medium on the neuritic side, indicating that the transition of Tau^{GFP} does not occur because of the release of exosomes of 1st order neurons into the conditioned medium of the 2nd order neurons and then internalized by 2nd order neurons at extrasynaptic sites. (2) There is no transmission of Tau^{GFP} exosomes from the 1st order to the young 2nd order neurons (DIV4) on the neuritic side (which lack synaptic connections), indicating that synaptic contacts are necessary for exosome-mediated Tau transmission. (3) In the 3-chamber microfluidic devices, no

transmission of Tau^{GFP} was observed from neurons in the 1st chamber to neurons in the 3rd chamber, when no neurons were seeded in the 2nd chamber. To the contrary, when neurons were cultured in all the three chambers of a 3-chamber microfluidic device, transmission of Tau^{GFP} was observed from neurons in the 1st chamber to neurons in the 2nd and the 3rd chamber. The difference between these two cases is that in the first case (only two populations of neurons) no synapses were formed between the two neuronal populations, while in the second case, synapses were formed between the 1st and 2nd order neurons and 2nd and 3rd order neurons **(Fig. 3.21e,f & schematic in Fig. 4.4)**. This confirms the role of synapses in transmitting Tau containing exosomes.

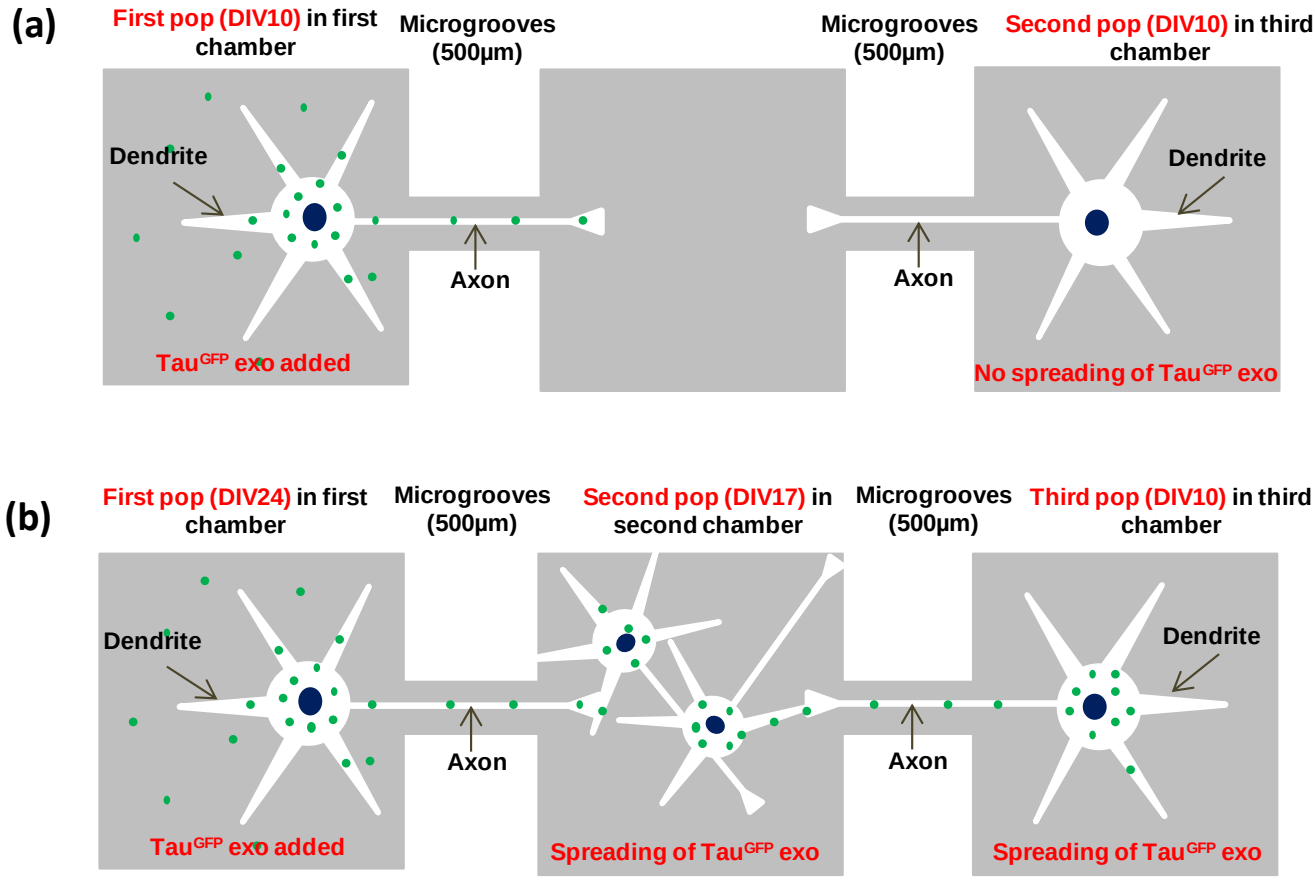

Fig. 4.4. Schematic representation of the spreading of exosomes containing Tau^{GFP} in neurons cultured in triple chamber microfluidic devices. (a) Neurons were cultured only in the first and the third chamber and Tau^{GFP} exosomes (green puncta) were added to the first population of neurons. No spreading of Tau^{GFP} exosomes was observed to the second population of neurons in the third chamber (absence of green puncta) due to lack of synapses between the first and the second populations of neurons. (b) Neurons were cultured in all the three chambers of a triple chamber microfluidic device and Tau^{GFP} exosomes (green puncta) were added to the first population of neurons. The spreading of Tau^{GFP} exosomes were observed in the second and the third populations of neurons indicating the essential role of synapses in the spreading of Tau pathology.

Our results argue that the trans-synaptic transmission of Tau^{GFP} occurs because exosomes are preferentially transmitted across the presynapses of the 1st order neurons to the postsynapses of the 2nd order neurons. However, it should be pointed out that the internalized exosomes added to the somal side are preferentially transmitted via pre-synaptic terminals to the neurons on the neuritic side. By contrast, the fusion of multivesicular bodies with membranes in cell bodies and dendrites may result in the release of “endogenous” exosomes at these sites as well (Lachenal et al., 2011). Taken together, our study implies that exosomes are capable of spreading of Tau pathology via trans-synaptic transmission.

5 Bibliography

ALZHEIMER, A. 1907. Über eine eigenartige Erkrankung der Hirnrinde. *Allgemeine Zeitschrift für Psychiatrie und Psychisch-gerichtliche Medizin,* 64**,** 146-8.

ALSHAMMARI, M. A., ALSHAMMARI, T. K. & LAEZZA, F. 2016. Improved Methods for Fluorescence Microscopy Detection of Macromolecules at the Axon Initial Segment. *Front Cell Neurosci,* 10**,** 5.

ANDREADIS, A., BROWN, W. M. & KOSIK, K. S. 1992. Structure and novel exons of the human tau gene. *Biochemistry,* 31**,** 10626-33.

ARONOV, S., ARANDA, G., BEHAR, L. & GINZBURG, I. 2001. Axonal tau mRNA localization coincides with tau protein in living neuronal cells and depends on axonal targeting signal. *J Neurosci,* 21**,** 6577-87.

ARRIAGADA, P. V., GROWDON, J. H., HEDLEY-WHYTE, E. T. & HYMAN, B. T. 1992. Neurofibrillary tangles but not senile plaques parallel duration and severity of Alzheimer's disease. *Neurology,* 42**,** 631-9.

BABU, J. R., GEETHA, T. & WOOTEN, M. W. 2005. Sequestosome 1/p62 shuttles polyubiquitinated tau for proteasomal degradation. *J Neurochem,* 94**,** 192-203.

BIERNAT, J. & MANDELKOW, E. M. 1999. The development of cell processes induced by tau protein requires phosphorylation of serine 262 and 356 in the repeat domain and is inhibited by phosphorylation in the proline-rich domains. *Mol Biol Cell,* 10**,** 727-40.

BINDER, L. I., FRANKFURTER, A. & REBHUN, L. I. 1985. The distribution of tau in the mammalian central nervous system. *J Cell Biol,* 101**,** 1371-8.

BOLAND, B., KUMAR, A., LEE, S., PLATT, F. M., WEGIEL, J., YU, W. H. & NIXON, R. A. 2008. Autophagy induction and autophagosome clearance in neurons: relationship to autophagic pathology in Alzheimer's disease. *J Neurosci,* 28**,** 6926-37.

BOLUDA, S., IBA, M., ZHANG, B., RAIBLE, K. M., LEE, V. M. & TROJANOWSKI, J. Q. 2015. Differential induction and spread of tau pathology in young PS19 tau transgenic mice following intracerebral injections of pathological tau from Alzheimer's disease or corticobasal degeneration brains. *Acta Neuropathol,* 129**,** 221-37.

BRAAK, E., BRAAK, H. & MANDELKOW, E. M. 1994. A sequence of cytoskeleton changes related to the formation of neurofibrillary tangles and neuropil threads. *Acta Neuropathol,* 87**,** 554-67.

BRAAK, H. & BRAAK, E. 1991. Neuropathological stageing of Alzheimer-related changes. *Acta Neuropathol,* 82**,** 239-59.

BRAAK, H. & BRAAK, E. 1996. Development of Alzheimer-related neurofibrillary changes in the neocortex inversely recapitulates cortical myelogenesis. *Acta Neuropathol,* 92**,** 197-201.

BRAAK, H. & DEL TREDICI, K. 2014. Are cases with tau pathology occurring in the absence of Abeta deposits part of the AD-related pathological process? *Acta Neuropathol,* 128**,** 767-72.

BRAUN, H. A., UMBREEN, S., GROLL, M., KUCKELKORN, U., MLYNARCZUK, I., WIGAND, M. E., DRUNG, I., KLOETZEL, P. M. & SCHMIDT, B. 2005. Tripeptide mimetics inhibit the 20 S proteasome by covalent bonding to the active threonines. *J Biol Chem,* 280**,** 28394-401.

BRETTSCHNEIDER, J., DEL TREDICI, K., LEE, V. M. & TROJANOWSKI, J. Q. 2015. Spreading of pathology in neurodegenerative diseases: a focus on human studies. *Nat Rev Neurosci,* 16**,** 109-20.

BROWN, M. R., BONDADA, V., KELLER, J. N., THORPE, J. & GEDDES, J. W. 2005. Proteasome or calpain inhibition does not alter cellular tau levels in neuroblastoma cells or primary neurons. *J Alzheimers Dis,* 7**,** 15-24.

CACERES, A. & KOSIK, K. S. 1990. Inhibition of neurite polarity by tau antisense oligonucleotides in primary cerebellar neurons. *Nature,* 343**,** 461-3.

CALAFATE, S., BUIST, A., MISKIEWICZ, K., VIJAYAN, V., DANEELS, G., DE STROOPER, B., DE WIT, J., VERSTREKEN, P. & MOECHARS, D. 2015. Synaptic Contacts Enhance Cell-to-Cell Tau Pathology Propagation. *Cell Rep,* 11**,** 1176-83.

CLAVAGUERA, F., AKATSU, H., FRASER, G., CROWTHER, R. A., FRANK, S., HENCH, J., PROBST, A., WINKLER, D. T., REICHWALD, J., STAUFENBIEL, M., GHETTI, B., GOEDERT, M. & TOLNAY, M. 2013. Brain homogenates from human tauopathies induce tau inclusions in mouse brain. *Proc Natl Acad Sci U S A,* 110**,** 9535-40.

CLAVAGUERA, F., BOLMONT, T., CROWTHER, R. A., ABRAMOWSKI, D., FRANK, S., PROBST, A., FRASER, G., STALDER, A. K., BEIBEL, M., STAUFENBIEL, M., JUCKER, M., GOEDERT, M. & TOLNAY, M. 2009. Transmission and spreading of tauopathy in transgenic mouse brain. *Nat Cell Biol,* 11**,** 909-13.

CONGDON, E. E., WU, J. W., MYEKU, N., FIGUEROA, Y. H., HERMAN, M., MARINEC, P. S., GESTWICKI, J. E., DICKEY, C. A., YU, W. H. & DUFF, K. E. 2012. Methylthioninium chloride (methylene blue) induces autophagy and attenuates tauopathy in vitro and in vivo. *Autophagy,* 8**,** 609-22.

COOK, C., CARLOMAGNO, Y., GENDRON, T. F., DUNMORE, J., SCHEFFEL, K., STETLER, C., DAVIS, M., DICKSON, D., JARPE, M., DETURE, M. & PETRUCELLI, L. 2014. Acetylation of the KXGS motifs in tau is a critical determinant in modulation of tau aggregation and clearance. *Hum Mol Genet,* 23**,** 104-16.

COUX, O., TANAKA, K. & GOLDBERG, A. L. 1996. Structure and functions of the 20S and 26S proteasomes. *Annu Rev Biochem,* 65**,** 801-47.

CROWTHER, T., GOEDERT, M. & WISCHIK, C. M. 1989. The repeat region of microtubule-associated protein tau forms part of the core of the paired helical filament of Alzheimer's disease. *Ann Med,* 21**,** 127-32.

CUERVO, A. M. & WONG, E. 2014. Chaperone-mediated autophagy: roles in disease and aging. *Cell Res,* 24**,** 92-104.

DE CALIGNON, A., POLYDORO, M., SUAREZ-CALVET, M., WILLIAM, C., ADAMOWICZ, D. H., KOPEIKINA, K. J., PITSTICK, R., SAHARA, N., ASHE, K. H., CARLSON, G. A., SPIRES-JONES, T. L. & HYMAN, B. T. 2012. Propagation of tau pathology in a model of early Alzheimer's disease. *Neuron,* 73**,** 685-97.

DEKOSKY, S. T. & SCHEFF, S. W. 1990. Synapse loss in frontal cortex biopsies in Alzheimer's disease: correlation with cognitive severity. *Ann Neurol,* 27**,** 457-64.

DESHPANDE, A., WIN, K. M. & BUSCIGLIO, J. 2008. Tau isoform expression and regulation in human cortical neurons. *FASEB J,* 22**,** 2357-67.

DING, W. X., NI, H. M., GAO, W., YOSHIMORI, T., STOLZ, D. B., RON, D. & YIN, X. M. 2007. Linking of autophagy to ubiquitin-proteasome system is important for the regulation of endoplasmic reticulum stress and cell viability. *Am J Pathol,* 171**,** 513-24.

DOTTI, C. G., BANKER, G. A. & BINDER, L. I. 1987. The expression and distribution of the microtubule-associated proteins tau and microtubule-associated protein 2 in hippocampal neurons in the rat in situ and in cell culture. *Neuroscience,* 23**,** 121-30.

DUJARDIN, S., BEGARD, S., CAILLIEREZ, R., LACHAUD, C., DELATTRE, L., CARRIER, S., LOYENS, A., GALAS, M. C., BOUSSET, L., MELKI, R., AUREGAN, G., HANTRAYE, P., BROUILLET, E., BUEE, L. & COLIN, M. 2014a. Ectosomes: a new mechanism for non-exosomal secretion of tau protein. *PLoS One,* 9**,** e100760.

DUJARDIN, S., LECOLLE, K., CAILLIEREZ, R., BEGARD, S., ZOMMER, N., LACHAUD, C., CARRIER, S., DUFOUR, N., AUREGAN, G., WINDERICKX, J., HANTRAYE, P., DEGLON, N., COLIN, M. & BUEE, L. 2014b. Neuron-to-neuron wild-type Tau protein transfer through a trans-synaptic mechanism: relevance to sporadic tauopathies. *Acta Neuropathol Commun,* 2**,** 14.

FAURE, J., LACHENAL, G., COURT, M., HIRRLINGER, J., CHATELLARD-CAUSSE, C., BLOT, B., GRANGE, J., SCHOEHN, G., GOLDBERG, Y., BOYER, V., KIRCHHOFF, F., RAPOSO, G., GARIN, J. & SADOUL, R. 2006. Exosomes are released by cultured cortical neurones. *Mol Cell Neurosci,* 31**,** 642-8.

FEUILLETTE, S., BLARD, O., LECOURTOIS, M., FREBOURG, T., CAMPION, D. & DUMANCHIN, C. 2005. Tau is not normally degraded by the proteasome. *J Neurosci Res,* 80**,** 400-5.

FEVRIER, B., VILETTE, D., ARCHER, F., LOEW, D., FAIGLE, W., VIDAL, M., LAUDE, H. & RAPOSO, G. 2004. Cells release prions in association with exosomes. *Proc Natl Acad Sci U S A,* 101**,** 9683-8.

FRANDEMICHE, M. L., DE SERANNO, S., RUSH, T., BOREL, E., ELIE, A., ARNAL, I., LANTE, F. & BUISSON, A. 2014. Activity-dependent tau protein translocation to excitatory synapse is disrupted by exposure to amyloid-beta oligomers. *J Neurosci,* 34**,** 6084-97.

FROST, B., JACKS, R. L. & DIAMOND, M. I. 2009. Propagation of tau misfolding from the outside to the inside of a cell. *J Biol Chem,* 284**,** 12845-52.

FRUHBEIS, C., FROHLICH, D., KUO, W. P., AMPHORNRAT, J., THILEMANN, S., SAAB, A. S., KIRCHHOFF, F., MOBIUS, W., GOEBBELS, S., NAVE, K. A., SCHNEIDER, A., SIMONS, M., KLUGMANN, M., TROTTER, J. & KRAMER-ALBERS, E. M. 2013. Neurotransmitter-triggered transfer of exosomes mediates oligodendrocyte-neuron communication. *PLoS Biol,* 11**,** e1001604.

GHIRARDI, M., BENFENATI, F., GIOVEDI, S., FIUMARA, F., MILANESE, C. & MONTAROLO, P. G. 2004. Inhibition of neurotransmitter release by a nonphysiological target requires protein synthesis and involves cAMP-dependent and mitogen-activated protein kinases. *J Neurosci,* 24**,** 5054-62.

GONG, C. X., LIU, F., GRUNDKE-IQBAL, I. & IQBAL, K. 2005. Post-translational modifications of tau protein in Alzheimer's disease. *J Neural Transm (Vienna),* 112**,** 813-38.

GUERRERO-MUNOZ, M. J., GERSON, J. & CASTILLO-CARRANZA, D. L. 2015. Tau Oligomers: The Toxic Player at Synapses in Alzheimer's Disease. *Front Cell Neurosci,* 9**,** 464.

HAMANO, T., GENDRON, T. F., KO, L. W. & YEN, S. H. 2009. Concentration-dependent effects of proteasomal inhibition on tau processing in a cellular model of tauopathy. *Int J Clin Exp Pathol,* 2**,** 561-73.

HAN, D. H., NA, H. K., CHOI, W. H., LEE, J. H., KIM, Y. K., WON, C., LEE, S. H., KIM, K. P., KURET, J., MIN, D. H. & LEE, M. J. 2014. Direct cellular delivery of human proteasomes to delay tau aggregation. *Nat Commun,* 5**,** 5633.

HANGER, D. P., ANDERTON, B. H. & NOBLE, W. 2009. Tau phosphorylation: the therapeutic challenge for neurodegenerative disease. *Trends Mol Med,* 15**,** 112-9.

HARDY, J. & ALLSOP, D. 1991. Amyloid deposition as the central event in the aetiology of Alzheimer's disease. *Trends Pharmacol Sci,* 12**,** 383-8.

HAROLD, D., JEHU, L., TURIC, D., HOLLINGWORTH, P., MOORE, P., SUMMERHAYES, P., MOSKVINA, V., FOY, C., ARCHER, N., HAMILTON, B. A., LOVESTONE, S., POWELL, J., BRAYNE, C., RUBINSZTEIN, D. C., JONES, L., O'DONOVAN, M. C., OWEN, M. J. & WILLIAMS, J. 2007. Interaction between the ADAM12 and SH3MD1 genes may confer susceptibility to late-onset Alzheimer's disease. *Am J Med Genet B Neuropsychiatr Genet,* 144B**,** 448-52.

HIROKAWA, N., FUNAKOSHI, T., SATO-HARADA, R. & KANAI, Y. 1996. Selective stabilization of tau in axons and microtubule-associated protein 2C in cell bodies and dendrites contributes to polarized localization of cytoskeletal proteins in mature neurons. *J Cell Biol,* 132**,** 667-79.

HOCHGRAFE, K., SYDOW, A., MATENIA, D., CADINU, D., KONEN, S., PETROVA, O., PICKHARDT, M., GOLL, P., MORELLINI, F., MANDELKOW, E. & MANDELKOW, E. M. 2015. Preventive methylene blue treatment preserves cognition in mice expressing full-length pro-aggregant human Tau. *Acta Neuropathol Commun,* 3**,** 25.

HOOVER, B. R., REED, M. N., SU, J., PENROD, R. D., KOTILINEK, L. A., GRANT, M. K., PITSTICK, R., CARLSON, G. A., LANIER, L. M., YUAN, L. L., ASHE, K. H. & LIAO, D. 2010. Tau mislocalization to dendritic spines mediates synaptic dysfunction independently of neurodegeneration. *Neuron,* 68**,** 1067-81.

HUANG, Y. & MUCKE, L. 2012. Alzheimer mechanisms and therapeutic strategies. *Cell,* 148**,** 1204-22.

HYMAN, B. T., VAN HOESEN, G. W., DAMASIO, A. R. & BARNES, C. L. 1984. Alzheimer's disease: cell-specific pathology isolates the hippocampal formation. *Science,* 225**,** 1168-70.

ITAKURA, E. & MIZUSHIMA, N. 2011. p62 Targeting to the autophagosome formation site requires self-oligomerization but not LC3 binding. *J Cell Biol,* 192**,** 17-27.

ITTNER, L. M., KE, Y. D., DELERUE, F., BI, M., GLADBACH, A., VAN EERSEL, J., WOLFING, H., CHIENG, B. C., CHRISTIE, M. J., NAPIER, I. A., ECKERT, A., STAUFENBIEL, M., HARDEMAN, E. & GOTZ, J. 2010. Dendritic function of tau mediates amyloid-beta toxicity in Alzheimer's disease mouse models. *Cell,* 142**,** 387-97.

JIANG, H., GUO, W., LIANG, X. & RAO, Y. 2005. Both the establishment and the maintenance of neuronal polarity require active mechanisms: critical roles of GSK-3beta and its upstream regulators. *Cell,* 120**,** 123-35.

KANAI, Y. & HIROKAWA, N. 1995. Sorting mechanisms of tau and MAP2 in neurons: suppressed axonal transit of MAP2 and locally regulated microtubule binding. *Neuron,* 14**,** 421-32.

KECK, S., NITSCH, R., GRUNE, T. & ULLRICH, O. 2003. Proteasome inhibition by paired helical filament-tau in brains of patients with Alzheimer's disease. *J Neurochem,* 85**,** 115-22.

KENESSEY, A. & YEN, S. H. 1993. The extent of phosphorylation of fetal tau is comparable to that of PHF-tau from Alzheimer paired helical filaments. *Brain Res,* 629**,** 40-6.

KERSCHER, O., FELBERBAUM, R. & HOCHSTRASSER, M. 2006. Modification of proteins by ubiquitin and ubiquitin-like proteins. *Annu Rev Cell Dev Biol,* 22**,** 159-80.

KHLISTUNOVA, I., PICKHARDT, M., BIERNAT, J., WANG, Y., MANDELKOW, E. M. & MANDELKOW, E. 2007. Inhibition of tau aggregation in cell models of tauopathy. *Curr Alzheimer Res,* 4**,** 544-6.

KIMURA, T., WHITCOMB, D. J., JO, J., REGAN, P., PIERS, T., HEO, S., BROWN, C., HASHIKAWA, T., MURAYAMA, M., SEOK, H., SOTIROPOULOS, I., KIM, E., COLLINGRIDGE, G. L., TAKASHIMA, A. & CHO, K. 2014. Microtubule-associated protein tau is essential for long-term depression in the hippocampus. *Philos Trans R Soc Lond B Biol Sci,* 369**,** 20130144.

KISHI, M., PAN, Y. A., CRUMP, J. G. & SANES, J. R. 2005. Mammalian SAD kinases are required for neuronal polarization. *Science,* 307**,** 929-32.

KLEIMAN, R., BANKER, G. & STEWARD, O. 1993. Inhibition of protein synthesis alters the subcellular distribution of mRNA in neurons but does not prevent dendritic transport of RNA. *Proc Natl Acad Sci U S A,* 90**,** 11192-6.

KLIONSKY, D. J. 2013. Why just eat in, when you can also eat out? *Autophagy,* 9**,** 119.

KNOPS, J., KOSIK, K. S., LEE, G., PARDEE, J. D., COHEN-GOULD, L. & MCCONLOGUE, L. 1991. Overexpression of tau in a nonneuronal cell induces long cellular processes. *J Cell Biol,* 114**,** 725-33.

KONZACK, S., THIES, E., MARX, A., MANDELKOW, E. M. & MANDELKOW, E. 2007. Swimming against the tide: mobility of the microtubule-associated protein tau in neurons. *J Neurosci,* 27**,** 9916-27.

KOPKE, E., TUNG, Y. C., SHAIKH, S., ALONSO, A. C., IQBAL, K. & GRUNDKE-IQBAL, I. 1993. Microtubule-associated protein tau. Abnormal phosphorylation of a non-paired helical filament pool in Alzheimer disease. *J Biol Chem,* 268**,** 24374-84.

KORKUT, C., LI, Y., KOLES, K., BREWER, C., ASHLEY, J., YOSHIHARA, M. & BUDNIK, V. 2013. Regulation of postsynaptic retrograde signaling by presynaptic exosome release. *Neuron,* 77**,** 1039-46.

KOROLCHUK, V. I., MANSILLA, A., MENZIES, F. M. & RUBINSZTEIN, D. C. 2009. Autophagy inhibition compromises degradation of ubiquitin-proteasome pathway substrates. *Mol Cell,* 33**,** 517-27.

KOSIK, K. S., CRANDALL, J. E., MUFSON, E. J. & NEVE, R. L. 1989. Tau in situ hybridization in normal and Alzheimer brain: localization in the somatodendritic compartment. *Ann Neurol,* 26**,** 352-61.

KOVACS, T. 2009. [Therapy of Alzheimer disease]. *Neuropsychopharmacol Hung,* 11**,** 27-33.

KRUGER, U., WANG, Y., KUMAR, S. & MANDELKOW, E. M. 2012. Autophagic degradation of tau in primary neurons and its enhancement by trehalose. *Neurobiol Aging,* 33**,** 2291-305.

KUNADT, M., ECKERMANN, K., STUENDL, A., GONG, J., RUSSO, B., STRAUSS, K., RAI, S., KUGLER, S., FALOMIR LOCKHART, L., SCHWALBE, M., KRUMOVA, P., OLIVEIRA, L. M., BAHR, M., MOBIUS, W., LEVIN, J., GIESE, A., KRUSE, N., MOLLENHAUER, B., GEISS-FRIEDLANDER, R., LUDOLPH, A. C., FREISCHMIDT, A., FEILER, M. S., DANZER, K. M., ZWECKSTETTER, M., JOVIN, T. M., SIMONS, M., WEISHAUPT, J. H. & SCHNEIDER, A. 2015. Extracellular vesicle sorting of alpha-Synuclein is regulated by sumoylation. *Acta Neuropathol,* 129**,** 695-713.

KUSSER, K. L. & RANDALL, T. D. 2003. Simultaneous detection of EGFP and cell surface markers by fluorescence microscopy in lymphoid tissues. *J Histochem Cytochem,* 51**,** 5-14.

LACHENAL, G., PERNET-GALLAY, K., CHIVET, M., HEMMING, F. J., BELLY, A., BODON, G., BLOT, B., HAASE, G., GOLDBERG, Y. & SADOUL, R. 2011. Release of exosomes from differentiated neurons and its regulation by synaptic glutamatergic activity. *Mol Cell Neurosci,* 46**,** 409-18.

LEBOUVIER, T., SCALES, T. M., WILLIAMSON, R., NOBLE, W., DUYCKAERTS, C., HANGER, D. P., REYNOLDS, C. H., ANDERTON, B. H. & DERKINDEREN, P. 2009. The microtubule-associated protein tau is also phosphorylated on tyrosine. *J Alzheimers Dis,* 18**,** 1-9.

LEE, G., NEWMAN, S. T., GARD, D. L., BAND, H. & PANCHAMOORTHY, G. 1998. Tau interacts with src-family non-receptor tyrosine kinases. *J Cell Sci,* 111 (Pt 21)**,** 3167-77.

LEE, J. H., SHIN, S. K., JIANG, Y., CHOI, W. H., HONG, C., KIM, D. E. & LEE, M. J. 2015. Facilitated Tau Degradation by USP14 Aptamers via Enhanced Proteasome Activity. *Sci Rep,* 5**,** 10757.

LEE, V. M., GOEDERT, M. & TROJANOWSKI, J. Q. 2001. Neurodegenerative tauopathies. *Annu Rev Neurosci,* 24**,** 1121-59.

LEVINE, B. & KROEMER, G. 2008. SnapShot: Macroautophagy. *Cell,* 132**,** 162 e1-162 e3.

LEWIS, J., MCGOWAN, E., ROCKWOOD, J., MELROSE, H., NACHARAJU, P., VAN SLEGTENHORST, M., GWINN-HARDY, K., PAUL MURPHY, M., BAKER, M., YU, X., DUFF, K., HARDY, J., CORRAL, A., LIN, W. L., YEN, S. H., DICKSON, D. W., DAVIES, P. & HUTTON, M. 2000. Neurofibrillary tangles, amyotrophy and progressive motor disturbance in mice expressing mutant (P301L) tau protein. *Nat Genet,* 25**,** 402-5.

LI, J., LIU, K., LIU, Y., XU, Y., ZHANG, F., YANG, H., LIU, J., PAN, T., CHEN, J., WU, M., ZHOU, X. & YUAN, Z. 2013. Exosomes mediate the cell-to-cell transmission of IFN-alpha-induced antiviral activity. *Nat Immunol,* 14**,** 793-803.

LI, X., KUMAR, Y., ZEMPEL, H., MANDELKOW, E. M., BIERNAT, J. & MANDELKOW, E. 2011. Novel diffusion barrier for axonal retention of Tau in neurons and its failure in neurodegeneration. *EMBO J,* 30**,** 4825-37.

LITMAN, P., BARG, J., RINDZOONSKI, L. & GINZBURG, I. 1993. Subcellular localization of tau mRNA in differentiating neuronal cell culture: implications for neuronal polarity. *Neuron,* 10**,** 627-38.

LIU, C. & GOTZ, J. 2013. Profiling murine tau with 0N, 1N and 2N isoform-specific antibodies in brain and peripheral organs reveals distinct subcellular localization, with the 1N isoform being enriched in the nucleus. *PLoS One,* 8**,** e84849.

LIU, F., GRUNDKE-IQBAL, I., IQBAL, K. & GONG, C. X. 2005. Contributions of protein phosphatases PP1, PP2A, PP2B and PP5 to the regulation of tau phosphorylation. *Eur J Neurosci,* 22**,** 1942-50.

LIU, L., DROUET, V., WU, J. W., WITTER, M. P., SMALL, S. A., CLELLAND, C. & DUFF, K. 2012. Trans-synaptic spread of tau pathology in vivo. *PLoS One,* 7**,** e31302.

LYNCH, S., SANTOS, S. G., CAMPBELL, E. C., NIMMO, A. M., BOTTING, C., PRESCOTT, A., ANTONIOU, A. N. & POWIS, S. J. 2009. Novel MHC class I structures on exosomes. *J Immunol,* 183**,** 1884-91.

MACCIONI, R. B. & CAMBIAZO, V. 1995. Role of microtubule-associated proteins in the control of microtubule assembly. *Physiol Rev,* 75**,** 835-64.

MANDELKOW, E. M. & MANDELKOW, E. 1998. Tau in Alzheimer's disease. *Trends Cell Biol,* 8**,** 425-7.

MANDELKOW, E. M. & MANDELKOW, E. 2012. Biochemistry and cell biology of tau protein in neurofibrillary degeneration. *Cold Spring Harb Perspect Med,* 2**,** a006247.

MANDELL, J. W. & BANKER, G. A. 1995. The microtubule cytoskeleton and the development of neuronal polarity. *Neurobiol Aging,* 16**,** 229-37; discussion 238.

MANN, G. J., DYNE, M. & MUSGROVE, E. A. 1987. Immunofluorescent quantification of ribonucleotide reductase M1 subunit and correlation with DNA content by flow cytometry. *Cytometry,* 8**,** 509-17.

MARZELLA, L., AHLBERG, J. & GLAUMANN, H. 1981. Autophagy, heterophagy, microautophagy and crinophagy as the means for intracellular degradation. *Virchows Arch B Cell Pathol Incl Mol Pathol,* 36**,** 219-34.

MATSUDAIRA, P. T. & BURGESS, D. R. 1978. SDS microslab linear gradient polyacrylamide gel electrophoresis. *Anal Biochem,* 87**,** 386-96.

MIGHELI, A., BUTLER, M., BROWN, K. & SHELANSKI, M. L. 1988. Light and electron microscope localization of the microtubule-associated tau protein in rat brain. *J Neurosci,* 8**,** 1846-51.

MOCANU, M. M., NISSEN, A., ECKERMANN, K., KHLISTUNOVA, I., BIERNAT, J., DREXLER, D., PETROVA, O., SCHONIG, K., BUJARD, H., MANDELKOW, E., ZHOU, L., RUNE, G. & MANDELKOW, E. M. 2008. The potential for beta-structure in the repeat domain of tau protein determines aggregation, synaptic decay, neuronal loss, and coassembly with endogenous Tau in inducible mouse models of tauopathy. *J Neurosci,* 28**,** 737-48.

MONDRAGON-RODRIGUEZ, S., TRILLAUD-DOPPIA, E., DUDILOT, A., BOURGEOIS, C., LAUZON, M., LECLERC, N. & BOEHM, J. 2012. Interaction of endogenous tau protein with synaptic proteins is regulated by N-methyl-D-aspartate receptor-dependent tau phosphorylation. *J Biol Chem,* 287**,** 32040-53.

MOREJOHN, L. C. & FOSKET, D. E. 1984. Taxol-induced rose microtubule polymerization in vitro and its inhibition by colchicine. *J Cell Biol,* 99**,** 141-7.

MORITA, T. & SOBUE, K. 2009. Specification of neuronal polarity regulated by local translation of CRMP2 and Tau via the mTOR-p70S6K pathway. *J Biol Chem,* 284**,** 27734-45.

MURRELL, J., FARLOW, M., GHETTI, B. & BENSON, M. D. 1991. A mutation in the amyloid precursor protein associated with hereditary Alzheimer's disease. *Science,* 254**,** 97-9.

MYEKU, N., CLELLAND, C. L., EMRANI, S., KUKUSHKIN, N. V., YU, W. H., GOLDBERG, A. L. & DUFF, K. E. 2016. Tau-driven 26S proteasome impairment and cognitive dysfunction can be prevented early in disease by activating cAMP-PKA signaling. *Nat Med,* 22**,** 46-53.

NAVE, K. A. & WERNER, H. B. 2014. Myelination of the nervous system: mechanisms and functions. *Annu Rev Cell Dev Biol,* 30**,** 503-33.

NEVE, R. L., HARRIS, P., KOSIK, K. S., KURNIT, D. M. & DONLON, T. A. 1986. Identification of cDNA clones for the human microtubule-associated protein tau and chromosomal localization of the genes for tau and microtubule-associated protein 2. *Brain Res,* 387**,** 271-80.

NIXON, R. A. 2013. The role of autophagy in neurodegenerative disease. *Nat Med,* 19**,** 983-97.

NIXON, R. A., WEGIEL, J., KUMAR, A., YU, W. H., PETERHOFF, C., CATALDO, A. & CUERVO, A. M. 2005. Extensive involvement of autophagy in Alzheimer disease: an immuno-electron microscopy study. *J Neuropathol Exp Neurol,* 64**,** 113-22.

ORNSTEIN, L & DAVIS, BJ. 1964. Disc electrophoresis-I: Background and theory. *Ann NY Acad Sci* ,121, 321–349.

PAPASOZOMENOS, S. C. & BINDER, L. I. 1987. Phosphorylation determines two distinct species of Tau in the central nervous system. *Cell Motil Cytoskeleton,* 8**,** 210-26.

PARTON, R. G., SIMONS, K. & DOTTI, C. G. 1992. Axonal and dendritic endocytic pathways in cultured neurons. *J Cell Biol,* 119**,** 123-37.

PEERAER, E., BOTTELBERGS, A., VAN KOLEN, K., STANCU, I. C., VASCONCELOS, B., MAHIEU, M., DUYTSCHAEVER, H., VER DONCK, L., TORREMANS, A., SLUYDTS, E., VAN ACKER, N., KEMP, J. A., MERCKEN, M., BRUNDEN, K. R., TROJANOWSKI, J. Q., DEWACHTER, I., LEE, V. M. & MOECHARS, D. 2015. Intracerebral injection of preformed synthetic tau fibrils initiates widespread tauopathy and neuronal loss in the brains of tau transgenic mice. *Neurobiol Dis,* 73**,** 83-95.

POLANCO, J. C., SCICLUNA, B. J., HILL, A. F. & GOTZ, J. 2016. Extracellular vesicles isolated from brains of rTg4510 mice seed tau aggregation in a threshold-dependent manner. *J Biol Chem*.

QIAN, W., SHI, J., YIN, X., IQBAL, K., GRUNDKE-IQBAL, I., GONG, C. X. & LIU, F. 2010. PP2A regulates tau phosphorylation directly and also indirectly via activating GSK-3beta. *J Alzheimers Dis,* 19**,** 1221-9.

RAJENDRAN, L., HONSHO, M., ZAHN, T. R., KELLER, P., GEIGER, K. D., VERKADE, P. & SIMONS, K. 2006. Alzheimer's disease beta-amyloid peptides are released in association with exosomes. *Proc Natl Acad Sci U S A,* 103**,** 11172-7.

REGAN, P., WHITCOMB, D. J. & CHO, K. 2016. Physiological and Pathophysiological Implications of Synaptic Tau. *Neuroscientist*.

REN, Q. G., LIAO, X. M., CHEN, X. Q., LIU, G. P. & WANG, J. Z. 2007. Effects of tau phosphorylation on proteasome activity. *FEBS Lett,* 581**,** 1521-8.

ROBERSON, E. D., SCEARCE-LEVIE, K., PALOP, J. J., YAN, F., CHENG, I. H., WU, T., GERSTEIN, H., YU, G. Q. & MUCKE, L. 2007. Reducing endogenous tau ameliorates amyloid beta-induced deficits in an Alzheimer's disease mouse model. *Science,* 316**,** 750-4.

RODRIGUEZ-NAVARRO, J. A., RODRIGUEZ, L., CASAREJOS, M. J., SOLANO, R. M., GOMEZ, A., PERUCHO, J., CUERVO, A. M., GARCIA DE YEBENES, J. & MENA, M. A. 2010. Trehalose ameliorates dopaminergic and tau pathology in parkin deleted/tau overexpressing mice through autophagy activation. *Neurobiol Dis,* 39**,** 423-38.

ROSSI, G., DALPRA, L., CROSTI, F., LISSONI, S., SCIACCA, F. L., CATANIA, M., DI FEDE, G., MANGIERI, M., GIACCONE, G., CROCI, D. & TAGLIAVINI, F. 2008. A new function of microtubule-associated protein tau: involvement in chromosome stability. *Cell Cycle,* 7**,** 1788-94.

RUBINSZTEIN, D. C., CUERVO, A. M., RAVIKUMAR, B., SARKAR, S., KOROLCHUK, V., KAUSHIK, S. & KLIONSKY, D. J. 2009. In search of an "autophagomometer". *Autophagy,* 5**,** 585-9.

RUBINSZTEIN, D. C., GESTWICKI, J. E., MURPHY, L. O. & KLIONSKY, D. J. 2007. Potential therapeutic applications of autophagy. *Nat Rev Drug Discov,* 6**,** 304-12.

SAMAN, S., KIM, W., RAYA, M., VISNICK, Y., MIRO, S., SAMAN, S., JACKSON, B., MCKEE, A. C., ALVAREZ, V. E., LEE, N. C. & HALL, G. F. 2012. Exosome-associated tau is secreted in tauopathy models and is selectively phosphorylated in cerebrospinal fluid in early Alzheimer disease. *J Biol Chem,* 287**,** 3842-9.

SARKAR, S., DAVIES, J. E., HUANG, Z., TUNNACLIFFE, A. & RUBINSZTEIN, D. C. 2007. Trehalose, a novel mTOR-independent autophagy enhancer, accelerates the clearance of mutant huntingtin and alpha-synuclein. *J Biol Chem,* 282**,** 5641-52.

SCHNEIDER, A., BIERNAT, J., VON BERGEN, M., MANDELKOW, E. & MANDELKOW, E. M. 1999. Phosphorylation that detaches tau protein from microtubules (Ser262, Ser214) also protects it against aggregation into Alzheimer paired helical filaments. *Biochemistry,* 38**,** 3549-58.

SCHNEIDER, A. & MANDELKOW, E. 2008. Tau-based treatment strategies in neurodegenerative diseases. *Neurotherapeutics,* 5**,** 443-57.

SIMON, D., GARCIA-GARCIA, E., ROYO, F., FALCON-PEREZ, J. M. & AVILA, J. 2012. Proteostasis of tau. Tau overexpression results in its secretion via membrane vesicles. *FEBS Lett,* 586**,** 47-54.

STAMER, K., VOGEL, R., THIES, E., MANDELKOW, E. & MANDELKOW, E. M. 2002. Tau blocks traffic of organelles, neurofilaments, and APP vesicles in neurons and enhances oxidative stress. *J Cell Biol,* 156**,** 1051-63.

STEINER, B., MANDELKOW, E. M., BIERNAT, J., GUSTKE, N., MEYER, H. E., SCHMIDT, B., MIESKES, G., SOLING, H. D., DRECHSEL, D., KIRSCHNER, M. W. & ET AL. 1990. Phosphorylation of microtubule-associated protein tau: identification of the site for Ca2(+)-calmodulin dependent kinase and relationship with tau phosphorylation in Alzheimer tangles. *EMBO J,* 9**,** 3539-44.

STEWARD, O. & LEVY, W. B. 1982. Preferential localization of polyribosomes under the base of dendritic spines in granule cells of the dentate gyrus. *J Neurosci,* 2**,** 284-91.

STEWARD, O. & SCHUMAN, E. M. 2003. Compartmentalized synthesis and degradation of proteins in neurons. *Neuron,* 40**,** 347-59.

SULTAN, A., NESSLANY, F., VIOLET, M., BEGARD, S., LOYENS, A., TALAHARI, S., MANSUROGLU, Z., MARZIN, D., SERGEANT, N., HUMEZ, S., COLIN, M., BONNEFOY, E., BUEE, L. & GALAS, M. C. 2011. Nuclear tau, a key player in neuronal DNA protection. *J Biol Chem,* 286**,** 4566-75.

TAKEDA, S., WEGMANN, S., CHO, H., DEVOS, S. L., COMMINS, C., ROE, A. D., NICHOLLS, S. B., CARLSON, G. A., PITSTICK, R., NOBUHARA, C. K., COSTANTINO, I., FROSCH, M. P., MULLER, D. J., IRIMIA, D. & HYMAN, B. T. 2015. Neuronal uptake and propagation of a rare phosphorylated high-molecular-weight tau derived from Alzheimer's disease brain. *Nat Commun,* 6**,** 8490.

TAYLOR, A. M., BLURTON-JONES, M., RHEE, S. W., CRIBBS, D. H., COTMAN, C. W. & JEON, N. L. 2005. A microfluidic culture platform for CNS axonal injury, regeneration and transport. *Nat Methods,* 2**,** 599-605.

TAYLOR, A. M., RHEE, S. W., TU, C. H., CRIBBS, D. H., COTMAN, C. W. & JEON, N. L. 2003. Microfluidic Multicompartment Device for Neuroscience Research. *Langmuir,* 19**,** 1551-1556.

TERABAYASHI, T., ITOH, T. J., YAMAGUCHI, H., YOSHIMURA, Y., FUNATO, Y., OHNO, S. & MIKI, H. 2007. Polarity-regulating kinase partitioning-defective 1/microtubule affinity-regulating kinase 2 negatively regulates development of dendrites on hippocampal neurons. *J Neurosci,* 27**,** 13098-107.

TERRY, R. D., PECK, A., DETERESA, R., SCHECHTER, R. & HOROUPIAN, D. S. 1981. Some morphometric aspects of the brain in senile dementia of the Alzheimer type. *Ann Neurol,* 10**,** 184-92.

THERY, C., AMIGORENA, S., RAPOSO, G. & CLAYTON, A. 2006. Isolation and characterization of exosomes from cell culture supernatants and biological fluids. *Curr Protoc Cell Biol,* Chapter 3**,** Unit 3 22.

THIES, E. & MANDELKOW, E. M. 2007. Missorting of tau in neurons causes degeneration of synapses that can be rescued by the kinase MARK2/Par-1. *J Neurosci,* 27**,** 2896-907.

TSENG, B. P., GREEN, K. N., CHAN, J. L., BLURTON-JONES, M. & LAFERLA, F. M. 2008. Abeta inhibits the proteasome and enhances amyloid and tau accumulation. *Neurobiol Aging,* 29**,** 1607-18.

TYTELL, M., BRADY, S. T. & LASEK, R. J. 1984. Axonal transport of a subclass of tau proteins: evidence for the regional differentiation of microtubules in neurons. *Proc Natl Acad Sci U S A,* 81**,** 1570-4.

USENOVIC, M., NIROOMAND, S., DROLET, R. E., YAO, L., GASPAR, R. C., HATCHER, N. G., SCHACHTER, J., RENGER, J. J. & PARMENTIER-BATTEUR, S. 2015. Internalized Tau Oligomers Cause Neurodegeneration by Inducing Accumulation of Pathogenic Tau in Human Neurons Derived from Induced Pluripotent Stem Cells. *J Neurosci,* 35**,** 14234-50.

VON BERGEN, M., FRIEDHOFF, P., BIERNAT, J., HEBERLE, J., MANDELKOW, E. M. & MANDELKOW, E. 2000. Assembly of tau protein into Alzheimer paired helical filaments depends on a local sequence motif ((306)VQIVYK(311)) forming beta structure. *Proc Natl Acad Sci U S A,* 97**,** 5129-34.

WANG, J. Z., GRUNDKE-IQBAL, I. & IQBAL, K. 1996. Glycosylation of microtubule-associated protein tau: an abnormal posttranslational modification in Alzheimer's disease. *Nat Med,* 2**,** 871-5.

WANG, Y. & MANDELKOW, E. 2012. Degradation of tau protein by autophagy and proteasomal pathways. *Biochem Soc Trans,* 40**,** 644-52.

WANG, Y. & MANDELKOW, E. 2016. Tau in physiology and pathology. *Nat Rev Neurosci,* 17**,** 22-35.

WANG, Y., MARTINEZ-VICENTE, M., KRUGER, U., KAUSHIK, S., WONG, E., MANDELKOW, E. M., CUERVO, A. M. & MANDELKOW, E. 2009. Tau fragmentation, aggregation and clearance: the dual role of lysosomal processing. *Hum Mol Genet,* 18**,** 4153-70.

WANG, Y. P., BIERNAT, J., PICKHARDT, M., MANDELKOW, E. & MANDELKOW, E. M. 2007. Stepwise proteolysis liberates tau fragments that nucleate the Alzheimer-like aggregation of full-length tau in a neuronal cell model. *Proc Natl Acad Sci U S A,* 104**,** 10252-7.

WEBER, K., RATHKE, P. C. & OSBORN, M. 1978. Cytoplasmic microtubular images in glutaraldehyde-fixed tissue culture cells by electron microscopy and by immunofluorescence microscopy. *Proc Natl Acad Sci U S A,* 75**,** 1820-4.

WEINGARTEN, M. D., LOCKWOOD, A. H., HWO, S. Y. & KIRSCHNER, M. W. 1975. A protein factor essential for microtubule assembly. *Proc Natl Acad Sci U S A,* 72**,** 1858-62.

WONG, E. & CUERVO, A. M. 2010. Integration of clearance mechanisms: the proteasome and autophagy. *Cold Spring Harb Perspect Biol,* 2**,** a006734.

WU, J. W., HERMAN, M., LIU, L., SIMOES, S., ACKER, C. M., FIGUEROA, H., STEINBERG, J. I., MARGITTAI, M., KAYED, R., ZURZOLO, C., DI PAOLO, G. & DUFF, K. E. 2013. Small misfolded Tau species are internalized via bulk endocytosis and anterogradely and retrogradely transported in neurons. *J Biol Chem,* 288**,** 1856-70.

WU, Y. T., TAN, H. L., SHUI, G., BAUVY, C., HUANG, Q., WENK, M. R., ONG, C. N., CODOGNO, P. & SHEN, H. M. 2010. Dual role of 3-methyladenine in modulation of autophagy via different temporal patterns of inhibition on class I and III phosphoinositide 3-kinase. *J Biol Chem,* 285**,** 10850-61.

YAMAMOTO, A., TAGAWA, Y., YOSHIMORI, T., MORIYAMA, Y., MASAKI, R. & TASHIRO, Y. 1998. Bafilomycin A1 prevents maturation of autophagic vacuoles by inhibiting fusion between autophagosomes and lysosomes in rat hepatoma cell line, H-4-II-E cells. *Cell Struct Funct,* 23**,** 33-42.

YAN, M. H., WANG, X. & ZHU, X. 2013. Mitochondrial defects and oxidative stress in Alzheimer disease and Parkinson disease. *Free Radic Biol Med,* 62**,** 90-101.

YANG, Y. P., HU, L. F., ZHENG, H. F., MAO, C. J., HU, W. D., XIONG, K. P., WANG, F. & LIU, C. F. 2013. Application and interpretation of current autophagy inhibitors and activators. *Acta Pharmacol Sin,* 34**,** 625-35.

YANG, Z. & KLIONSKY, D. J. 2010. Eaten alive: a history of macroautophagy. *Nat Cell Biol,* 12**,** 814-22.

YEW, E. H., CHEUNG, N. S., CHOY, M. S., QI, R. Z., LEE, A. Y., PENG, Z. F., MELENDEZ, A. J., MANIKANDAN, J., KOAY, E. S., CHIU, L. L., NG, W. L., WHITEMAN, M., KANDIAH, J. & HALLIWELL, B. 2005. Proteasome inhibition by lactacystin in primary neuronal cells induces both potentially neuroprotective and pro-apoptotic transcriptional responses: a microarray analysis. *J Neurochem,* 94**,** 943-56.

ZEMPEL, H., LUEDTKE, J., KUMAR, Y., BIERNAT, J., DAWSON, H., MANDELKOW, E. & MANDELKOW, E. M. 2013. Amyloid-beta oligomers induce synaptic damage via Tau-dependent microtubule severing by TTLL6 and spastin. *EMBO J,* 32**,** 2920-37.

ZEMPEL, H. & MANDELKOW, E. 2014. Lost after translation: missorting of Tau protein and consequences for Alzheimer disease. *Trends Neurosci,* 37**,** 721-32.

ZEMPEL, H., THIES, E., MANDELKOW, E. & MANDELKOW, E. M. 2010. Abeta oligomers cause localized Ca(2+) elevation, missorting of endogenous Tau into dendrites, Tau phosphorylation, and destruction of microtubules and spines. *J Neurosci,* 30**,** 11938-50.

ZHU, L. Q., ZHENG, H. Y., PENG, C. X., LIU, D., LI, H. L., WANG, Q. & WANG, J. Z. 2010. Protein phosphatase 2A facilitates axonogenesis by dephosphorylating CRMP2. *J Neurosci,* 30**,** 3839-48.

6 Appendix

Probesets used for fluorescence insitu hybridization:

The binding region of probe sets is RED and the binding region of the blocking probe (BL) is GREEN on rat Tau mRNA (see **Fig. 2.2** in 'Materials and Methods').

cDNA sequence of Rattus norvegicus microtubule-associated protein Tau (Mapt), mRNA. [Rattus norvegicus] ref|NM_017212|

gtctccgccacccaccagctccagcaccagcagcagcgccggcgccaccgcccaccttctgctgtcgccgccgcc
acaaccaccttcccctccgctgtcctcttctgtcctcgcctcctgtcgattatcaggctttgaagcagcatggct
gaaccccgccaggagtttgacacaatggaagaccaggccggagattacactatgctccaagaccaagaaggagac
atggaccatggcttaaaagctgaagaagcaggcatcggagacaccccgaacatggaggaccaagctgctgggcat
gtgactcaagctcgagtggccggcgtaagcaaagacaggacaggaaatgacgagaagaaagccaagggcgccgat
ggcaaaacgggggcgaagatcgccacacctcggggagcagccactccgggccagaaaggcacatccaatgccacc
aggatcccagccaagaccacacccagcccaaagactcctccaggatcaggtgaaccaccaaaatccggagaacga
agcggctacagcagccccggctcgcccggaacccctggcagtcgctcccgtaccccatccctaccaacgccgccc
acccgagagcccaaaaaggtggcagtggttcgcactccccctaagtcaccgtctgccagtaagagccgcctacag
actgcccctgtgcccatgccagacctaaagaacgtcaggtccaagattggctccactgagaacctgaagcaccag
ccgggaggcggcaaggtgcagataattaataagaagctggatcttagcaacgtccagtccaagtgtggctcaaag
gacaatatcaaacacgtcccgggcggaggcagtgtgcaaatagtctacaagccagtggacctgagcaaggtgacc
tccaagtgtggttccttagggaacatccatcacaagccaggaggtggccaggtagaagtaaaatcagagaagctg
gacttcaaggatagagtccagtcgaagattggctccttggataacatcacccatgtccctggaggagggaataag
aagattgaaacccacaagctgaccttcagggagaatgccaaagccaagacagaccatggagcagaaatcgtgtac
aagtcacctgtggtgtctggggacacatctccacggcacctcagcaacgtctcctccacgggcagcatcgacatg
gtggactctccacagcttgccacgttagccgatgaagtgtccgcctctttggccaagcagggtttgtgatcaggc
ccctggggccgtcactgatcatggagagaagagagagtgagagtgtggaaaaaaaaaaaaaaaaaaagaatgacct
ggcccctcaccctctgccctccccgctgctcctcatagacaggctgaccagcttgtcacctaacctgcttttgtg
gctcgggtttggctcgggacttcaaaatcagtgatgggaaaaagtaaatttcatctttccaaattgatttgtggg
ctagtaataaaatatttttaaggaaggaaaaaaaaaaaaacacgtaaaaccatggccaaacaaaacccaacattt
ccttggcaattgttattgaccccgcccccccctctgagttttagagggtgaaggaggctttggatggaggctgc
ttctggggattggctgagggactagggcaactaattgcccacagccccatcttaggggcatcagggacagcggca
gcaatgaaagacttgggacttggtgtgtttgtggagccgtaggcaggtgatgttaactttgtgtgggtttgaggg
aggactgtgatagtgaaggctgagagatgggtgggctgggagtcagaggagagaggtgaggaagacaggttggga
gaggggacattggctccttgccaaggagcttgggaagcacaggtagccctggctgcctgcagcagtcttagctag
cacagatgcctgcctgagaaagcacagtggggtacagtgggtgtgtgtgccccttctgaagggcagcccatggga
gaaggggtattgggcagaaggaaggtaggccagaaggtggcaccttgtagattggttctctgaaggctgaccttg
ccatcccagggcactggctcccaccctccagggagggaggtcctgagctgaggagcttccctttgctctcacagg
aaaacctgtgttactgagttctgaagtttggaactacagccatgattttggccaccatacagacctgggacttta
gggctaaccagttctttgtaaggacttgtgcctcttgcgggaacatctgcctgttctcaagcctggtcctctggc
acttctgcagtgtgagggatgggggtggtattctgggatgtgggtcccangcctcccatccctcgcacagccact
gtatcccctctacctgtcctatcatgcccacgtctgccatgagagccagtcactgccgtccatacatcacgtctc
accgtcctgagtgcccagcctccccaagccccatccctggcccctgggtagttatggccaatatctgctctacac
taggggttggagtccagggaaggcaaagatttgggccttggtctctagtcctacgttgcacgaatccaaccagtg
tgcctcccacaaggaaccttacaaccttgtttggtttgctccatcatttcccatcgtggatgggagtccgtgtgt
gcctggagattaccctggacacctctgctttttttttttactttagcggttgcctcctaggcctgactccttcc
catgttgaactggaggcagccacgttaggtgtcaatgtcctggcatcagtatgaacagtcagtagtcccagggca
gggccacacttctcccatcttctgcttccaccccagcttgtgattgctagcctcccagagctcagccgccattaa
gtccccatgcacgtaatcagcccttcataccccaatttggggaacataccccttgattgaaatgttttccctcca
gtcctatggaagcggtgctgcctgccctgctggagcagccagccatctccagagacgcagccctttctctcctgt
ccgcaccctgttgcgctgtagtcggattcgtctgtttgtctgggttcaccagagtgactatgatagtgaaaagaa
aaagaaaaagaaaaaagaaaaaagaaaaaaaaaaaaggacgcatgttatcttgaaatatttgtcaaaaggttgta
gcccaccgcagggattggagggcctggatattccttgtcttcttcgtgacttaggtccaggccggtgcagtgcta
ccctgctgggacatcccatgttttgaagggtttcttcttcatctgggaccctgcagacactggattgtgacattg
gaggtctatgacattggccaaggcctgaagcacaggacccgttagaggcagcaggctccgactgtcagggagagc
ttgtggctggcctgtttctctgagtgaagatggtcctctctaatcacaacttcaagtcccacagcagccctggca
gacatctaagaactcctgcatcacaagagaaaaggacactagtaccagcagggagagctgtggccctagaaattc

catgactctccactacatatccgtgggtcctttccaagccttggcctcgtcaccaagggcttgggatggactgcc
ccactgatgaaagggacatctttggagacccccttggtttccaaggcgtcagccccctgaccttgcatgacctcc
tacagctgtaaggatgaggcctttaaagattaggaacctcaggcccaggtcggccactttgggcttgggtacagt
tagggacgatgcggtagaaggaggtggccaacctttcccatataagagttctgtgtgcccagagctaccctattg
tgagctccccactgctgatggactttagctgtccttagaagtgaagagtccaacggaggaaaaggaagtgtggtt
tgatggtctgtggtcccttcatcatggttacctgttgtggttttctctcgtatacccatttacccatcctgcagt
tcctgtccttgaataggggtgggggtactctgccatatctcttgtagggcagtcagcccccaagtcatagtttgg
agtgatctggtcagtgctaataggcagtttacaaaggaattctggcttgttacttcagtgaggacaatcccccaa
gggccctggcacctgtcctgtctttccatggctctccactgcagagccaatgtctttgggtgggctagatagggt
gtacaatttgcctggttcctccaagctcttaatccactttatcaatagttccatttaaattgacttcaatgataa
gagtgtatcccatttgagattgcttgtgttgtggggtaaaggggggaggaggaacatgttaagataattgacatg
ggcaaggggaagtcttgaagtgtagcagttaaaccatcttgtagccccattcatgatgttgaccacttgctagag
agaagaggtgccataaggctagaacctagaggcttggctgtcccaccaacaggcaggcttttgcaaggcagaggc
agccagctaggtccctgacttcccagccaggtgcagctctaagaactgctcttgcctgctgccttcttgtggtgt
ccagagcccacagccaatgcctcctcaaaaccctggcttccttccttctaatccactggcacatcagcatcacct
ccggattgacttcagatccacagcctacactactagcagtgggtaagaccacttcctttgtccttgtctgttctc
cagaaaagtgggcatggaggcggtgttaataactataggtctgtggctttatgagccttcaaacttctctctagc
ttctgaaagggttacttttgggcagtattgcagtctcaccctcccgatgggctgtagcctgtgcagttgctgtac
tgggcatgatctccagtgcttgcaagtcccatgatttctttggtgattttgagggtgggggagggacatgaatc
atcttagcttagcttcctgtctgtgaatgtccatatagtgtactgtgttttaacaaacgatttacactgactgtt
gctgtacaagtgaatttggaaataaagttattactctgattaaacaaaaaaaaaaaaa

Quantigene ViewRNA ISH cell assay kit components and storage conditions:

Component	**Description**	**Storage**
10X PBS	Aqueous buffered solution	15-30deg
Detergent solution	Aqueous buffered solution	15-30deg
Protease	Aqueous buffered solution	2-8deg
Probe Set Diluent	Aqueous buffered solution containing formamide and detergent	2-8deg
Amplifier Diluent	Aqueous buffered solution containing formamide and detergent	2-8deg
Label probe diluent	Aqueous buffered solution containing detergent	2-8deg
PreAmplifier Mix	DNA in aqueous buffered solution containing PreAmp4	-20deg

Amplifier Mix	DNA in aqueous buffered solution containing Amp4	-20deg
Label Probe Mix	Fluorescent dye-labeled oligonucleotides in aqueous buffered solution containing LP4-488	-20deg
Wash Buffer Component 1	Aqueous buffered solution containing detergent	15-30deg
Wash Buffer Component 1	Aqueous buffered solution	15-30deg
QuantiGene ViewRNA Probe Set	RNA-specific DNA oligonucleotides designed against a target of interest and are compatible with Type 4 Signal Amplifiers	-20deg

Adapted from Affymetrix ‘QuantiGene ViewRNA ISH Cell Assay User Manual’

7 Acknowledgement

I sincerely thank Prof. Dr. Eckhard Mandelkow and Dr. Eva Mandelkow for giving me an opportunity to carry out my projects and providing me with all the necessary facilities. Their guidance was immensely important in my projects. I also thank them for their constant encouragement and fruitful discussions throughout this work.

Special thanks to Dr. Eva Mandelkow for introducing me to the latest techniques which are highly demanded in the field of neuroscience.

I thank Dr. Yipeng Wang for his tremendous amount of input in my projects, participating in discussions related to my projects, advising me during critical times of my projects, helping me with my papers and my thesis.

I thank Julia Ludtke, Sabrina Huebschman and Johanna Roth for their excellent technical assistance and ordering things as quick as possible.

I thank Dr. Bikash Choudhary, Dr. Senthil Kaniyappan, Dr. Jeelani Pir and Dr. Maria Joseph for their assistance.

I thank all my other lab members for their help during the various stages of my PhD.

Last but not least, I would like thank my family and my dear friend, Deepika for extending tremendous amount of moral support although from a remote distance.